High precision spectroscopy in muonic hydrogen

The measurement of the hyperfine transition in muonic hydrogen $\Delta E_{HFS}(\mu p)_{1S}$

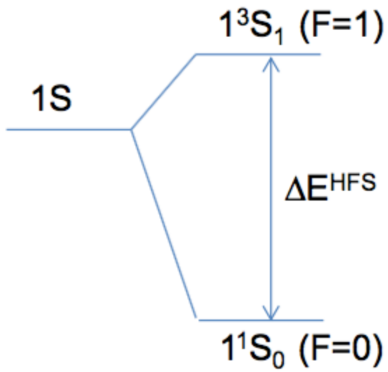

F : total angular momentum

Andrea Vacchi on behalf of the FAMU Collaboration

Bologna 2 Marzo 2018

FAMU Collaboration

RIKEN Nishina Center
"The RIKEN-RAL Muon Facility"
(International Research Collaboration between RIKEN and SFTC (Science and Technology Facility Council) in the UK)

INFN Trieste: V. Bonvicini, H. Cabrera, E. Furlanetto, E. Mocchiutti, C. Pizzolotto, A. Rachevsky, L. Stoychev, A. Vacchi (also *Università di Udine*), E. Vallazza, G. Zampa, **Elettra-Sincrotrone**: M. Danailov, A. Demidovich, **ICTP**: J. Niemela, K.S. Gadedjisso-Tossou

INFN Bologna: L. Andreani, G. Baldazzi, G. Campana, I. D'Antone, M. Furini, F. Fuschino, A. Gabrielli, C. Labanti, A. Margotti, M. Marisaldi, S. Meneghini, G. Morgante, L. P. Rignanese, P. L. Rossi, M. Zuffa

INFN Milano Bicocca: A. Baccolo, R. Benocci, R. Bertoni, M. Bonesini, T. Cervi, F. Chignoli, M. Clemenza, A. Curioni, V. Maggi, R. Mazza, M. Moretti, M. Nastasi, E. Previtali, R. Ramponi (also Politecnico Milano CNR)

INFN Pavia: A. De Bari, C. De Vecchi, A. Menegolli, M. Rossella, R. Nardò, A. Tomaselli

INFN Roma3: L. Colace, M. De Vincenzi, A. Iaciofano, L. Tortora, F. Somma

INFN Seconda Università di Napoli: L. Gianfrani, L. Moretti

INFN – GSSI: D. Guffanti,

RIKEN-RAL: K. Ishida

INP, Polish Academy of Sciences: A. Adamczak

INRNE, Bulgarian Academy of Sciences: D. Bakalov, M. Stoilov, P. Danev

• FAMU 2017 activity in one slide

- Spectroscopic measurement of the hyperfine transition of the 1S state of muon hydrogen. Information on proton structure and muon-nucleon interaction

Highlights 2017:

- At RAL, experimental optimization and study of the final set-up and background noise in presence of pure hydrogen were performed.
- Analysis of the data collected in 2014 has been completed and published.
- The publications relating to the 2016 data analysis are in the final In the drafting phase.
- The procurement phase of the FAMU Laser components is completed.
- In progress the study of the optical cavity of the experiment.
- Simulations and engineering study of the target for the final spectroscopic measurements based on the data collected in 2016 and the theoretical calculations are being concretized.
- The LaBr detectors with active high voltage divider were upgraded.
- A new odoscope for detailed study of the beam has been realized.
- A study on the focusing of low-energy muons has been initiated.
- The preparation of the experimental area started at RAL.
- Two collaboration meetings.

Experimental activity @ Rutherford lab (UK)

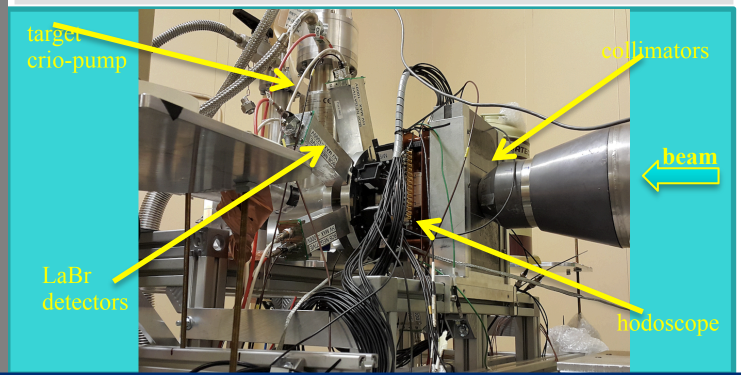

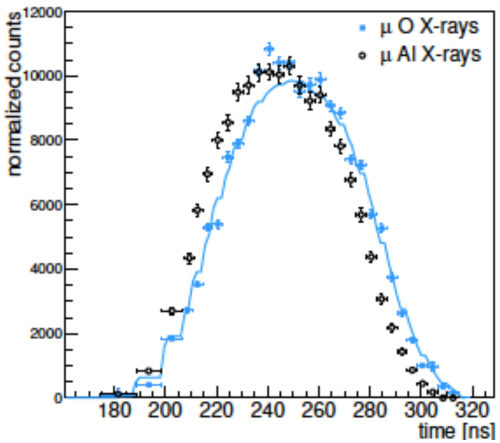

Fig 1 time evolution of X-rays emission from aluminium and oxygen. Line fit to the oxygen distribution [1].

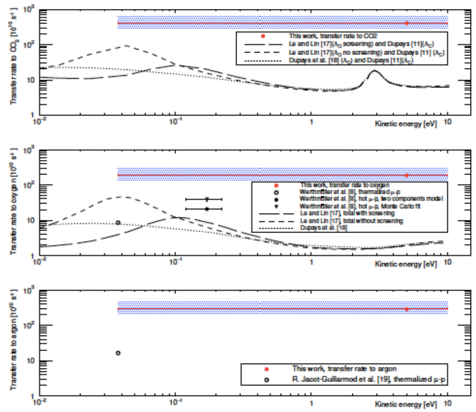

Figure 3. From top to bottom: measured transfer rate to CO_2, oxygen and argon. Shaded regions represent the limits of the estimated systematic uncertainties. Horizontal lines associated to points represent the energy ranges of the measurements, the points are placed at the arithmetic mean of the interval. Statistical error bars are included in the points when not visible. Dashed lines represent theoretical calculations of the transfer rate to oxygen and to CO_2.

Activities 2018:

- Laser implementation and optimization
- March new beam test:
  - first focusing test
  - high pressure high temperature last test
  - low pressure checks for final conditions
- realization of the final cryo-gas-optical-target:
  - optical cavity
  - cryostat
  - optimized optical and beam windows
- Collaboration meeting in June
- Assembly of the experiment at RAL
- First beam tests with lasers and cavities

[1] Emiliano Mocchiutti *et al.*, "First FAMU observation of muon transfer from mu-p atoms to higher-Z elements,"\\ *arXiv:1708.03172 [physics]*, Aug. 2017.

[2] G. Baldazzi *et al.*, "The LaBr 3 (Ce) based detection system for the FAMU experiment," *J. Inst.*, vol. 12, no. 03, p. C03067, 2017.

[3] M. Bonesini *et al.*, "The construction of the Fiber-SiPM beam monitor system of the R484 and R582 experiments at the RIKEN-RAL muon facility," *Journal of Instrumentation*, vol. 12, no. 03, pp. C03035–C03035, Mar. 2017.

[4] Vacchi, A. *et al.*, RIKEN Accel. Prog. Rep. 50, (2017).

[5] E. Mocchiutti et al., "FAMU: studies of the muon transfer process in a mixture of hydrogen and higher Z gas", INFN-CNAF Annual Report 2016. www.cnaf.infn.it/annual-report, ISSN 2283-5490

OUTLINE

- FAMU background & motivations
- The method to measure the hfs
- laser
- beam
- target
- detectors
- muon transfer rate measurements
- conclusions

Simple atomic systems

High precision studies of the energy spectra of hydrogenic atoms like

muonic hydrogen

provide ***very high accuracy tests of quantum electrodynamics and the theory of electromagnetic bound states.***

Moreover, ***the values of the fundamental physical constants (particle masses, fine structure constant, proton charge radius, etc.) can be determined more precisely***.

and how universal is (lepton) universality?

Muonic hydrogen

Muon (e^-'s heavier twin) orbiting the proton instead of electron.

$$m_\mu = 207 m_e$$

$$r_\mu = \frac{1}{186} r_e$$

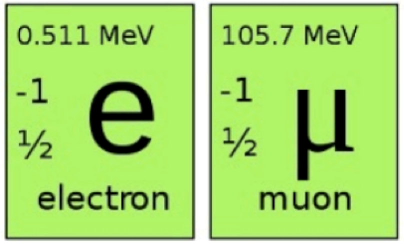

$$m\mu/me \approx 2x10^2$$

- the ***radius of the muon orbit*** is ~ $a_0/200$ so ***that the energy levels of muonic hydrogen are orders of magnitude more "sensitive" to the details of the proton structure than the levels of normal hydrogen***.
- the binding energy of the ground state of muonic hydrogen is of the order of 200 Ry,

FAMU

INFN
Istituto Nazionale di Fisica Nucleare

Rydberg constant R_H

The constant appearing in the Balmer formula for spectral lines of the hydrogen atom. For a hydrogen atom, the effective mass must be taken as the reduced mass of the proton and electron. In MKS, this gives the Rydberg constant

$$\frac{m_e m_p}{m_e + m_p} \frac{e^4}{8c\epsilon_0^2 h^3} \qquad 1.09678 \times 10^5 \text{ cm}^{-1}$$

The hydrogen atom consists of a single proton surrounded by a single electron. It is thus the simplest of all atoms. For the hydrogen atom, the (nonrelativistic) Schrödinger equation takes the form

$$\left[\frac{\tilde{\mathbf{p}}^2}{2\mu} + V(r)\right]\psi(\mathbf{r}) = E\psi(\mathbf{r}),$$

where μ here is the reduced mass of the nucleus and electron. This equation may be attacked in one of two ways: solution of the Schrödinger equation or using operators (matrix mechanics).

- Charge radius (r_E, based on the distribution of charge) and a
- Zemach radius (r_Z, reflects the spatial distribution of $\vec{\mu}$ smeared out by $\rho(\vec{r})$).

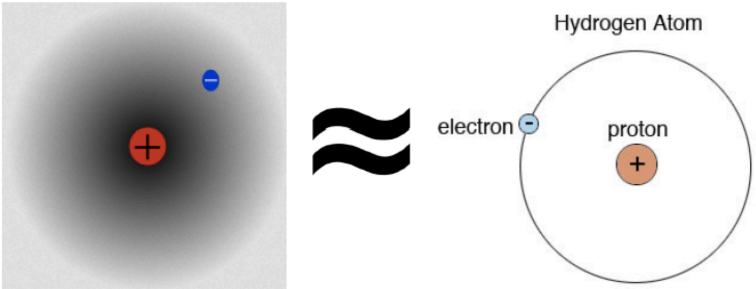

The proton is the lightest and simplest stable hadronic system.

proton structure

r_c & r_Z

- The **charge radius r_c = sqr(⟨r^2⟩)**

determined by **the charge distribution of the proton** is *one of the universal fundamental physical constants* extracted from:

  - **scattering** experiment & empirical fitting,
  - ***hydrogen*** Lamb shift measurements.
  - ***muonic hydrogen*** Lamb shift measurements

- **The magnetic radius r_Z** has been determined only by means of electron-proton ***scattering***, whose value is not free of controversies.

Electron Compton wave length and the Bohr radius

The **increase of the lepton mass** when we change the *electronic hydrogen to the muonic hydrogen* leads to the **decrease of the Bohr radius** in the μp. As a result the **electron Compton wave length** and the Bohr radius are of the same order

$$\frac{\hbar^2}{\mu c^2} \div \frac{\hbar}{m_e c} = 0.737384$$

m_e is the electron mass, μ is the reduced mass in the atom μp

The important consequence is the increased the role of the electron vacuum polarization effects in the energy spectrum of the μp

FAMU

INFN Istituto Nazionale di Fisica Nucleare

The muon is 200 time closer to the nucleus
Muonic hydrogen
is a good probe of the proton structure

E and M charge distribution $\rho_E(r)$, $\rho_M(r)$:

$$r_c=\left(\int \rho_E(r)\, r^2\, d^3r\right)^{1/2}$$

$$\Delta E_{LS} = 206.0669 - 5.2275\, r_{ch}^2$$

$$r_Z= \int\left(\int \rho_E(r')\, \rho_M(r-r')\, d^3r'\right) r\, d^3r$$

$$\Delta E^{HFS}_{1S} = 184.087 - 1.281\, r_Z$$

FAMU

INFN
Istituto Nazionale di Fisica Nucleare

For each lepton probe the **proton charge radius** can be extracted from two independent methods

The proton radius puzzle

The proton charge radius is measured from

- electron-proton interactions: 0.8770 ± 0.0045 fm
  - eH spectroscopy
  - $e - p$ scattering
- muon-proton interactions: 0.8409 ± 0.0004 fm
  - μH Lamb shift (2S-2P energy splittings) measurements at PSI (Switzerland)
    Pohl *et al.*, Nature (2010); Antognini *et al.*, Science (2013)

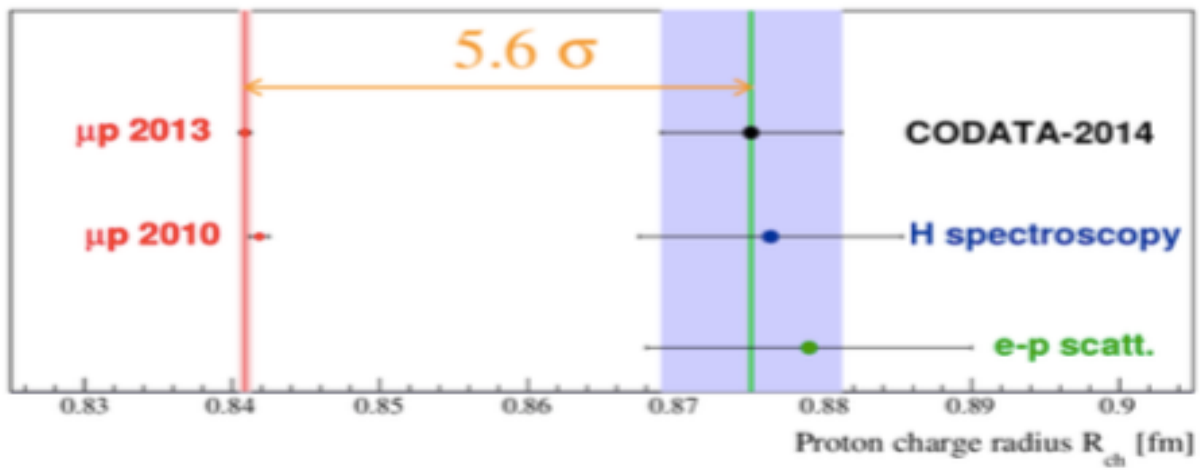

For each lepton probe the **proton charge radius** can be extracted from two independent methods

1. The first is through **lepton-proton scattering data**, where the radius is given by the slope of the electric form factor at $Q^2 = 0$:

$$\langle r_p^2 \rangle \equiv -6\hbar^2 \frac{dG_E(Q^2)}{dQ^2}\bigg|_{Q^2=0}$$

2. The second method measures the **Lamb shift in hydrogen** which is directly sensitive to the proton radius. **For electronic** measurements, these **two methods agree** and give a radius of **0.88 fm.**

- However, the **muonic hydrogen Lamb Shift** measurements yield a radius of **0.84 fm**.

FAMU

INFN Istituto Nazionale di Fisica Nucleare

PUZZLE! A recent summary of proton charge radius extractions

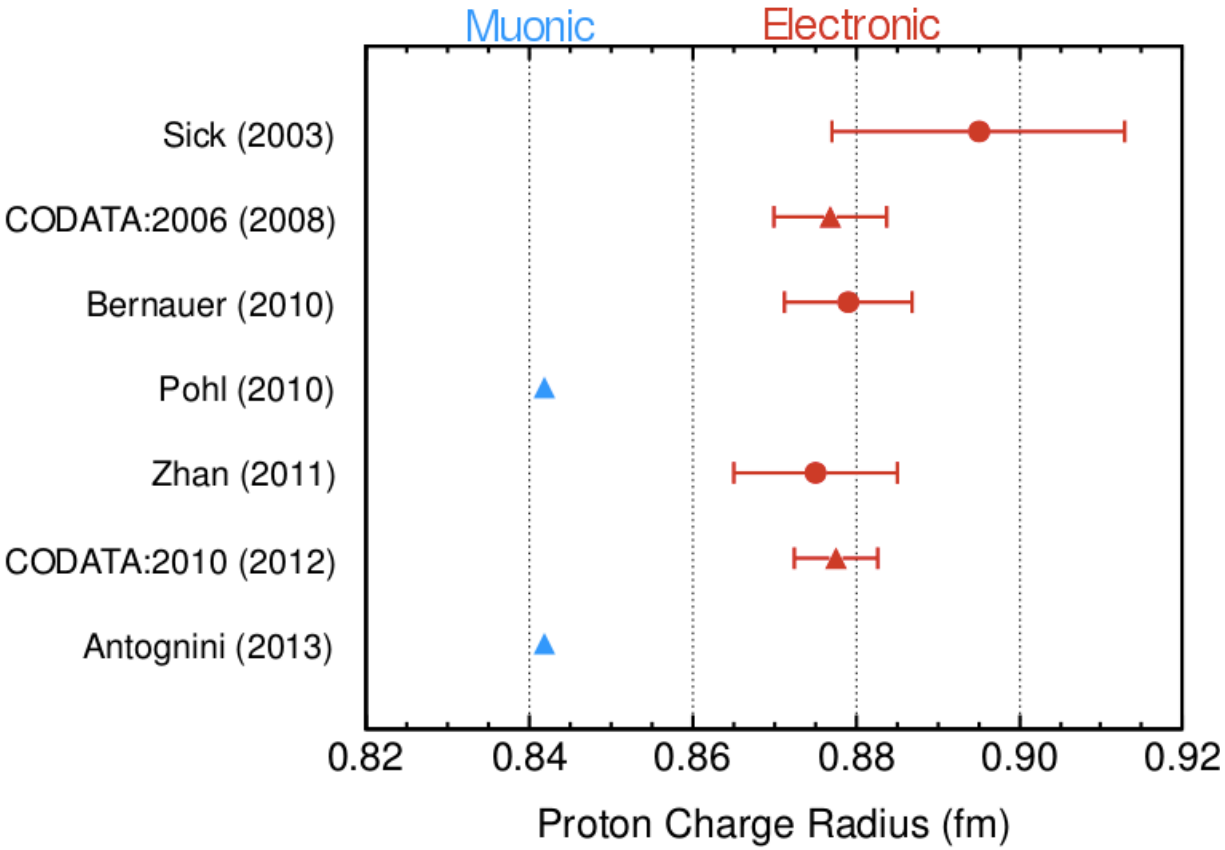

The CODATA value of the proton charge radius as obtained from a combination of 24 transition frequency measurements in H and deuterium and several results from elastic electron scattering is **0.88 fm .** However, the **muonic hydrogen Lamb Shift** measurements yield a radius of **0.84 fm**.

Proton radius from μp Lamb shift

Lamb Shift: 2S-2P splitting in atomic spectrum Pic: Pohl *et al.* Nature (201(

- **prompt X-ray ($t \sim 0$s):** μ^- stopped in H_2 gases

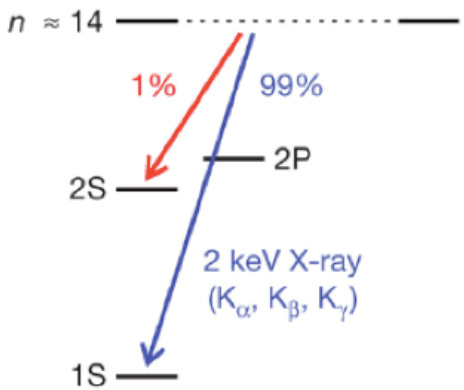

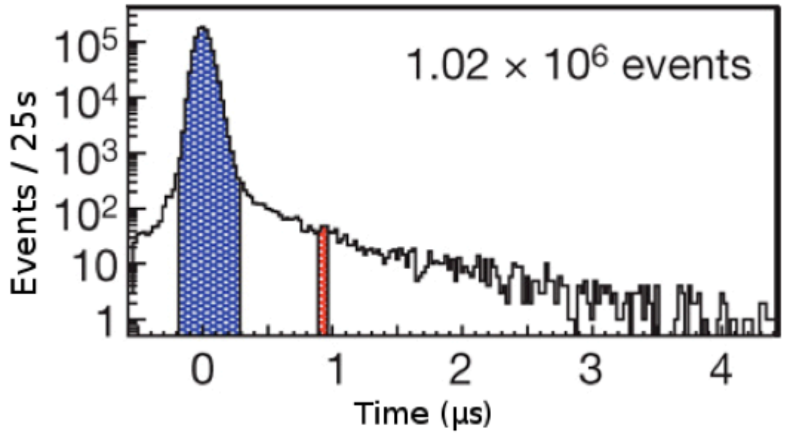

- **delayed X-ray ($t \sim 1\mu$s):** laser induced 2S→2P

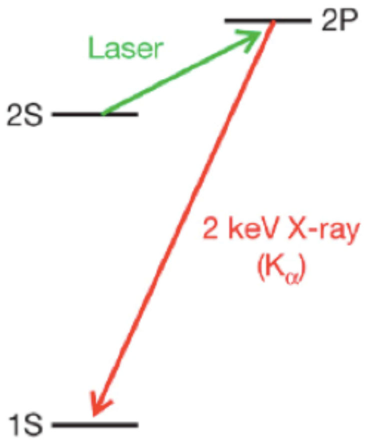

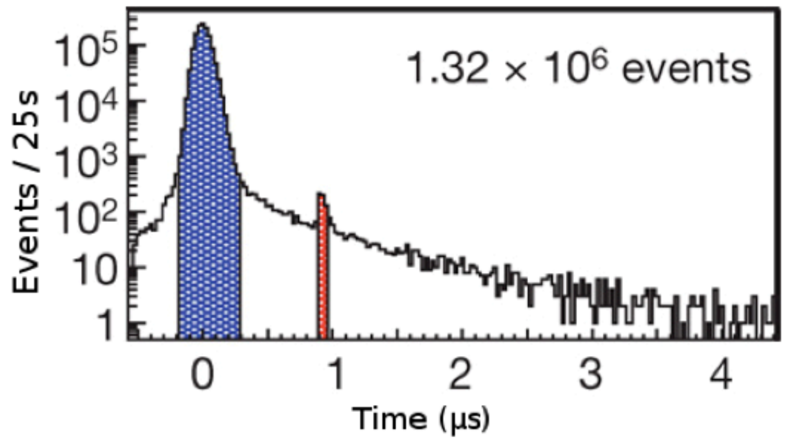

Proton radius from μp Lamb shift

Lamb Shift: 2S-2P splitting in atomic spectrum   Pic: Pohl *et al.* Nature (201(

- **prompt X-ray ($t \sim 0$s):** μ^- stopped in H_2 gases

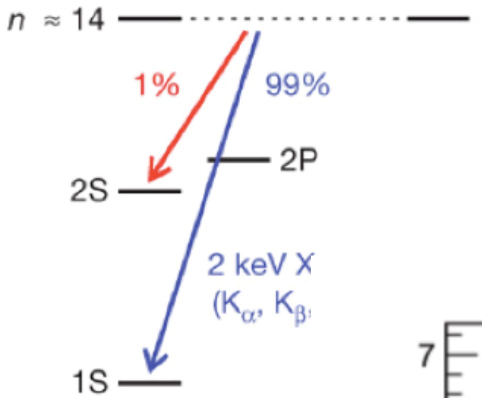

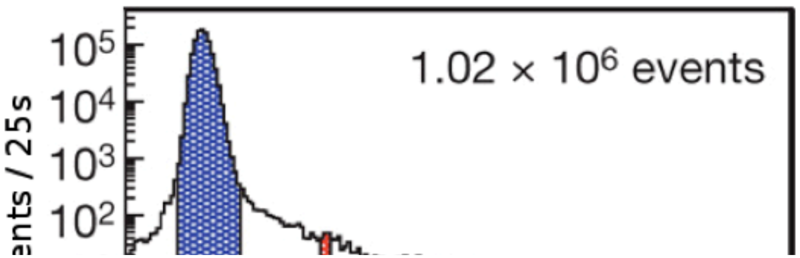

- **delayed X-ray (**

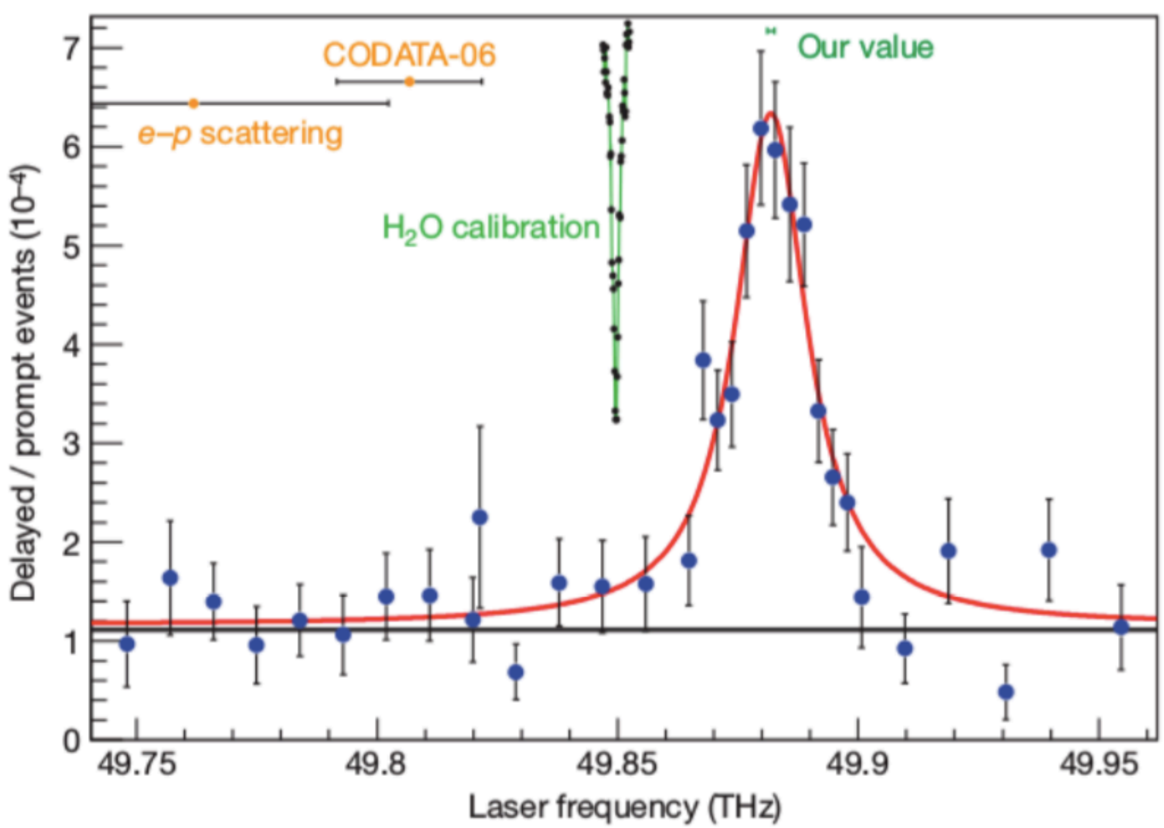

Proton radius from μp Lamb shift

Further measurement and analysis did not ease the discrepancy.

R. Pohl et al., Ann. Rev. Nucl. Part. Sci. 63 (2013)242001

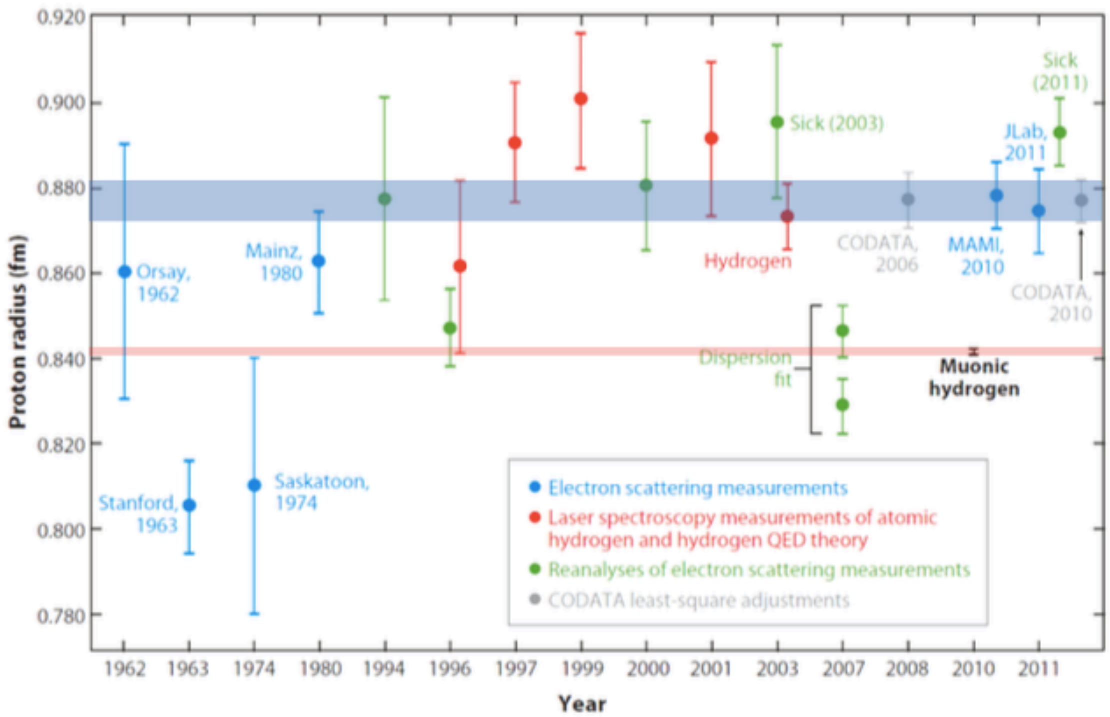

Errors in measurement?
Theoretical corrections wrong?
Broke lepton universality? new physics?

=> So far, no satisfactory explanation is given.

The Rydberg constant and proton size
from *atomic* hydrogen 2S-4P transition frequency

At the core of the "proton radius puzzle" is a five–standard deviation discrepancy between the proton root-mean-square charge radii (r_c) determined from the regular hydrogen (H) and the muonic hydrogen (μp) atoms.
Using a cryogenic beam of H atoms, we measured the 2S-4P transition frequency in H, yielding the values of the Rydberg constant R=10973731.568076(96) per meter and

r_p = 0.8335(95) femtometer.

this r_p value is 3.3 combined standard deviations smaller than the previous H world data, but in good agreement with the μp value.

FAMU

Beyer et al., Science 358, 79–85 (2017) 6 October 2017

INFN Istituto Nazionale di Fisica Nucleare

The Rydberg constant R links the natural energy scale of atomic systems and the SI unit system.

It connects the mass of the electron m_e, the fine structure constant α, Planck's constant h, and the speed of light in vacuum c.
Precision spectroscopy of H has been used to determine R by means of the following Eq. with a relative uncertainty of 6 parts in 10^{12}, making it one of the most precisely determined constants of nature to date and a cornerstone in the global adjustment of fundamental constants. The energy levels in H can be expressed as :

$$E_{nlj} = R_\infty \left(-{}^{1}\!/_{n^2} + f_{nlj}\left(\alpha, \frac{m_e}{m_p}, ...\right) + \delta_{l0} \frac{C_{NS}}{n^3} r_p^2\right)$$

$$R_\infty = {}^{m_e \alpha^2 c}\!/_{2h}$$

where n, l, and j are the principal, orbital, and total angular momentum quantum numbers, respectively. The first term describes the gross structure of H as a function of n and was first observed in the visible H spectrum and explained empirically by Rydberg.
Later, the Bohr model, in which the electron is orbiting a point like and, infinitely heavy proton, provided a deeper theoretical understanding.

The second term,

- $f_{nlj}(\alpha, me/mp, \ldots.) = X_{20}\alpha^2 . X_{30}\alpha^3 . X_{31}\alpha^3(\ln \alpha) . X_{40}\alpha^4 . \ldots,$

accounts for relativistic corrections, contributions coming from the interactions of the bound-state system with the quantum electrodynamics (QED) vacuum fields, and other corrections calculated in the framework of QED.

- The electron-to proton mass ratio me/mp enters the coefficients X20, X_{30}, … through recoil corrections caused by the finite proton mass.

The last term in with coefficient C_{NS} is the leading-order correction originating from the finite charge radius of the proton, rp. It only affects atomic S states (with l = 0) for which the electron's wave function is nonzero at the origin.

Higher-order nuclear charge distribution contributions are included in $f_{nlj}(\alpha; me/mp; \ldots.)$

Higher-order nuclear charge distribution contributions are included in $f_{nlj}(\alpha; me/mp ;.....)$

Considering the fact that $f_{nlj}(\alpha; me/mp ;.....)$ is known with sufficiently high accuracy, one finds a very strong correlation between $R\infty$ and r_p.

CODATA quotes a correlation coefficient of 0.9891.

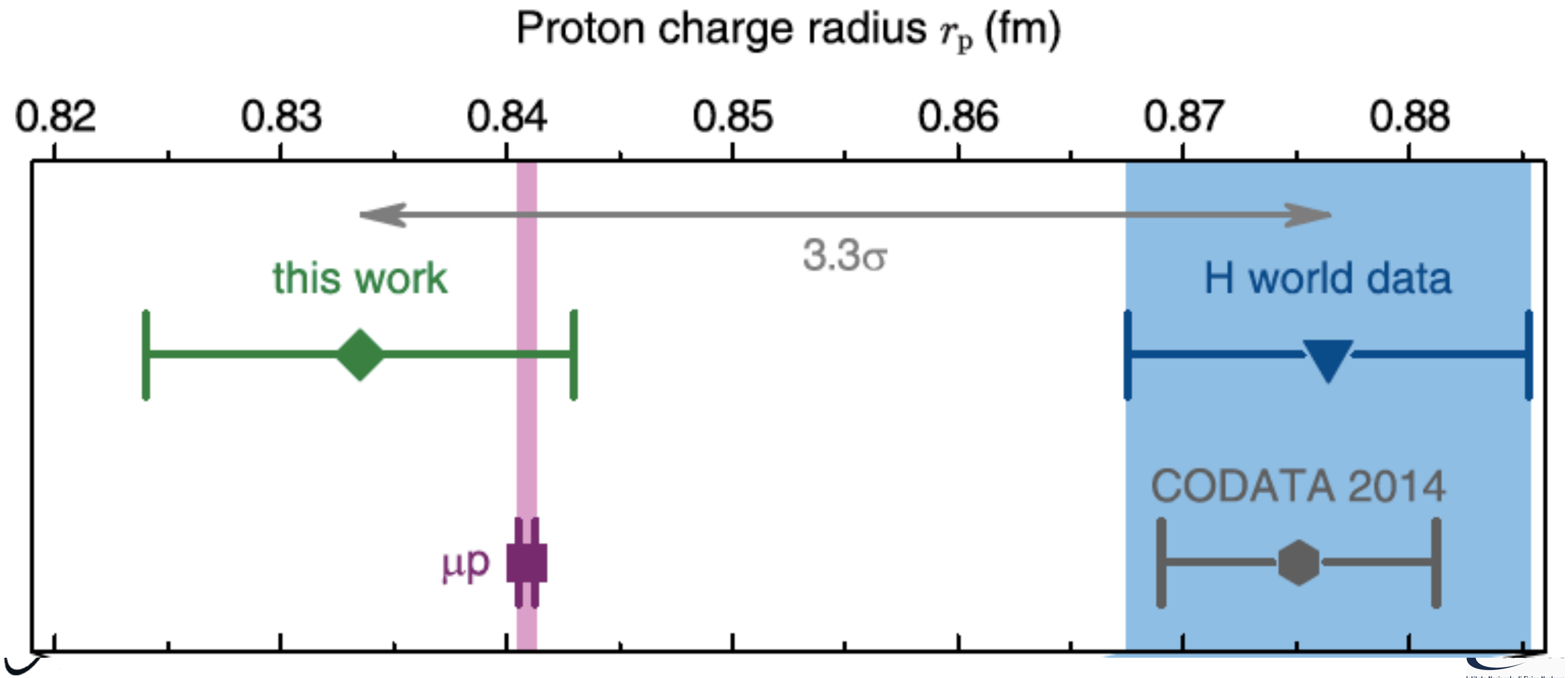

why measuring $\Delta E^{hfs}(\mu^- p)_{1S}$?

New independent high precision measurements on $\mu^- p$ are needed.

the hyperfine splitting of bound systems involving protons is the directly observable quantity which is most sensitive to the Zemach radius of the proton $\mathbf{r_Z}$.

The spectroscopic measurement of the hyperfine splitting (hfs) in the 1S state of muonic hydrogen $\Delta E^{hfs}(\mu^- p)_{1S}$, will :

- **provide the proton Zemach radius $\mathbf{r_Z}$** with high precision, disentangling discordant theoretical values
- **quantify any level of discrepancy** between values of r_Z as extracted from normal and muonic hydrogen atoms leading to new information **on proton structure and muon-nucleon interaction**.

The experimental value of r_Z sets important restrictions on the theoretical models of proton electromagnetic structure and, in particular, on the parametrization of proton form factors, in terms of which the theoretical values are calculated.

FAMU

INFN Istituto Nazionale di Fisica Nucleare

current status

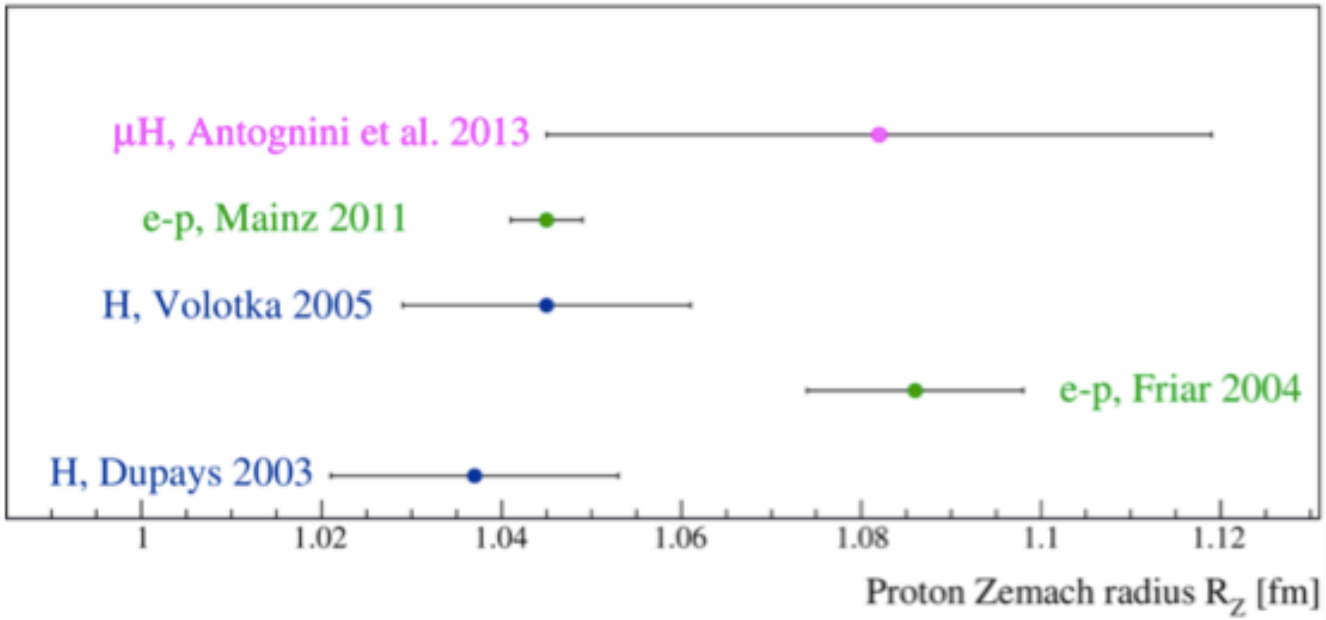

current status of $(\mu^- p)^{hfs}_{1S}$

units fm	rms charge radius r_{ch}	Zemach radius R_p
e^--p scattering & spectroscopy	r_{ch} = **0.8751(61)**	R_p=1.037(16) Dupays&*al*' 03 R_p=1.086(12) s Friar&Sick' 04 R_p=1.047(16) Volotka&*al*' 05 R_p=1.045(4) s Distler&*al*' 11
μ^--p Lamb shift spectroscopy	r_{ch}=0.84087(39)	a 20 years old idea: R_p from HFS of $(\mu^- p)_{1S}$ Either confirm a e^-p value or admit: e^-p and μ^-p differ

Recently : R_p = 1.082(37) [PSI'12] from HFS of $(\mu^- p)_{2S}$

=> we need new indipendent measurements

FAMU

INFN Istituto Nazionale di Fisica Nucleare

Muonic hydrogen Hyperfine splitting

$$\Delta E^{hfs}_{theor} = \Delta E^{F}.(1+\delta^{QED}+\delta^{str})$$

$$E^{F} = \frac{8}{3}\alpha^{4}\frac{m_{\mu}^{2}m_{p}^{2}}{(m_{\mu}+m_{p})^{3}}\mu_{p}$$

$$\hbar = c = 1$$

μ_p = magnetic moment of the proton

δE^{QED} = correction term related to higher order QED

δ^{str} = correction term related to proton electromagnetic interaction due to strong interaction

δ^{QED} => contribution of higher-order quantum-electrodynamical effects.
This correction is known with an accuracy 10^{-7}.
Note that the expression for δ^{QED} does not involve the mass ratio ml /mp ;
all terms which depend on proton mass or come from strong interactions are included in δ^{str}

Dupays et.al. PHYSICAL REVIEW A 68, 052503 - 2003

FAMU

INFN
Istituto Nazionale di Fisica Nucleare

Hyperfine structure of $\mu^- p(1s)$

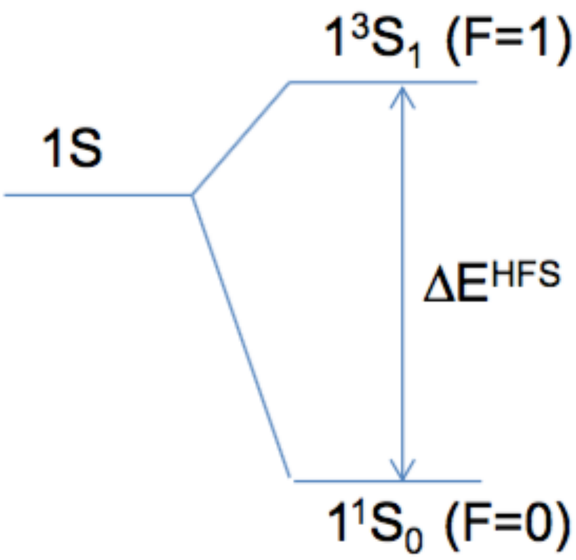

F : total angular momentum

- $\Delta E = \Delta E^F (1 + \delta^{QED} + \delta^{str})$
- $\delta^{QED} = a_e + \alpha^2 (\ln 2 - 1) + \ldots$
- $\delta^{str} = \delta^{rigid} + \delta^{pol} + \delta^{hvp} + \ldots$
- $\delta^{rigid} = \delta^{Zemach} + \delta^{recoil}$
- $\delta^{Zemach} = -2\, \alpha\, m\, R_p + O(\alpha^2)$

$R_p = \langle r \rangle_{E \circ M}$ (HFS)

$R_p^2 \neq r_{sq}^2$ (Lamb shift)

Muonic hydrogen Hyperfine splitting

$$\delta^{str} = \delta^{rigid} + \delta^{hvp} + \delta^{pol}$$

$$\Delta E^{hfs}_{theor} = \Delta E^{F} .(1 + \delta^{QED} + \delta^{rigid} + \delta^{hvp} + \delta^{pol})$$

In turn, $\boldsymbol{\delta}^{\mathbf{str}}$ splits into:

- a "static" part $\boldsymbol{\delta}^{\mathbf{rigid}}$ that accounts for the elastic electromagnetic form factors of the proton and can be calculated using data from elastic scattering experiments,
- a part $\boldsymbol{\delta}^{\mathbf{pol}}$ that comes from the internal dynamics of the proton and could only be evaluated using data on inelastic processes with protons,
- and a part $\boldsymbol{\delta}^{\mathbf{hvp}}$ describing the strong interaction effects outside the proton, such as hadron vacuum polarization:

FAMU

INFN
Istituto Nazionale di Fisica Nucleare

Muonic hydrogen Hyperfine splitting

Two types of "static" proton structure corrections are incorporated in δ^{rigid}, associated with the spatial distribution of the charge and magnetic moment within the proton and with recoil effects, respectively:

$$\delta^{rigid} = \delta^{Zemach} + \delta^{recoil}$$

$$\Delta E^{hfs}_{theor} = \Delta E^{F} . (1 + \delta^{QED} + \delta^{Zemach} + \delta^{recoil} + \delta^{hvp} + \delta^{pol})$$

δ^{recoil} denotes the contribution of all terms which depend on the ratio ml /mp

δ^{Zemach} has been calculated in the leading order approximation by Zemach

$$\delta^{Zemach} = \delta^{Zemach}_{(1)} + O(\alpha^2)$$

$$\delta^{Zemach}_{(1)} = 2\alpha \frac{m_{lp}}{\pi} \int \frac{d^3 p}{P^4} \left(\frac{1}{\mu_p} G_E(-P^2) \cdot G_M(-P^2) - 1 \right) = -2\alpha m_{lp} r_z$$

$$m_{lp} = \frac{m_l \cdot m_p}{m_l + m_p}$$

G_E(k) and G_M(k) are the charge and magnetic form factors of the proton, and

Rp is the first moment of the convolution of the proton charge and magnetic moment distributions, also known as Zemach radius of the proton.

R_p from Muonic hydrogen Hyperfine splitting

Two types of "static" proton structure corrections are incorporated in δ^{rigid}, associated with the spatial distribution of the charge and magnetic moment within the proton and with recoil effects, respectively:

$$\Delta E^{hfs}_{theor} = \Delta E^{F} . (1 + \delta^{QED} + \delta^{Zemach} + \delta^{recoil} + \delta^{hvp} + \delta^{pol})$$

$$\delta^{Zemach} = \delta^{Zemach}_{(1)} + O(\alpha^2)$$

$$\delta^{Zemach}_{(1)} = -2\alpha m_{lp} R_p$$

the explicit expression of the Zemach term becomes $\delta^{Zemach} = -xx \cdot 2\alpha m_{lp} R_p$.

were xx accounts also for the radiative corrections to $\delta^{Zemach}_{(1)}$

for hydrogen $\delta^{Zemach} = -1{,}0152 \cdot \alpha m_{lp} R_p$

Order of magnitude of the various terms

$$\Delta E^{hfs}_{theor} = \Delta E^{F} \cdot (1+\delta^{QED}+\delta^{Zemach}+\delta^{recoil}+\delta^{hvp}+\delta^{pol})$$

	Hydrogen		Muonic hydrogen	
	Magnitude	Uncertainty	Magnitude	Uncertainty
E^{F}	1418.84 MHz	0.01 ppm	182.443 meV	0.1 ppm
δ^{QED}	1.13×10^{-3}	$<0.001\times10^{-6}$	1.13×10^{-3}	10^{-6}
δ^{rigid}	39×10^{-6}	2×10^{-6}	7.5×10^{-3}	0.1×10^{-3}
δ^{recoil}	6×10^{-6}	10^{-8}	$1{,}7\times10^{-3}$	10^{-6}
δ^{pol}	1.4×10^{-6}	0.6×10^{-6}	0.46×10^{-3}	0.08×10^{-3}
δ^{hvp}	10^{-8}	10^{-9}	0.02×10^{-3}	0.002×10^{-3}

The overall uncertainty of ΔE_{th}^{hfs} is of the order of 2-3 ppm and is entirely due to proton structure effects.

Dupays et.al. PHYSICAL REVIEW A 68, 052503 - 2003

r_Z from Muonic hydrogen Hyperfine splitting

assuming that the theoretical values of **δ^{QED}, δ^{recoil}, δ^{hvp} and δ^{pol} are accurate** and use the experimental data to determine the Zemach radius of the proton Rp as:

$$r_z = -\left(\frac{\Delta E^{hfs}_{\exp}}{\Delta E^{F} - 1 - \delta^{QED} - \delta^{recoil} - \delta^{hvp} - \delta^{pol}} \right) \Big/ \left(1{,}0152 x 2 m_{ep} \alpha\right)$$

The above assumption is justifiable since all four correction terms are objects of QED, the only difference of δ^{hvp} and δ^{pol} from the former two being that their evaluation requires the use of additional phenomenological information beyond first principles.

From theory

$\Delta E_{theor}^{hfs}(\mu^- p)_{1S} = 182.725$ meV

- The total splitting of the 1*S* state is 182.725 meV; this value can be used as a reliable estimate in conducting a corresponding experiment with an accuracy of 30 ppm.

- Corrections of orders α^5 and α^6 to the hyperfine ground-state structure of the muonic hydrogen atom have been calculated. The calculations takes into account the effects of the structure of the nucleus on one and two loop Feynman amplitudes with the help of the electromagnetic form factors of the proton and the modification of the hyperfine part of the Breit potential caused by the electronic polarization of the vacuum.

Contribution to the HFS of the μp atom	Contribution, meV	Refs.
Fermi energy E^F	182.443	[18], (12)
Correction for the anomalous magnetic moment of the muon $a_\mu E^F$ of order α^5, α^6	0.213	[18]
Relativistic correction $(3/2)(Z\alpha)^2 E^F$ of order α^6	0.015	[43]
Relativistic and radiative corrections for recoil taking into account κ of the nucleus of order α^6	0.014	[30]
Contribution of one-loop electronic polarization of the vacuum to 1γ interaction of order α^5	0.398	(18)
Contribution of one-loop muonic polarization of the vacuum to 1γ interaction of order α^6	0.004	(19)
Second-order perturbation theory corrections determined by the polarization of the vacuum of orders α^5 and α^6	0.797	(30) + (33)
Correction for the structure of the nucleus of order α^5	–1.215	[22], (40)
Correction for the structure of the nucleus of order α^6	–0.014	[8]
Contribution of the electronic polarization of the vacuum + corrections for the structure of the nucleus of order α^6	–0.021	(43)
Contribution of the two-loop electronic polarization of the vacuum to 1γ interaction of order α^6	0.003	(21) + (24)
Correction for the intrinsic muon energy + corrections for the structure of the nucleus of order α^6	0.008	(50)
Vertex corrections + corrections for the structure of the nucleus of order α^6	–0.014	(61)
Jellyfish diagram correction + corrections for the structure of the nucleus of order α^6	0.004	(66)
Correction for the hadronic polarization of the vacuum of order α^6	0.004	(45)
Correction for the polarizability of the proton of order α^5	0.084	[16]
Contribution of weak interaction	0.002	[36]
Total correction	182.725 ± 0.062	

TABLE I: Corrections of orders α^5, α^6 to the ground state HFS in the muonic hydrogen.

Contribution to HFS of μp	Numerical value in meV	Reference
The Fermi energy E^F	182.443	[18], (12)
Muon AMM correction $a_\mu E^F$ of order α^5, α^6	0.213	[18]
Relativistic correction $\frac{3}{2}(Z\alpha)^2 E^F$ of order α^6	0.015	[43]
Relativistic and radiative recoil corrections with the account proton AMM of order α^6	0.014	[30]
One-loop electron vacuum polarization contribution of 1γ interaction of order α^5	0.374	(18)
One-loop muon vacuum polarization contribution of 1γ interaction of order α^6	002	(19)
Vacuum polarization corrections of orders α^5, α^6 in the second order of perturbative series	0.736	(30)+(33)
Proton structure corrections of order α^5	-1.215	[22], (40)
Proton structure corrections of order α^6	-0.014	[8]
Electron vacuum polarization contribution+ proton structure corrections of order α^6	-0.021	(43)
Two-loop electron vacuum polarization contribution of 1γ interaction of order α^6	0.003	(21)+(24)
Muon self energy + proton structure correction of order α^6	0.008	(50)
Vertex corrections + proton structure corrections of order α^6	-0.014	(61)
"Jellyfish" diagram correction + proton structure corrections of order α^6	0.004	(66)
HVP contribution of order α^6	0.004	(45)
Proton polarizability contribution of order α^5	0.084	[16]
Weak interaction contribution	0.002	[44]
Summary contribution	182.638 ± 0.062	

These estimates show that the current theoretical uncertainty of $\mathbf{r_Z}$ significantly exceeds the experimental one, and that the experimental results on the proton Zemach radius may be used as a test for the quality of models of the proton in the limit of low transfer momenta.

The hyperfine splitting is more sensitive to the proton structure than the Lamb shift

- The **main nuclear structure dependent contribution** (so-called 'Zemach correction') is of the form

$$\Delta\nu(Zemach) = \nu_F \frac{2Z\alpha m_e}{\pi^2} \int \frac{d^3\mathbf{q}}{\mathbf{q}^4} \left[\frac{G_E(-\mathbf{q}^2) G_M(-\mathbf{q}^2)}{1+\kappa} - 1 \right]$$

- the comparison of theory and experiment leads *for the hydrogen* hyperfine splitting to

$$\frac{\nu_{hfs}(exp) - \nu_{hfs}(theo)}{\nu_{hfs}(exp)} = \Big(0.48 \pm 0.56\Big)\, ppm.$$

- Proton polarizability is not included in ν_{hfs}(theo) and the difference above has to be interpreted as its contribution.

FAMU

INFN Istituto Nazionale di Fisica Nucleare

Comparing the theoretical prediction with the experiment, deduce $\mathbf{r_Z}$ with a relative accuracy better than 5×10^{-3}

limited by the relative accuracy on the polarizability contribution.

The theoretical prediction for the 1S-hfs in μp can be written approximately:

$$\mathbf{\Delta E^{hfs}_{th}(\mu^- p)_{1S}} = 182.819(1)[\mathrm{meV}] - 1.30[\mathrm{meV/fm}]\ \mathbf{r_Z} + 0.064(21)\ [\mathrm{meV}]$$

- where the first term includes the Fermi energy, QED corrections, hadronic vacuum polarization, recoil corrections and weak interactions,
- the second term, proportional to $\mathbf{r_Z}$, is the finite size contribution containing also some higher order mixed radiative finite size corrections,
- and the third term is given by the proton polarizability contribution.

FAMU

INFN Istituto Nazionale di Fisica Nucleare

D_{21} from ($\mu^- p$) hfs

Determination of the proton Zemach r_Z radius is essential for:

1. understanding ***the proton charge and magnetic structure***
2. Testing bound-state QED by measuring

$$D_{21} = \Delta E^{1S}_{HFS} - 8 \times \Delta E^{2S}_{HFS}$$

The difference is weakly affected by the effects of the nuclear structure and thus may be calculated with a high accuracy. The leading nuclear structure contributions are determined by two photon exchanges with a high momentum transfer and have the hard structure and, therefore, cancel when calculating difference.

The current status of the determination of corrections to the hyperfine splitting of the ground state in hydrogen

- Improved calculations are provided taking into account the most recent value for the proton charge radius. Comparing experimental data with predictions for the hyperfine splitting, the

  Zemach radius of the proton is deduced to be 1.045(16) fm.
- Employing exponential parametrizations for the electromagnetic form factors we determine

  the magnetic radius of the proton to be 0.778(29) fm.
- Both values are compared with the corresponding ones derived from the data obtained in electron-proton scattering experiments and the data extracted from a rescaled difference between the hyperfine splittings in hydrogen and muonium.

The FAMU experiment goals

Currently 3 independent experiments plan to measure RZ

- Measure the Hyperfine Splitting (HFS) of $\mu^- p$ with accuracy 10^{-5}
- Extract the Zemach radius of the proton with an accuracy of better than 1%

Hyperfine Splitting (HFS) of $\mu^- p$ with accuracy 10^{-5}
Zemach radius of the proton with an accuracy of better than 1%

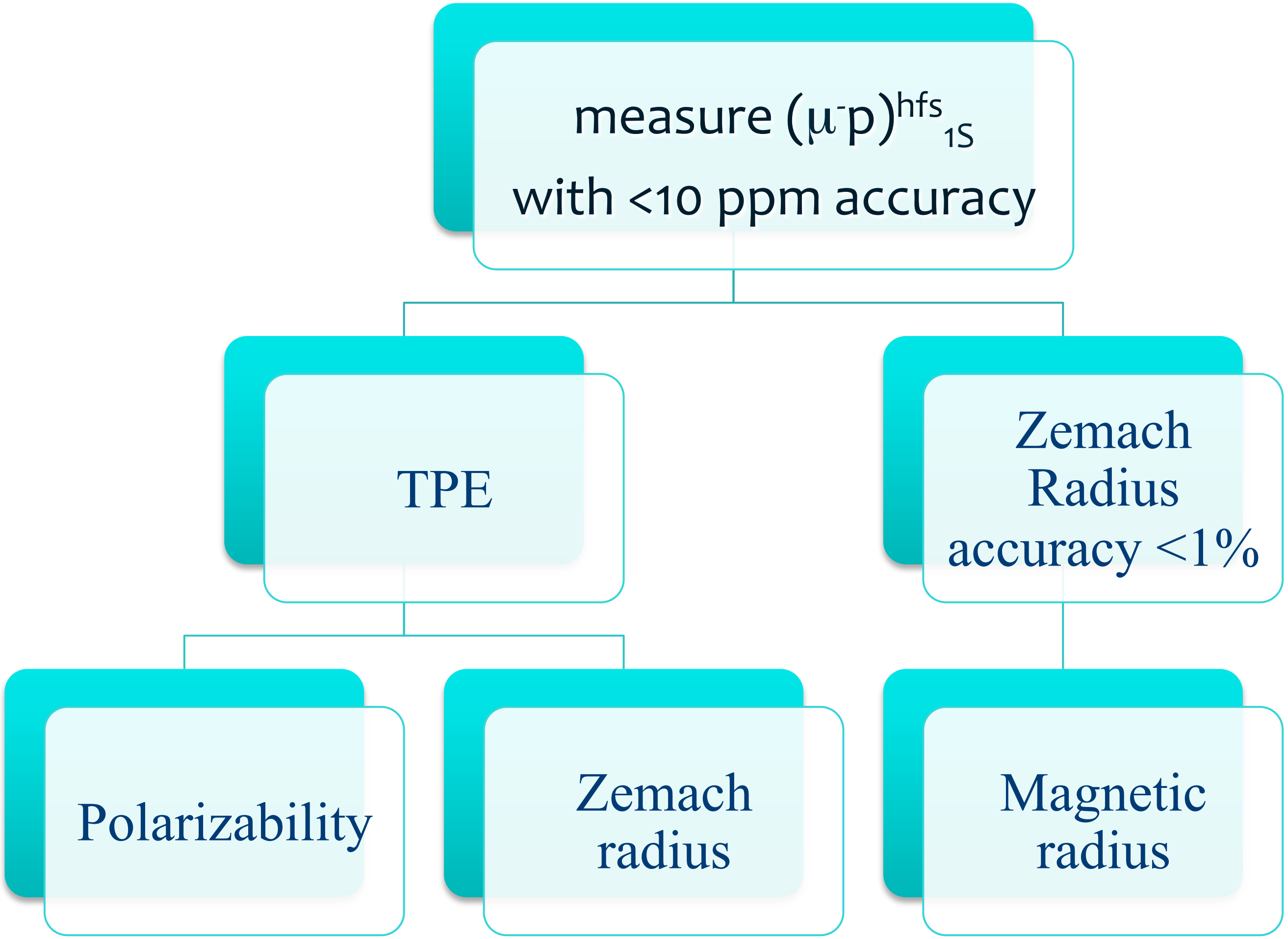

Impact

- In the measurement of $\mathbf{\Delta E^{hfs}}$ **in** $(\mu p)_{1s}$ **,** the proton structure corrections δ^{str} scale approximately as ($m\mu$ /me), are enhanced (compared to hydrogen) by a factor of 2 10^{2}, QED effects are overshadowed by the proton structure corrections.

- *In both hydrogen and muonic hydrogen*, the proton structure corrections δ^{str} is dominated by two independent terms: **the Zemach term** δ^{rigid} **and the polarizability term** δ^{pol} .
  - while the Zemach term is directly related to the Zemach radius of the proton r_Z, a well defined physical parameter,
  - δ^{pol} is expressed in terms of the form factors and polarized structure functions of the proton in an indirect and case-dependent way and is not associated with a single parameter.
- the measurements of ΔE^{hfs} in hydrogen and muonic hydrogen atoms may be regarded as repeated experimental determination of the Zemach radius of the proton.

Impact

- The repeated measurements of Rp in hydrogen and muonic hydrogen are the best way to verify the theoretical evaluation:
  - compatible values of Rp extracted from the hyperfine splitting in hydrogen and muonic hydrogen will confirm the reliability of the theoretical values of δ^{pol} and vice versa.
- The accuracy of Rp depends on the uncertainty of δ^{pol} ;
  - a measurement of the hyperfine splitting of the ground state of muonic hydrogen based on the available theoretical predictions would give the value of Rp accurate to 1%.
  - such an accuracy would allow to filter the numerous theoretical estimates of Rp and detect a deviation of GE /GM from 1 by distinguishing the values of Rp obtained with and without account of the JLab experimental results.
- It would be preferable for this purpose to have the value of Rp accurate to 0.5% or better, that requires in turn that the theoretical uncertainty of δ^{pol} be brought below $3\ 10^{-5}$ and that the experimental error of ΔE_{exp}^{hfs} not exceed 30 ppm.

Impact

- The proton structure correction δ^{str} in muonic hydrogen is enhanced (compared to hydrogen) by a factor of 2 10^2. Therefore, a measurement of ΔE^{hfs} in $(\mu p)_{1s}$ can not be a good test of QED since QED effects are overshadowed by the proton structure corrections.
- Further on, in both hydrogen and muonic hydrogen, the proton structure corrections δ^{str} is dominated by two independent terms: the Zemach term δ^{rigid} and the polarizability term δ^{pol} .
  - while the Zemach term is directly related to a well defined physical parameter, the Zemach radius of the proton Rp,
  - δ^{pol} is expressed in terms of the form factors and polarized structure functions of the proton in an indirect and case-dependent way and is not associated with a single parameter.
- Compared to hydrogen, both these terms scale approximately as ($m\mu$ /me). This all brings us to the conclusion that the measurements of ΔE^{hfs} in hydrogen and muonic hydrogen atoms are not complementary in a sense which would let us extract the values of two universal parameters of the proton, characterizing its charge and magnetic distribution and polarizability.
- These measurements may be regarded as repeated experimental determination of the Zemach radius of the proton.

Impact

- These measurements may be regarded as repeated experimental determination of the Zemach radius of the proton. The repeated measurements of Rp in hydrogen and muonic hydrogen are the best way to verify the theoretical evaluation:
  - compatible values of Rp extracted from the hyperfine splitting in hydrogen and muonic hydrogen will confirm the reliability of the theoretical values of δ^{pol} and vice versa.
- The accuracy of Rp depends on the uncertainty of δ^{pol} ; a measurement of the hyperfine splitting of the ground state of muonic hydrogen based on the available theoretical predictions would give the value of Rp accurate to 1%.
- As already mentioned, such an accuracy would fairly allow to filter the numerous theoretical estimates of Rp and detect a deviation of GE /GM from 1 by distinguishing the values of Rp obtained with and without account of the JLab experimental results.
- It would be preferable for this purpose to have the value of Rp accurate to 0.5% or better, that requires in turn that the theoretical uncertainty of δ^{pol} be brought below $3\ 10^{-5}$ and that the experimental error of ΔE_{exp}^{hfs} not exceed 30 ppm.

OUTLINE

- FAMU background & motivations
- The method to measure the hfs
- laser
- beam
- target
- detectors
- muon transfer rate measurements
- conclusions

a 25 years old idea

Physics Letters A 172 (1993) 277–280
North-Holland

PHYSICS LETTERS A

Experimental method to measure the hyperfine splitting of muonic hydrogen $(\mu^- p)_{1S}$

D. Bakalov [1], E. Milotti, C. Rizzo, A. Vacchi and E. Zavattini

Dipartimento di Fisica dell'Università di Trieste, via Valerio 2, Trieste 34017, Italy
and Sezione INFN di Trieste, Area di Ricerca, Padriciano 99, Trieste 34012, Italy

Received 31 July 1992; revised manuscript received 17 October 1992; accepted for publication 8 November 1992
Communicated by B. Fricke

We propose an experimental method to measure the hyperfine splitting of the energy level of the muonic hydrogen ground state $(\mu^- p)_{1S}$ by inducing a laser-stimulated para-to-ortho transition. The method requires an intense low energy pulsed μ^- beam and a high power tunable pulsed laser.

1. Introduction

The theoretical expression for the hyperfine splitting

FAMU

INFN
Istituto Nazionale di Fisica Nucleare

Exploit the ***energy dependence of the muon transfer*** from muonic hydrogen to higher-Z gas is to detect the spin flip transition in μp.

- For few gases the muon-transfer rate λ_{pZ} is energy independent ***Oxygen exhibits a peak in the muon transfer rate λ_{pZ}^{epith} at the epithermal energy.***
- Adding small quantities of oxygen to hydrogen one can observe the number of HPF transitions which take place from the muon-transfer events this by measuring the time distribution of the oxygen characteristic X-rays of the added gas.

$$\mu p + Z \Rightarrow \mu Z^{**} + p$$

A. Werthmüller et al. / Muon transfer to oxygen 3

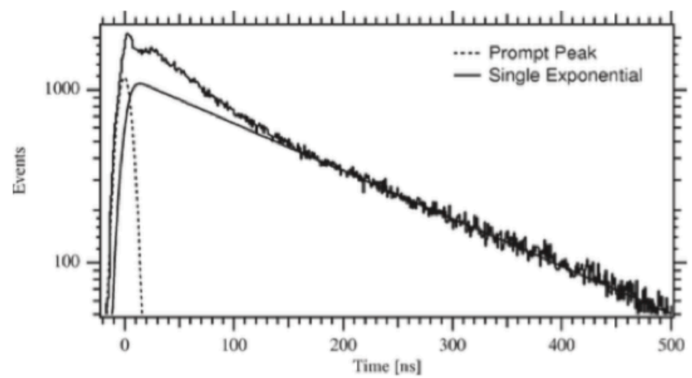

Figure 2. Background subtracted time distribution of muonic oxygen $\mu O(2\text{–}1)$ X-rays measured in a gaseous mixture of $H_2 + 0.4\% O_2$ at 15 bar and room temperature. The prompt peak corresponds essentially to muons directly captured in oxygen whereas the delayed part is due to muon transfer from the ground state of the $(\mu p)_{1s}$ atom. The solid line represents a pure exponential function to stress the additional structure.

D. Bakalov, A. Adamczak et al., Phys. Lett. A379 (2014).
A. Adamczak et al. Hyperfine Interactions 136: 1–7, 2001.
F. Mulhauser, H. Schneuwly, Hyperfine Interact. 82 (1993).
A. Werthmüller, et al., Hyperfine Interact. 116 (1998).

FAMU

Laser spectroscopy for ΔE^{HFS}_{1S}

HOW ?

Method relying on a two-steps process

excited μp* with n >14

are formed in a hydrogen gas target,
in subsequent collisions with H2 molecules,
the μp de-excite to the

$\mu^{-}p(\uparrow\downarrow)$

thermalized μp in the (1S) F =0 state.

first step
Tunable laser shot

$\mu^{-}p(\uparrow\downarrow)$ absorbs a photon @ ***resonance wavelength***

$\lambda_0 = hc/\Delta E^{1S}_{HFS}$ ~ 6.8 μ ~ 0.183 eV

Converts the spin state of the ($^{-}\mu p$) atoms from $^{1}S_{0}$ to $^{3}S_{1}$

$\mu^{-}p(\uparrow\downarrow) \rightarrow \mu^{-}p(\uparrow\uparrow)$

FAMU

INFN Istituto Nazionale di Fisica Nucleare

second-step
energy dependent μ transfer

2. $\mu^{-}p(\uparrow\uparrow)$ $^{3}S_{1}$ atoms are collisionally de-excited and the transition energy is converted into additional kinetic energy of the μp system

$\mu^{-}p(\uparrow\downarrow)$ $^{1}S_{0}$ and accelerated by ~ 0.12 eV ~ 2/3 ΔE^{HFS}_{1S}

Energy-dependent muon transfer rates change the time distribution of the cascade X-ray events from $\mu^{-}Z^{**}$

λ_{0} is recognized by maximal response in the time distribution

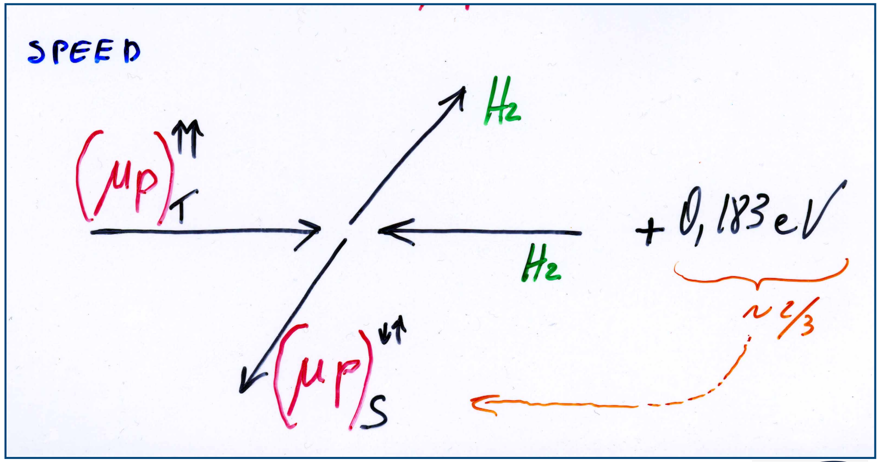

D. Bakalov, et al., Phys. Lett. A172 (1993).
A. Dupays, **Phys. Rev. A 68**, p. 052503, 2003.
D. Bakalov, et al., NIM B281 (2012).

FAMU

INFN
Istituto Nazionale di Fisica Nucleare

FAMU Principle of operation

μp formation =>>

μp termalization =>>

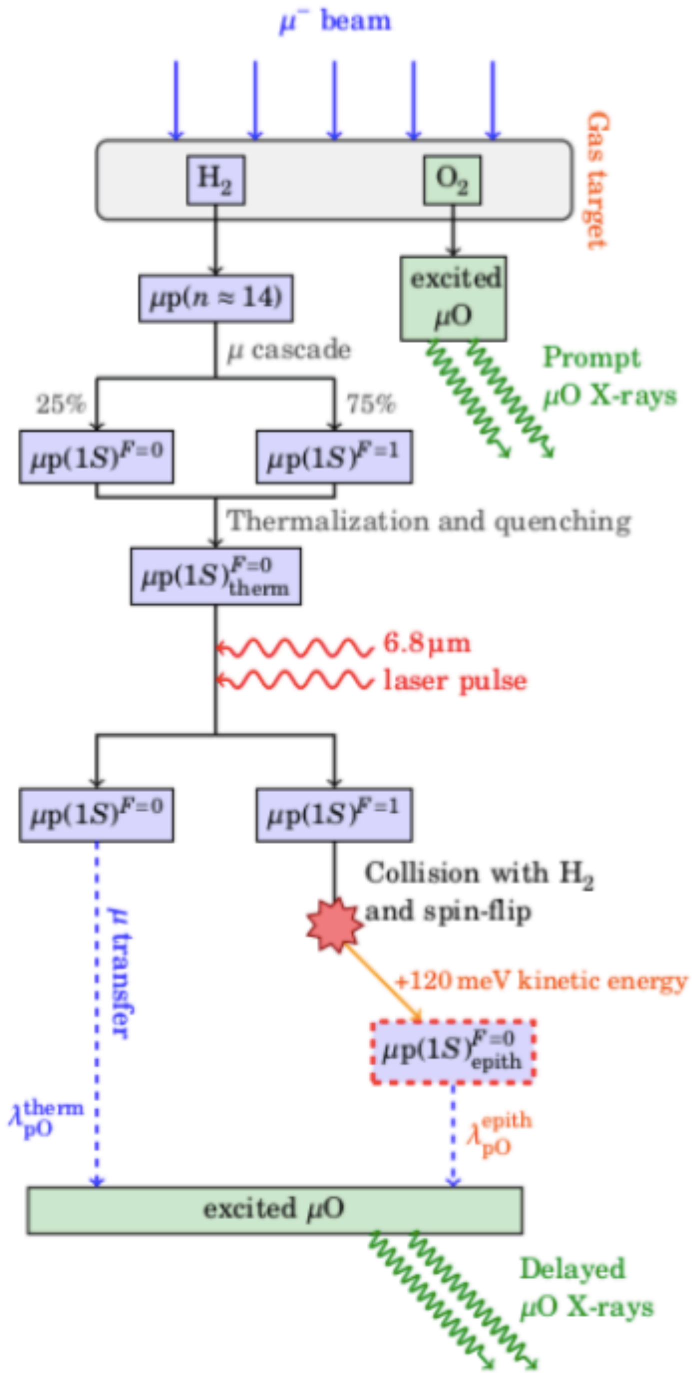

Lay-Out of the experiment

laser exitation F=0 F=1 =>>

μ enhanced transfer to O =>>

μO X-ray time distribution =>

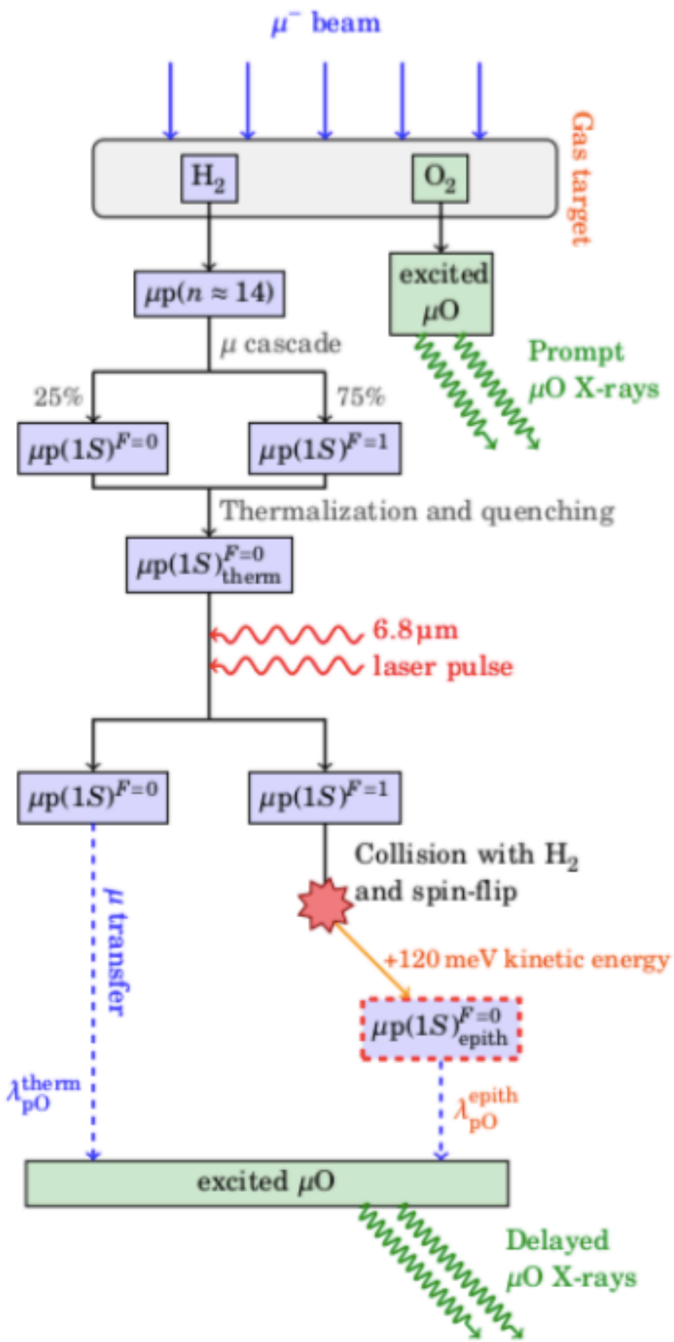

FAMU

INFN
Istituto Nazionale di Fisica Nucleare

Lay-Out of the experiment

laser exitatio

λ_0 resonance is determined by the maximizing the time distribution of μ^- transferred events.

μ enhanced transfer to O =>>

μO X-ray time distribution =>

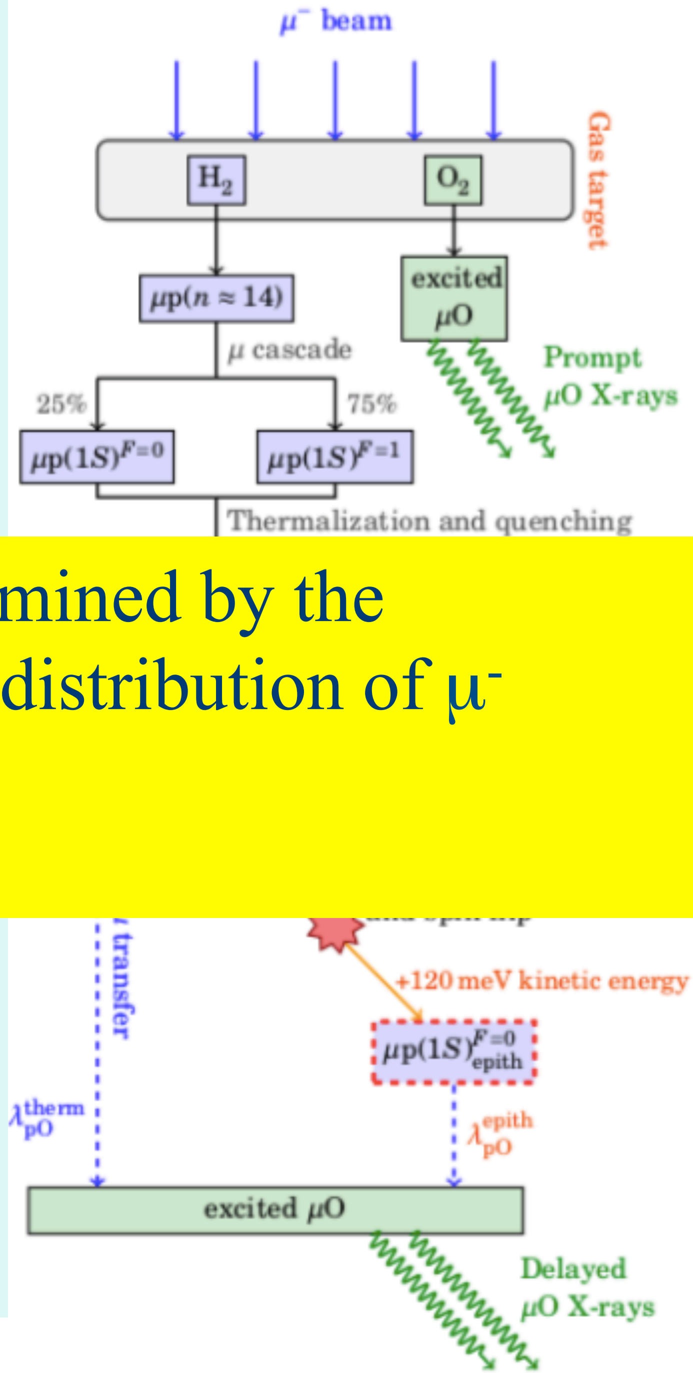

Study of best setup to maximize signal

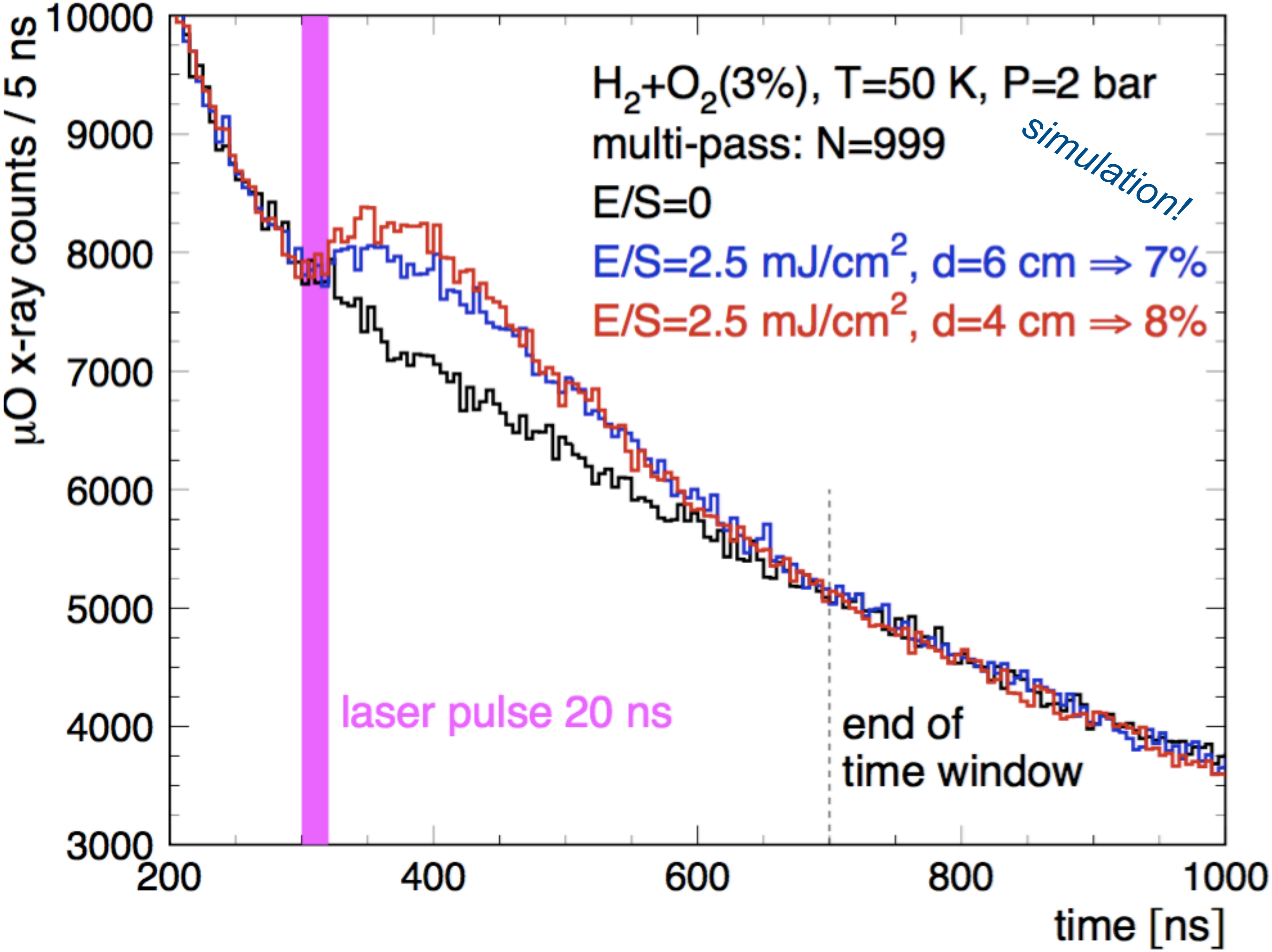

OUTLINE

- FAMU background & motivations
- The method to measure the hfs
- laser
- beam
- target
- detectors
- muon transfer rate measurements
- conclusions

FAMU: key ingredients

- innovative high energy MIR fine-tunable laser
- pulsed high intensity muon beam
- proper target & gas mixture
- best X-rays detectors (fast and accurate)

FAMU key elements high energy MIR laser

Tunable pulsed IR laser at λ=6.8μ

Direct difference frequency generation
in non-oxide non linear crystals using
single-mode Nd:YAG laser and tunable Cr:forsterite laser

Wavelength:	λ =6785 nm	44.22 THz
Line width:	$\Delta\lambda$ = 0.07 nm	450 MHz
Tunability range:	6785 +- 10 nm	130 GHz
Tunability step	= 0.007nm	45 MHz
Repetition rate:	25 Hz	

(L.Stoychev, EOSAM '14)

Proc. of SPIE Vol. 9135, 91350J · © 2014 SPIE · CCC code: 0277-786X/14

The Nd:YAG will be at "fixed" wavelength 1064.14nm with linewidth max - 0.34pm (90MHz) and min - 0.11pm (30MHz).

The Cr:forsterite will have linewidth max - 1pm (188MHz) and min - 0.5pm (90MHz).

The Cr:forsterite will be tunable from 1252nm to 1272 nm which corresponds to tunability from 6500nm to 7090nm, which is 3765GHz. The required tunability 6760nm ±3nm corresponds to tunability range ~ 39GHz.

Final scheme of the DFG based laser system for the FAMU experiment

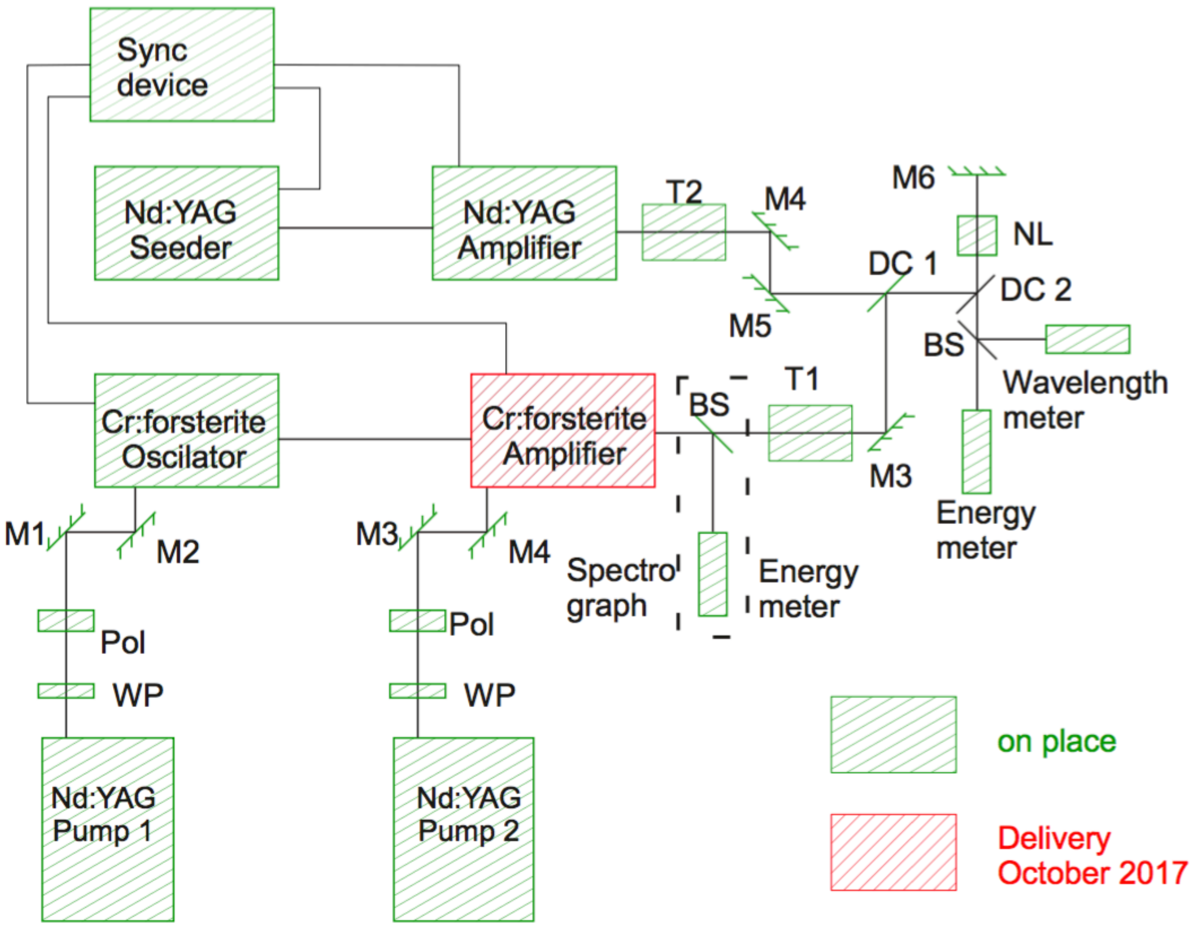

WP - waveplate, Po - polarizer, M1-M5 - mirrors, T1 and T2 - telescopes, BS - beamsplitters, DC1 - dichroic mirror (reflecting 1.26μm, transmitting1.06μm), DC2 - dichroic mirror (reflecting 1.06 and 1.26 μm, transmitting 6.76μm)

A possible solution to further increase the energy

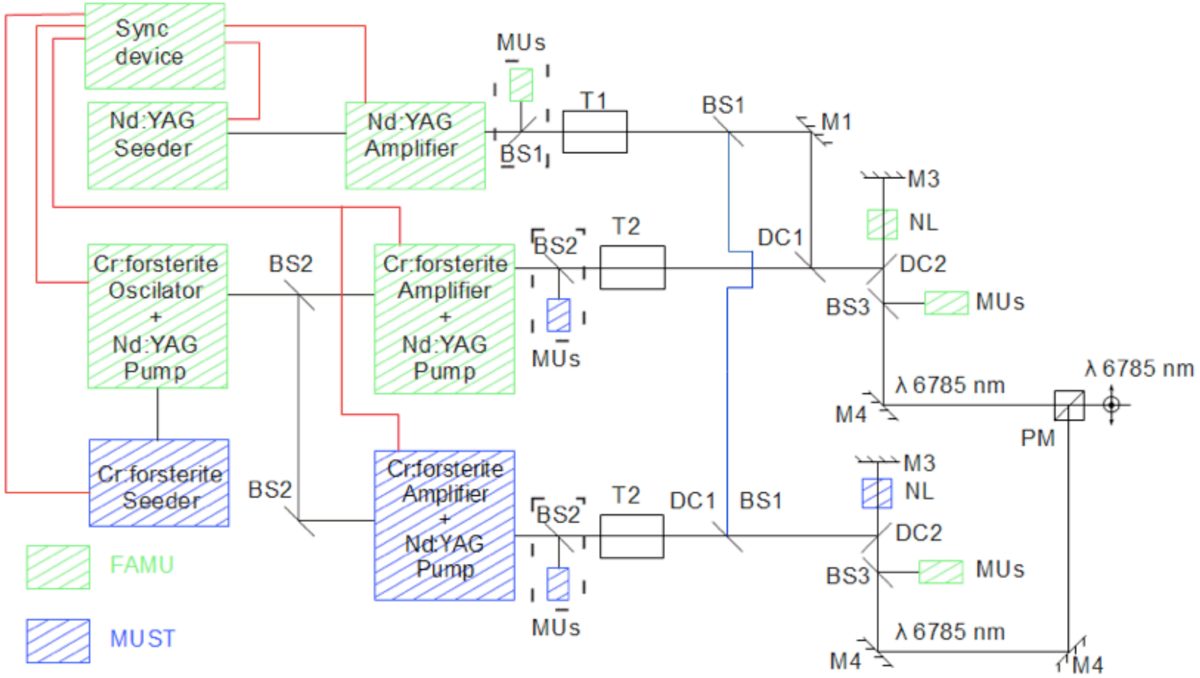

M1 – mirror HR 1064 nm, M2 – mirror HR 1262 nm, M3 – mirrors HR 1064&1262&6785 nm, M1 – mirror HR 6785 nm, T1 and T2 - telescopes, BS1 – beamsplitters/beamsampler 1064 nm, BS – beamsplitters/beamsampler 1262 nm, BS1 – beamsampler 6785 nm, DC1 - dichroic mirror (reflecting 1.26μm, transmitting1.06μm), DC2 - dichroic mirror (reflecting 1.06 and 1.26 μm, transmitting 6.76μm), MUs – measuring units: λ meters, energy meters, PM – polarization mixer

Fig. 2 The must (final) laser system evolution, in dashed blue the parts which will contribute to the final high energy system allowing the high precision measurements.

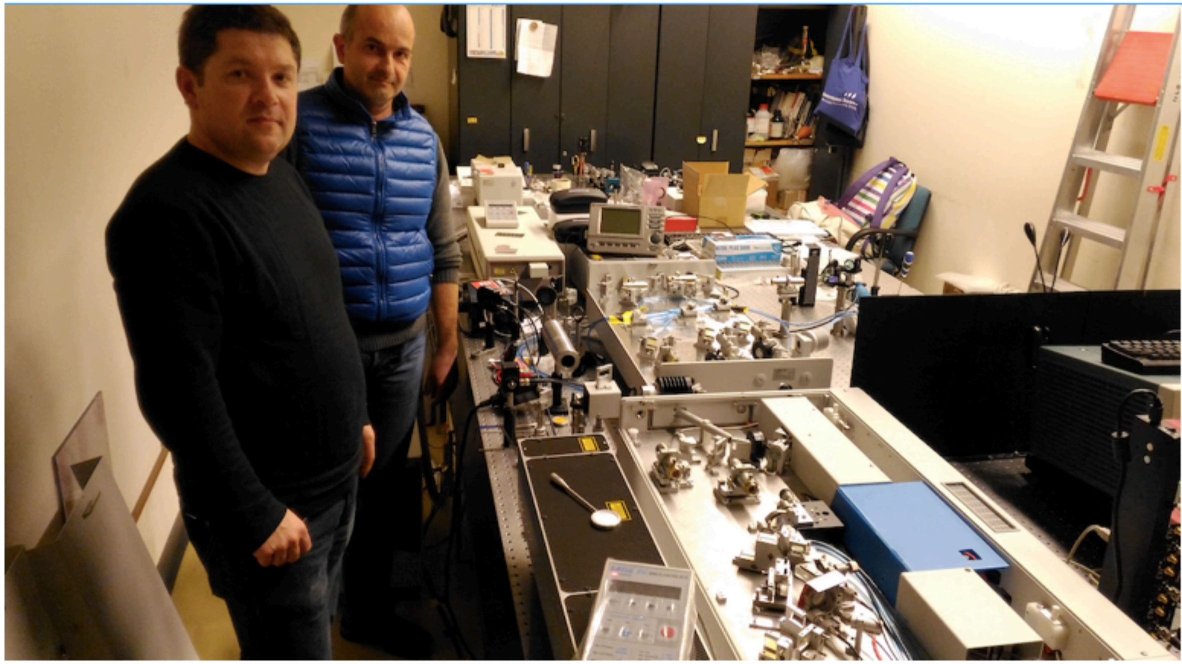

Fig. 3 Dr. Stoychev and the specialist of LOTIS working on the Cromium Forsterite laser, such a device has never been realized with the quality and energy needed for the FAMU experiment

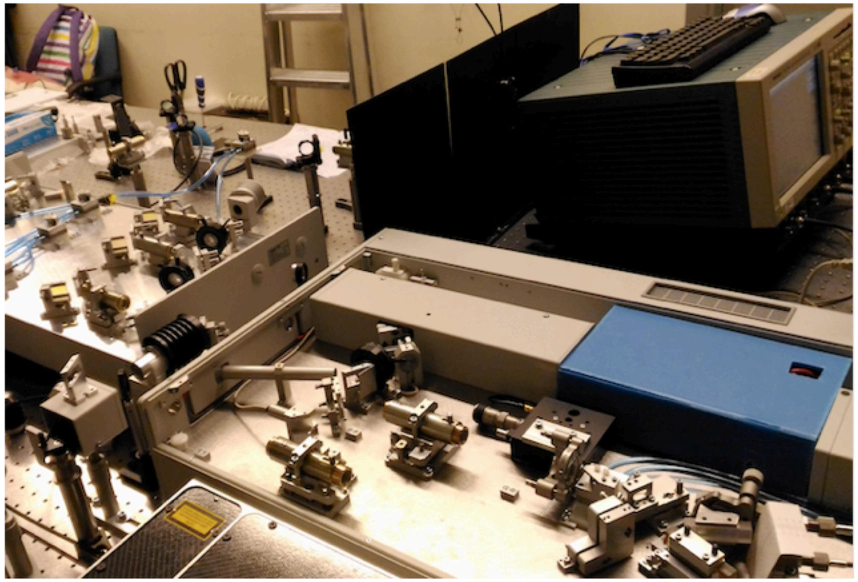

two sections are visible left the amplifier right the oscillator

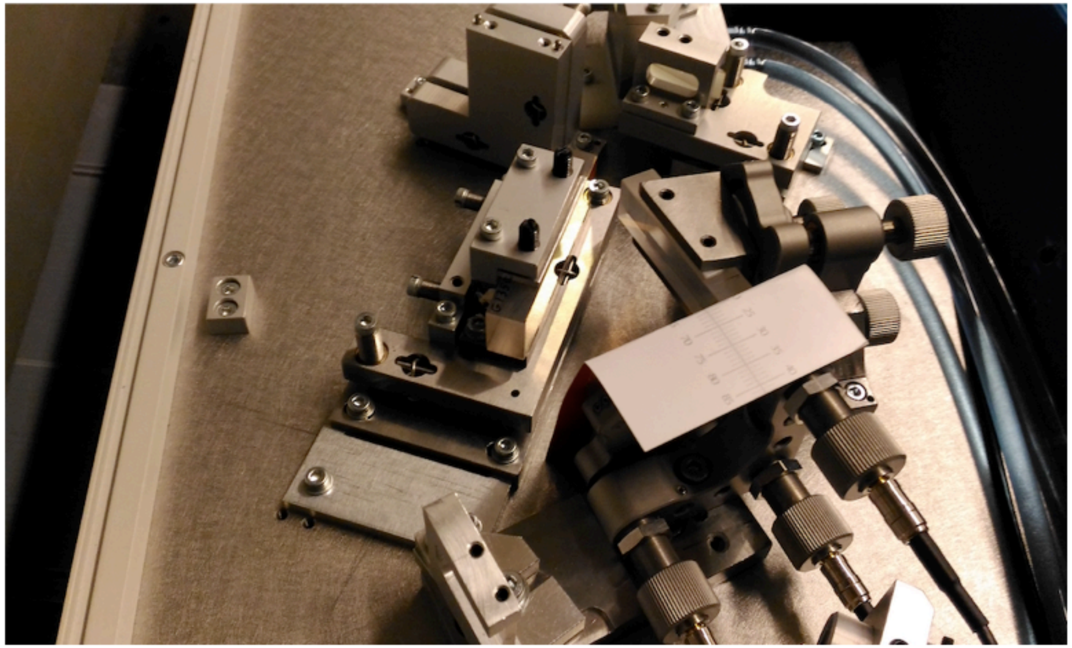

Fig. 5 a detail of the oscillator

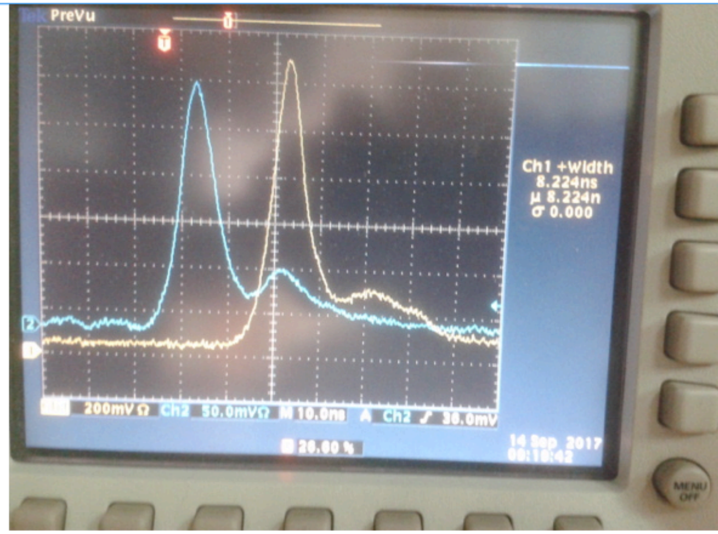

Fig.7 An oscillogram of the pulses of generation of the Cr:forsterite oscillator (blue) and amplifier (yellow).

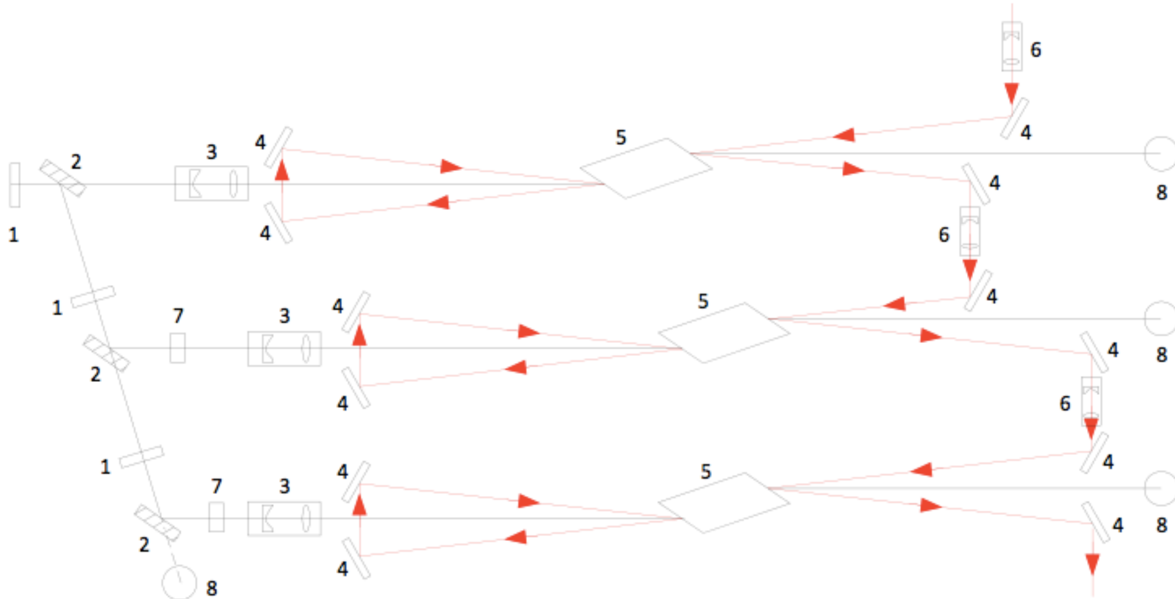

Fig. 6 Amplifying module: 1 – half-wave plates (λ/2, λ = 1064 nm); 2 – polarizers (λ = 1064 nm); 3 – decreasing telescopes (λ = 1064 nm); 4 – turning mirrors (λ = 1262 nm); 5 – Cr:Forsterite crystals; 6 – increasing telescopes (λ = 1262 nm); 7 - rotators (90°, λ = 1064 nm); 8 – beam stops

Expected output energies at 6760 - 6780 nm

E ~ 1 – 1.5 mJ

Available crystals at the moment

7x7x20 - ~ 2mJ < ~ 2 times compared to 4,6mJ

8x8x18 - ~ 2,2mJ (10x10x20 crystal)

Increasing the E_{output}:

- two crystals in parallel
- pump lasers with longer pulse duration (implementing beams with higher power densities)
- optimazing the pozition of the rear mirror/s and using mirrors with higher reflectivity
- Top-Hat beam profiling of pump beams

Cavity reflectivity

(R = 99.97% or better)
can be achieved with a ThF_4 /ZnSe coating,

(LohnStar Optics, 1863 Commercial St., Escondido, CA 92029, USA.)
OPTICS EXPRESS 13051 2 June 2014 | Vol. 22, No. 11 | DOI:10.1364/OE.22.013050 |

- the small amount of alpha particles emitted from the coating tolerable.

$P=2\times10^{-5}\times W/((1-R)\times S\times\sqrt{T})$ OK!

W= 5 mJ;
T= 70 K;
S=some cm^{-2};
R=0.9995

P will reach ~20%.

High intensity muon beam

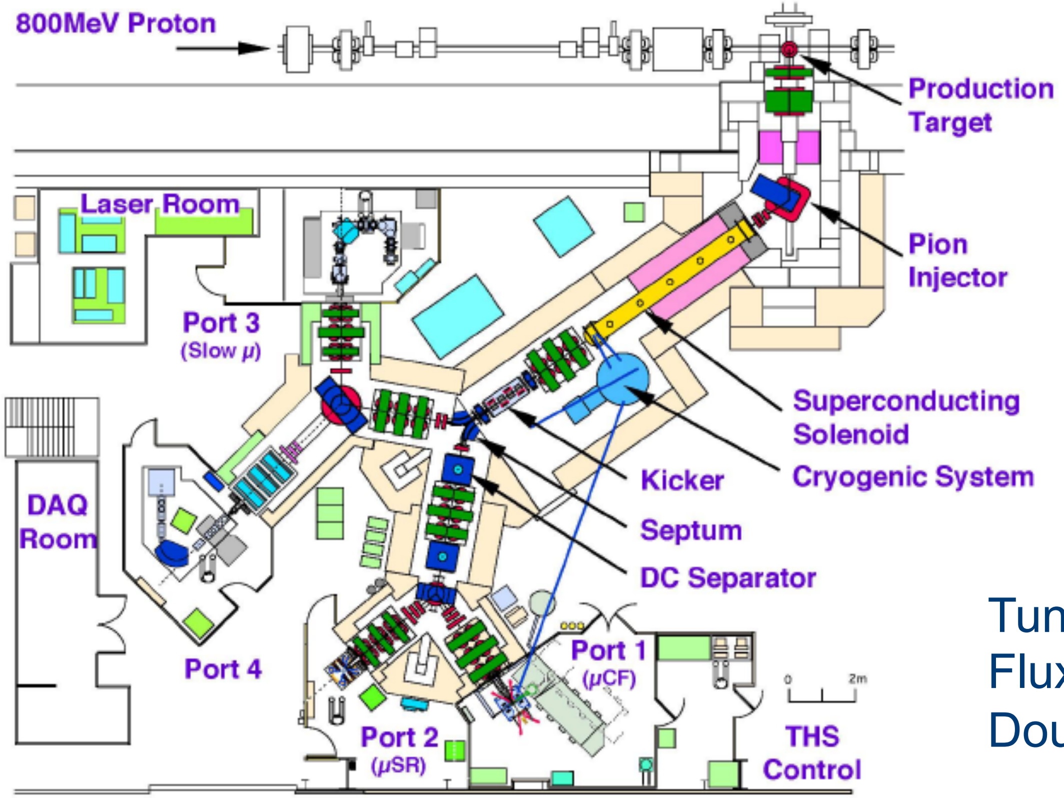

Tunable momentum: 20 – 120 MeV/c

Flux μ^- : 7 x 10^4 muons/s

Double pulsed beam

Beam time structure

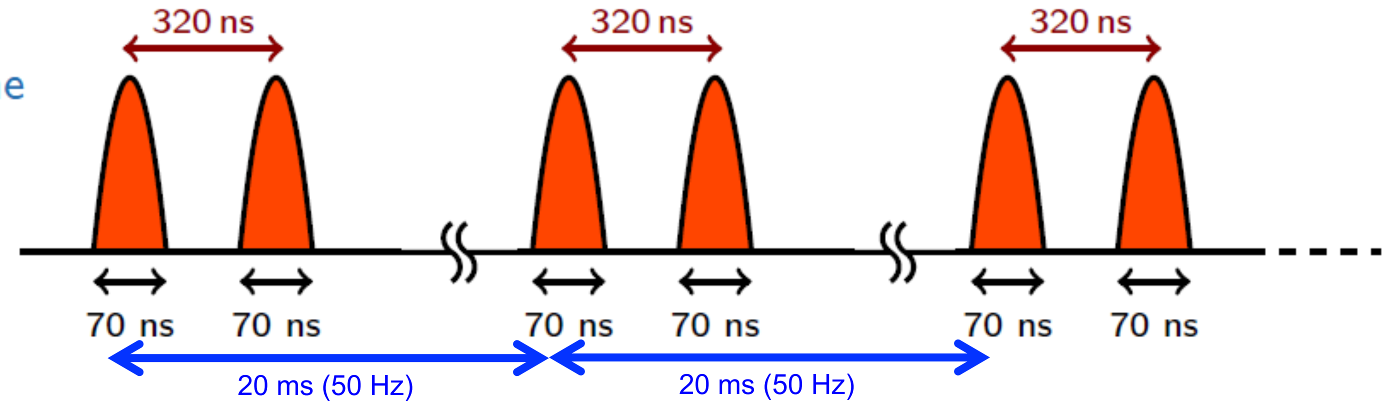

FAMU Key elements

Muon Beam at RIKEN-RAL

Beam properties

surface μ^+ (20~30MeV/c) and
decay μ^+/ μ^- (20~120MeV/c)
typical beam size 10cm²
$\bar{x}\Delta p/p$ FWHM 10%(decay), 5%(surface)
Double pulse structure
(Choice of single pulse
with magnetic kicker (<30 MeV/c))
Operation
160 days/y of ISIS beam time
~40 days for UK
~120 days for RIKEN

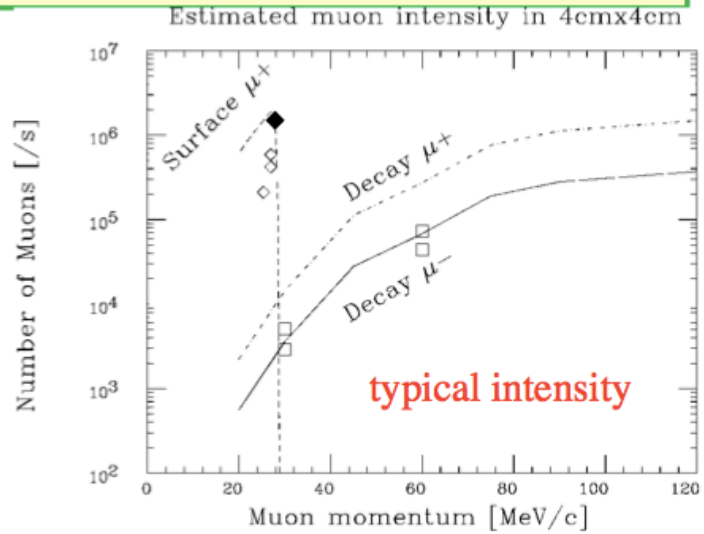

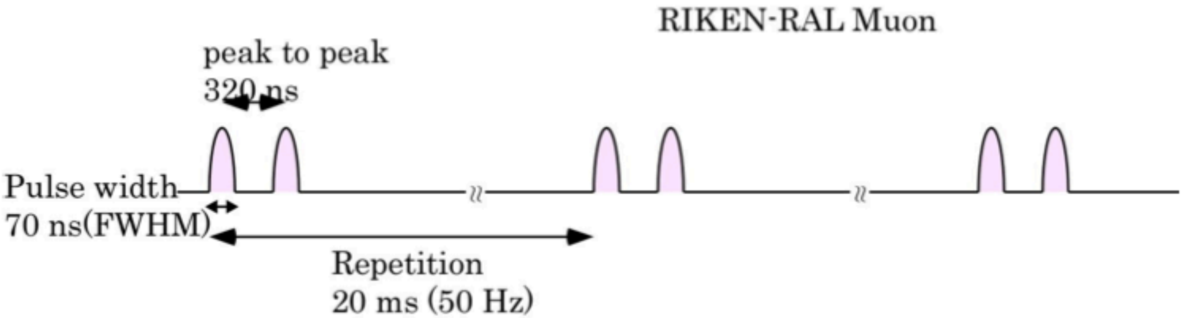

The RIKEN-RAL Muon Facility

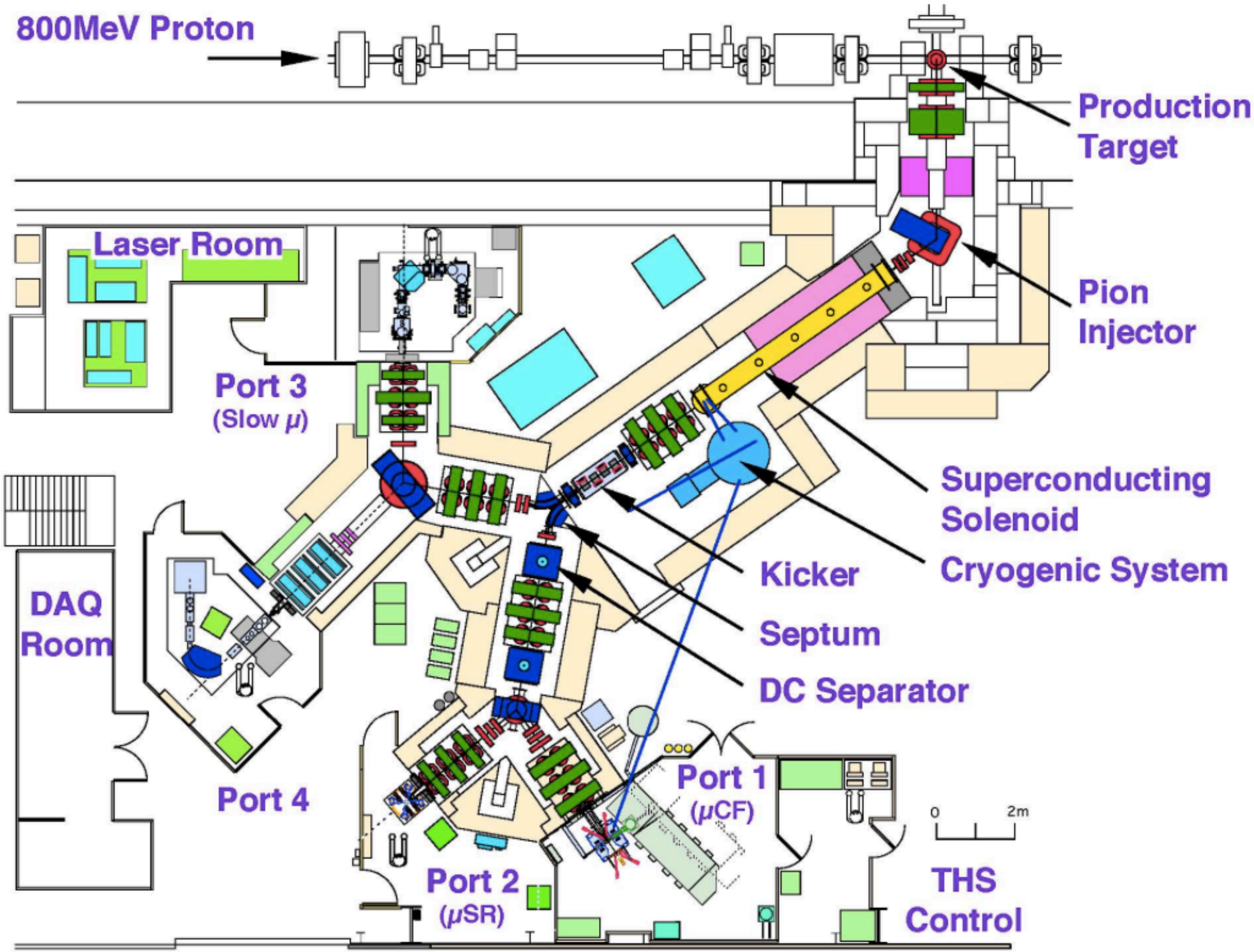

Moderator Study
Sofia group

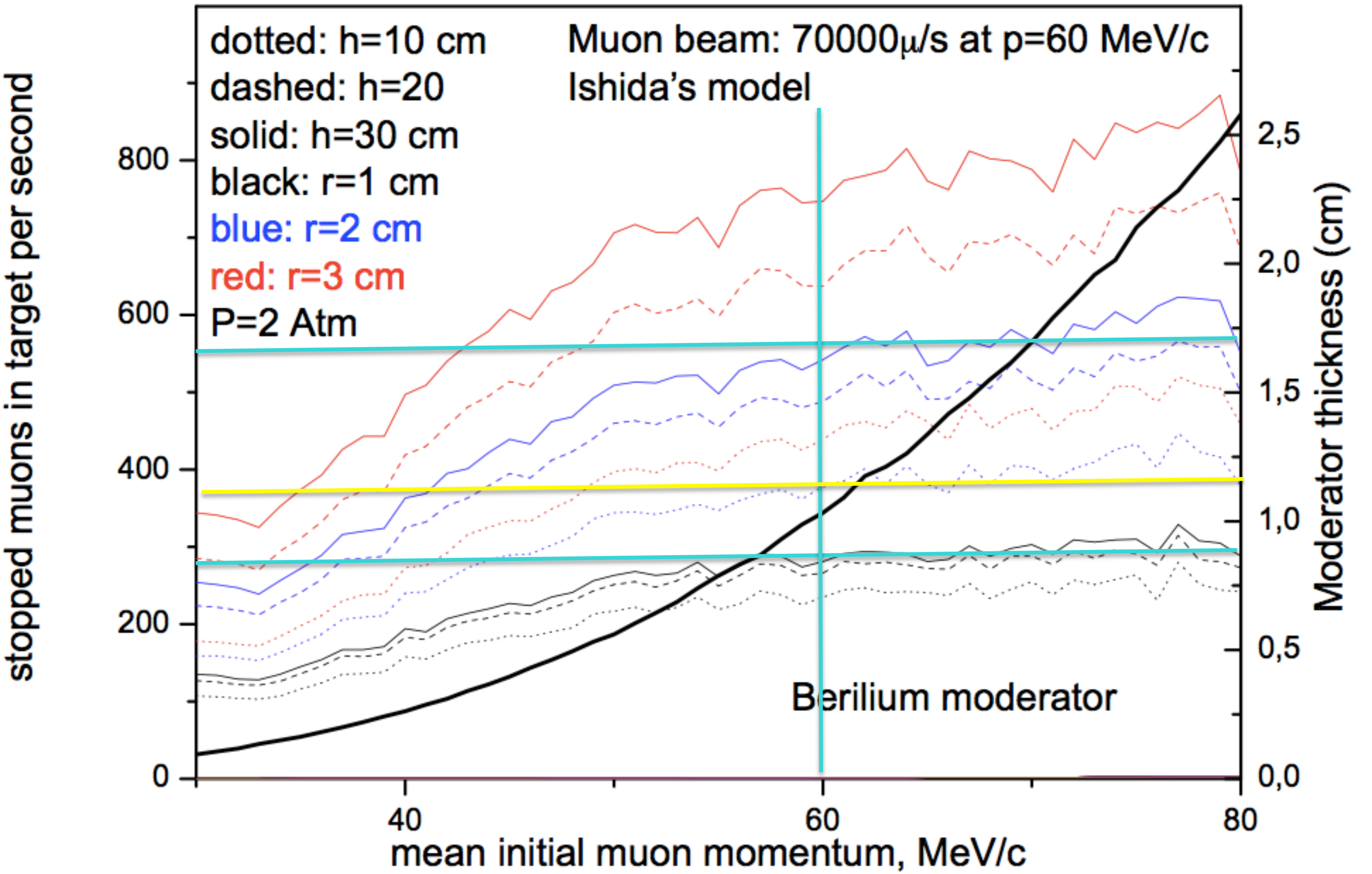
dotted: h=10 cm
dashed: h=20
solid: h=30 cm
black: r=1 cm
blue: r=2 cm
red: r=3 cm
P=2 Atm
Muon beam: 70000μ/s at p=60 MeV/c
Ishida's model
Berilium moderator
stopped muons in target per second
Moderator thickness (cm)
mean initial muon momentum, MeV/c
0
200
400
600
800
40
60
80
0,0
0,5
1,0
1,5
2,0
2,5

Max at 60 MeV/c; r=2cm; h=30cm; M_{Be}=1.5cm 550mu/s

Max at 60 MeV/c; r=1cm; h=30cm; M_{Be}=0.8cm 240mu/s

Max at 60 MeV/c; r=2cm; h=30cm; M_{ch}=2.2cm 500mu/s

Max at 60 MeV/c; r=1cm; h=30cm; M_{ch}=1.0cm 240mu/s

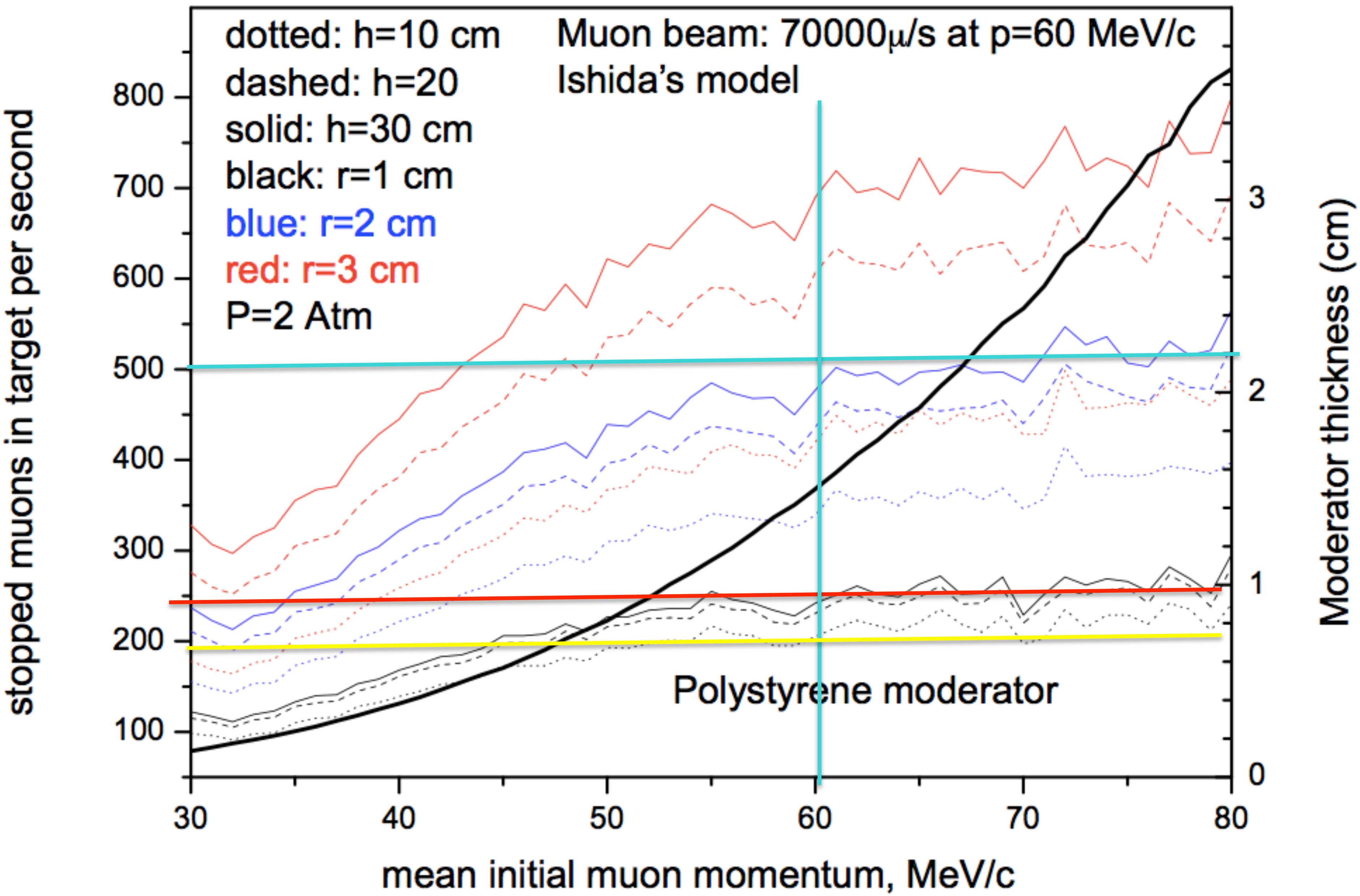

dotted: h=10 cm
dashed: h=20
solid: h=30 cm
black: r=1 cm
blue: r=2 cm
red: r=3 cm
P=2 Atm
Muon beam: 70000μ/s at p=60 MeV/c
Ishida's model
Polystyrene moderator
stopped muons in target per second
Moderator thickness (cm)
mean initial muon momentum, MeV/c
100
200
300
400
500
600
700
800
0
1
2
3
30
40
50
60
70
80

Si vedono alcunecose:

1) per via delle perdite laterali nmu/s=f(MeV/c) satura
2) si guadagna un fattore 2 lavorando a 60MeV/c con moderatore
3) Cambiando moderatore il guadagno in nmu/s e' piccolo
4) se il concentratore funziona possiamo aumentare ulteriormente recuperando dalle perdite laterali
5) La lunghezza del bersaglio è non porta molto quando r=1cm si potrebbe lavorare con h=10cm

2017:
RIKEN RAL Port 1 experimental setup

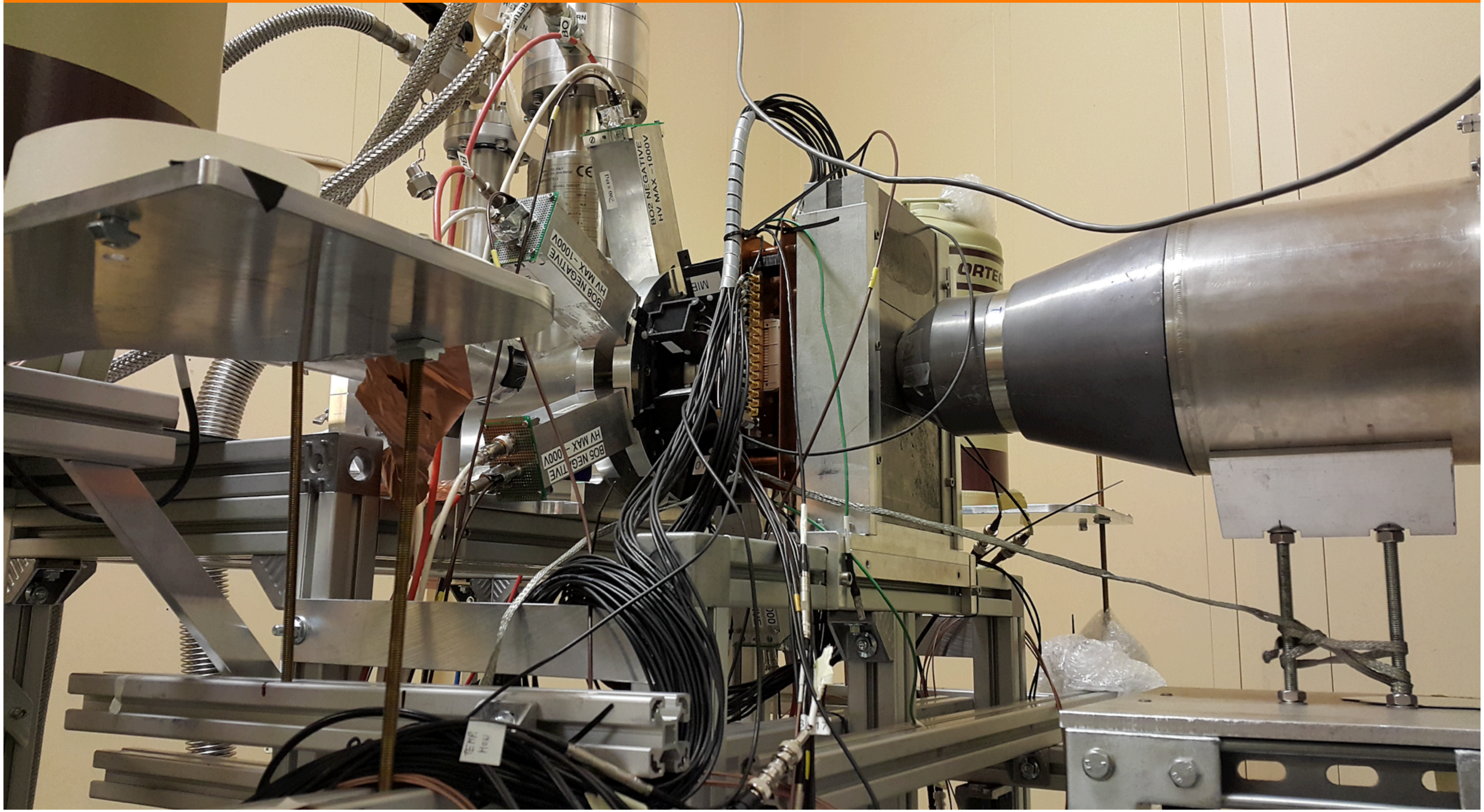

FAMU focusing team

Simulation set-up (optics material = Copper, Trapezoid tube)

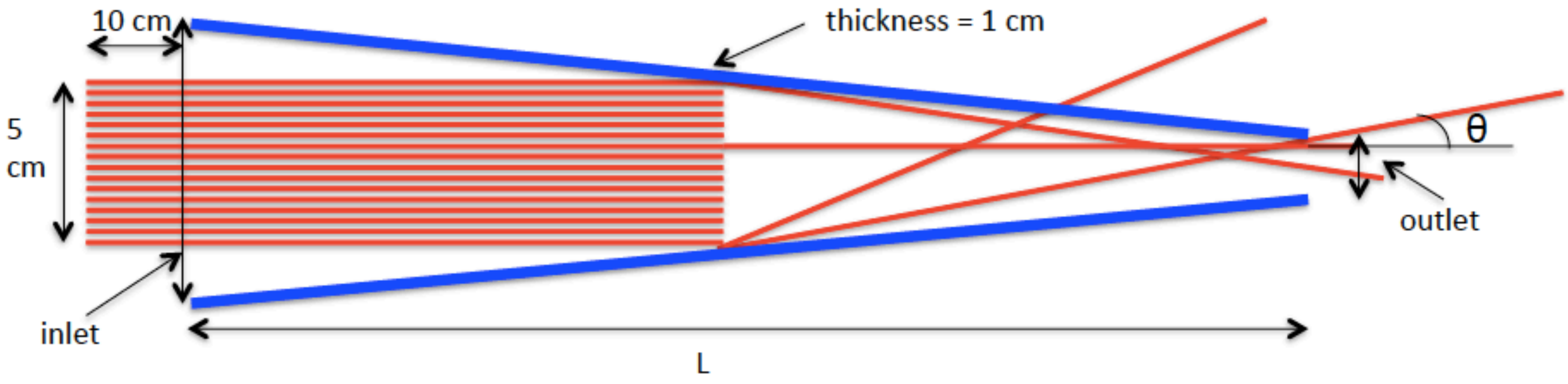

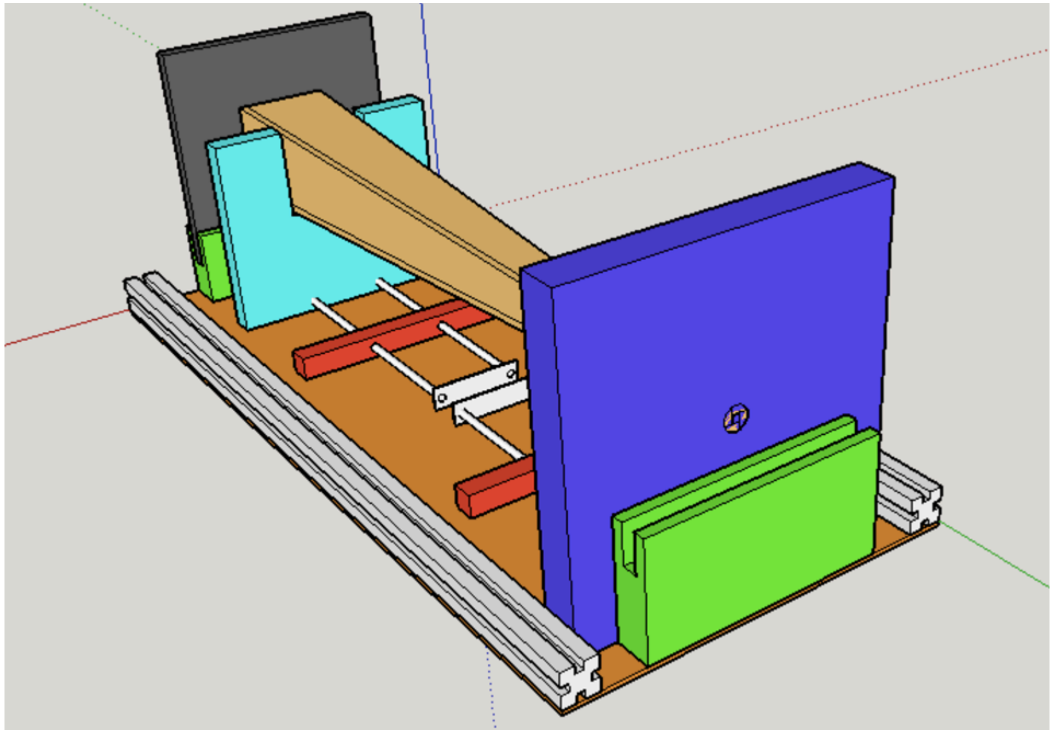

FAMU experiment context

Aim: muon momentum at exit about 30 MeV/c (in AIR)
test case: 1000 mm (length), 100 mm inlet, 10 mm outlet

- input momentum = 30 MeV/c
  - no modulator
  - total exiting muons = 0.2%
  - exit momentum = 20 MeV/c
- input momentum = 60 MeV/c
  - modulator
  - 20x muons wrt 30 MeV/c
  - total exiting muons = 0.14% = 2.8% considering 20x factor
  - exit momentum = 30 - 35 MeV/c
- input momentum = 80 MeV/c
  - modulator
  - 100x muons wrt 30 MeV/c
  - exiting muons = 0.03% = 3% considering 100x factor
  - exit momentum = 30 - 35 MeV/c

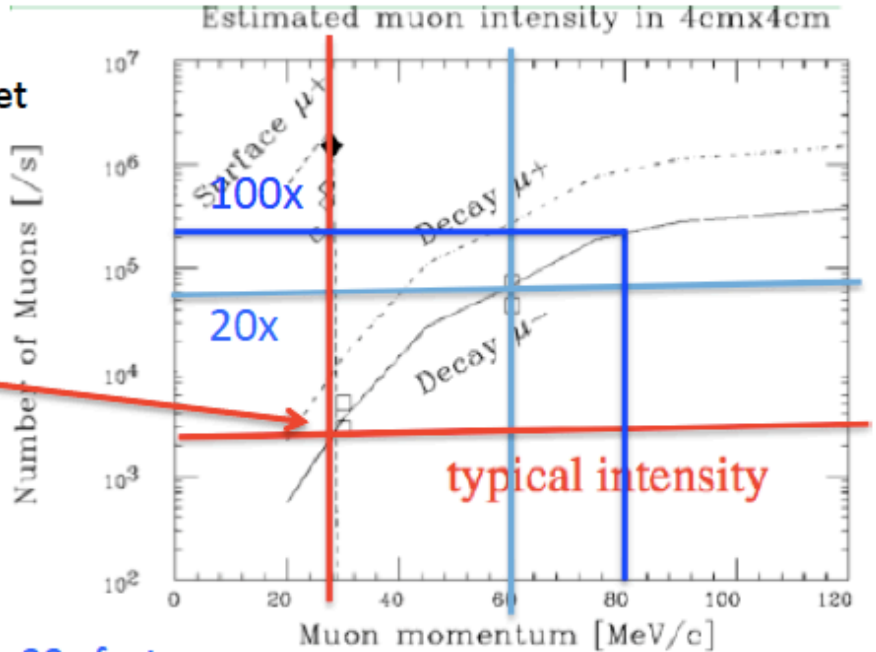

at 60MeV/c
10mm exit area
#50000x0.028
#1400 muons/s

Hodoscope for beam shape monitoring

Final version:
two planes (X and Y) of 32 scintillating fibers 1 x 1 mm^2 square section
SiPM reading with fast electronics
3D printed supports

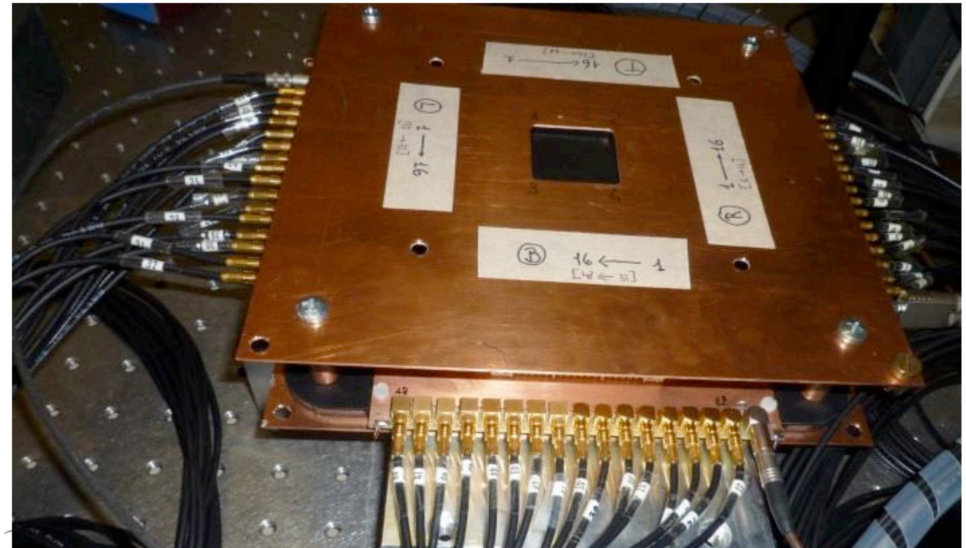

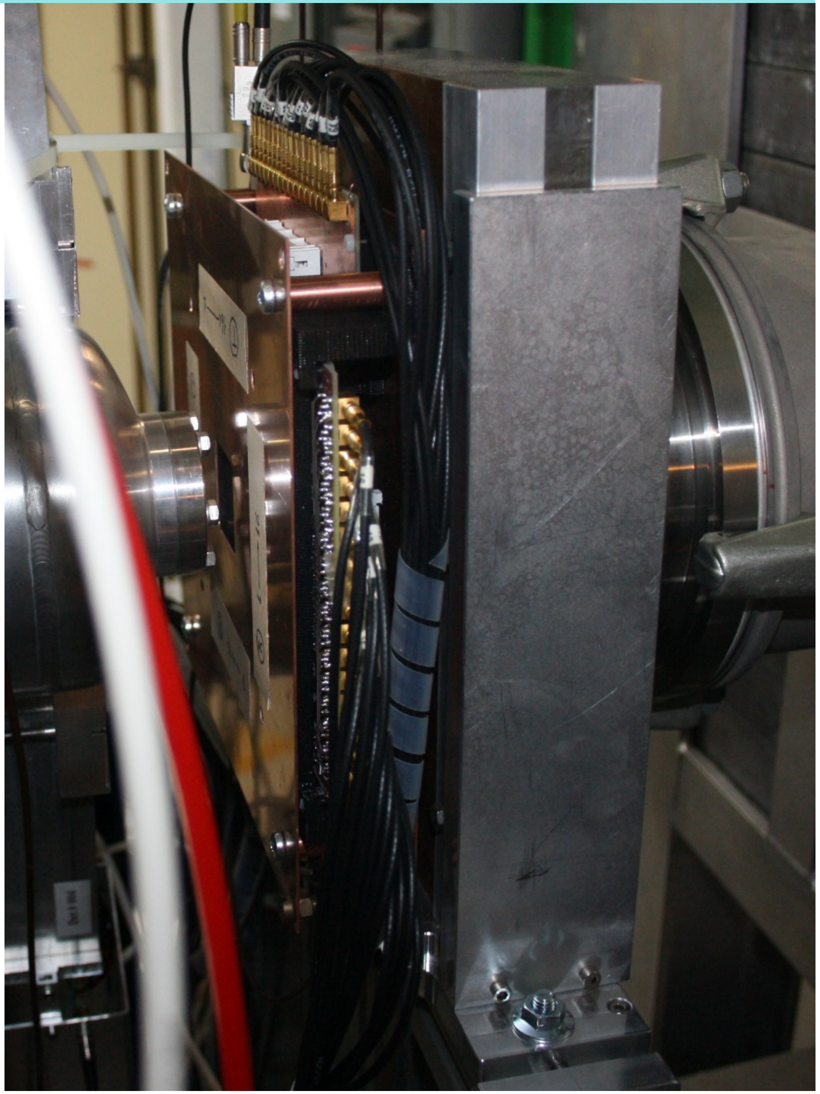

hodoscope in the 2016 setup

Hodoscope: PORT1 commissioning

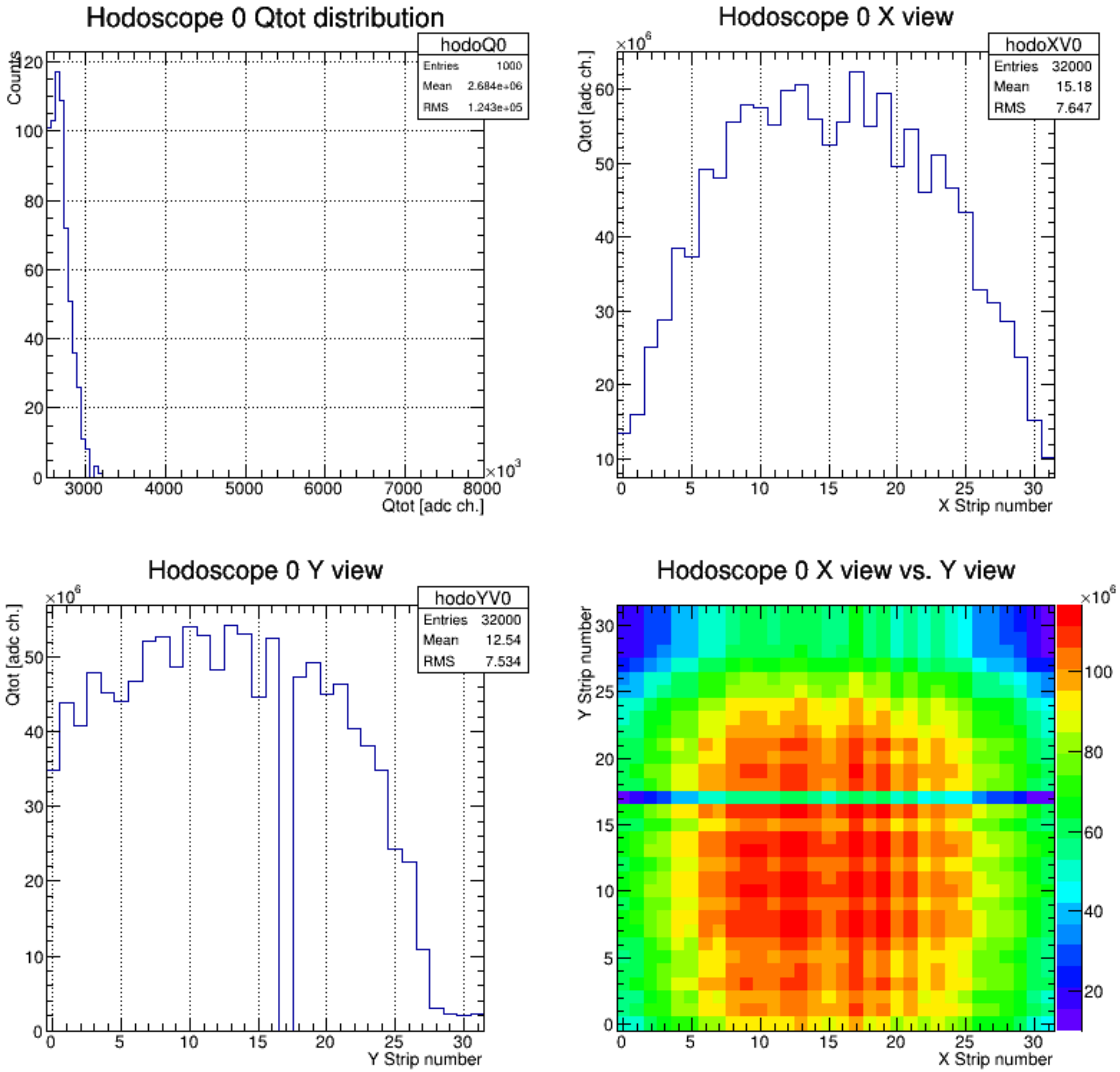

2017 data at PORT1:

tuning magnets currents to change beam shape with millimetric resolution

Hodoscope: PORT1 commissioning

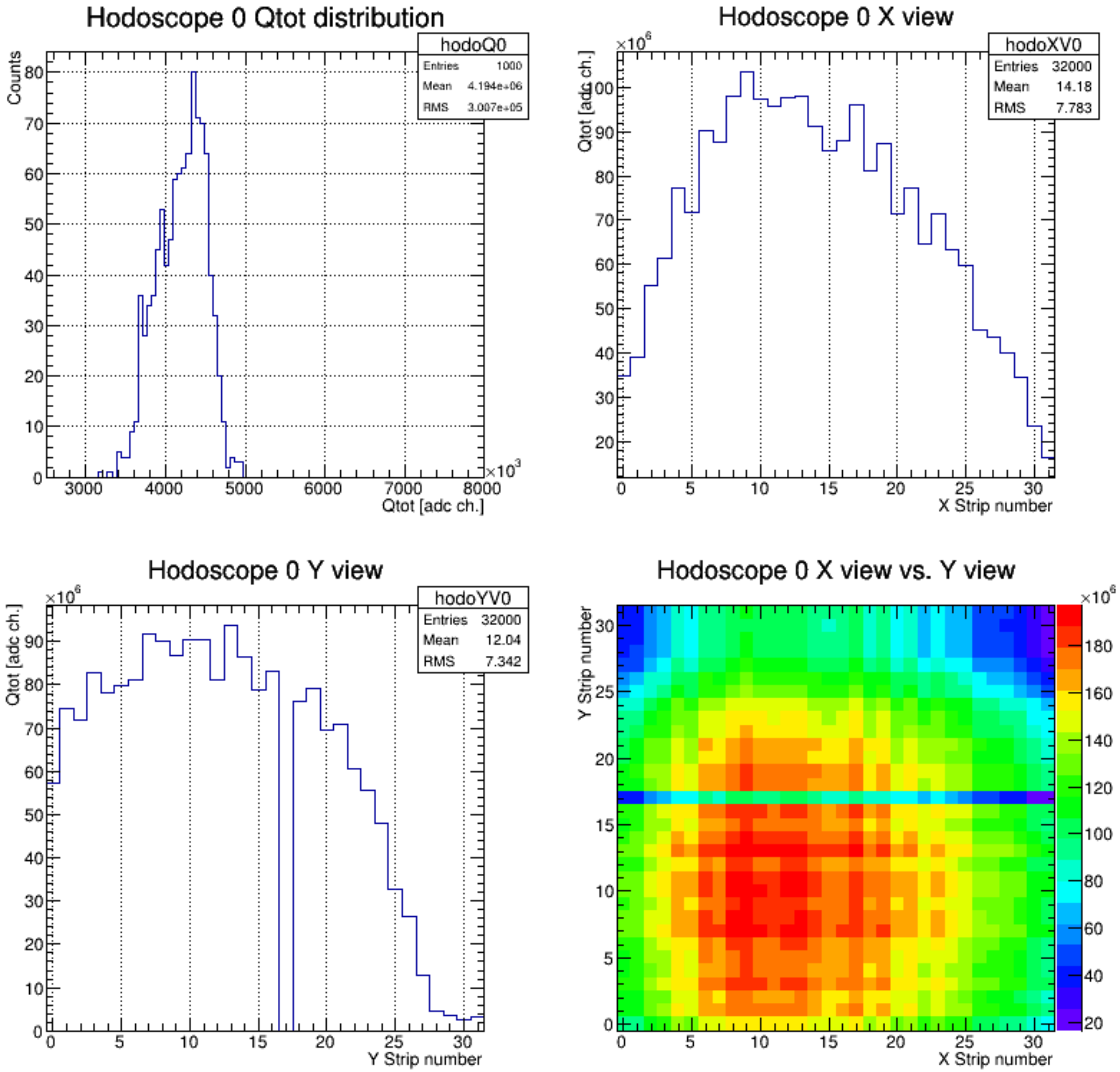

2017 data at PORT1:

tuning magnets currents to change beam shape with millimetric resolution

INFN
Istituto Nazionale di Fisica Nucleare

Hodoscope: PORT1 commissioning

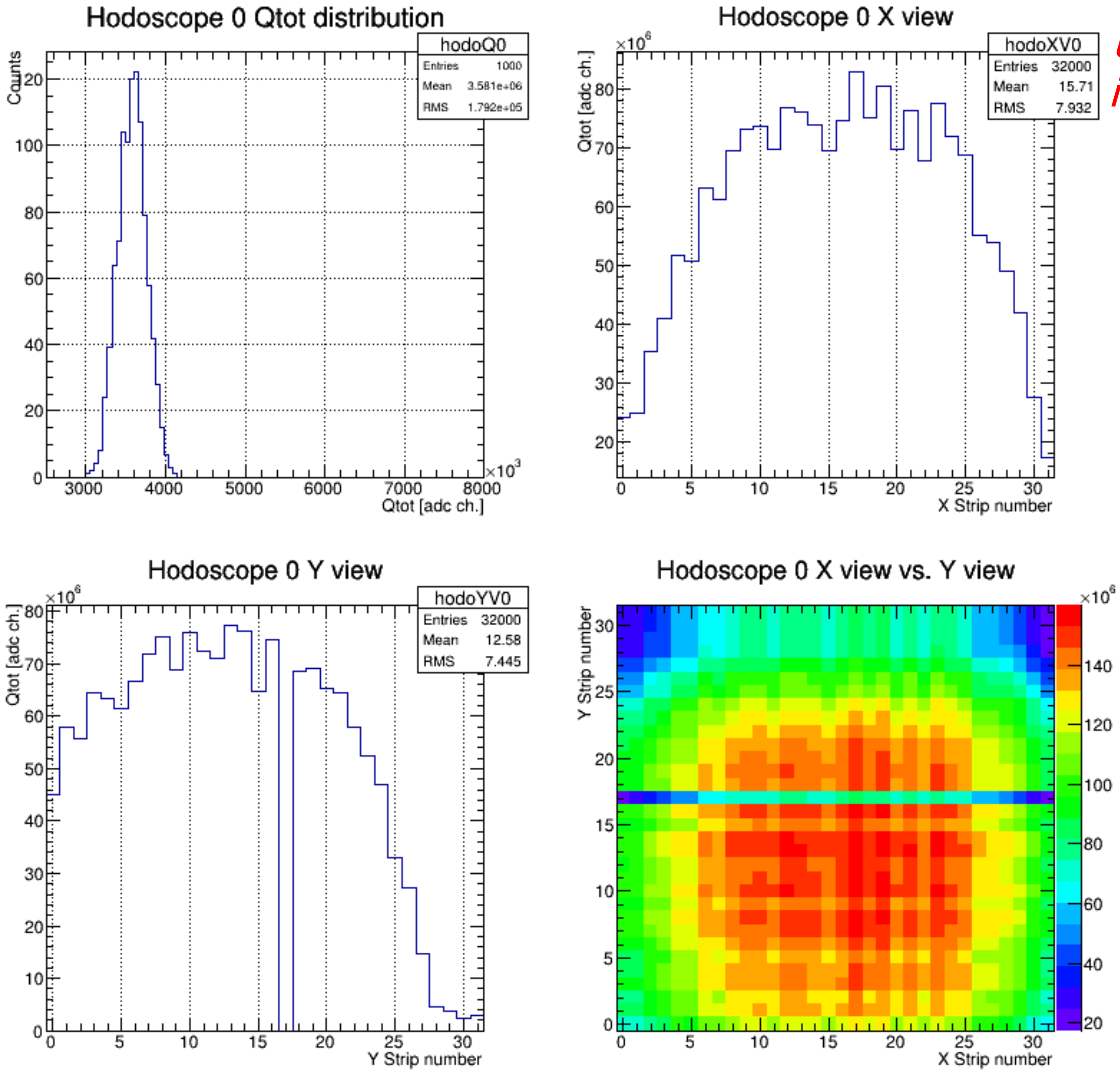

unprecedented precision in beam monitoring at RAL

2017 data at PORT1:

tuning magnets currents to change beam shape with millimetric resolution

Target: a challenge itself

- 2015 target:
detectors and beam test and validation

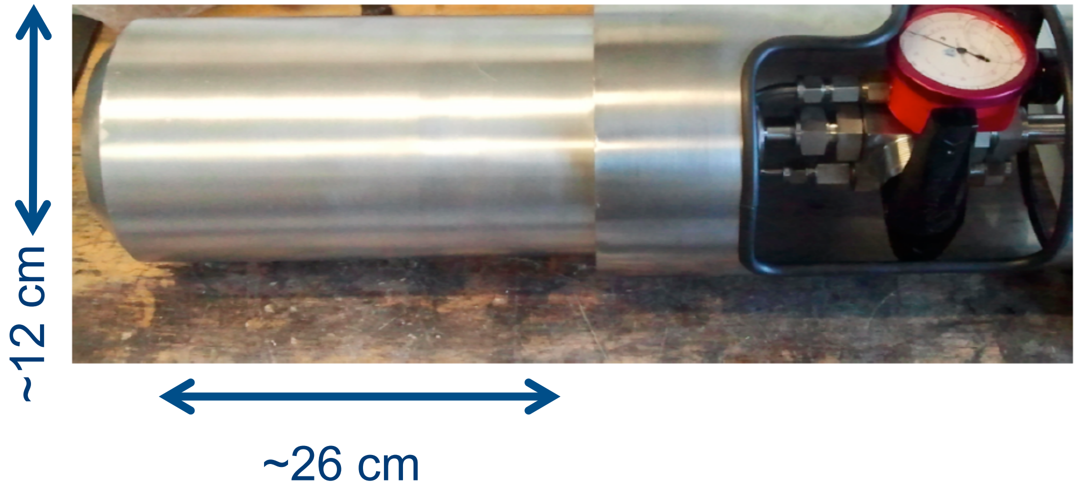

- 2016 target:
cryogenic target,
transfer rate measurement

- 2018 target: cryogenic target + optical path and cavity, Zemach radius measurement

2016 Target: a necessary trade-off

Main requirements:

-Operating temperature range: 40 K ≤ T ≤ 325 K

-Temperature control for measurement runs at fixed T steps from 300 K to 50K

-Gas @ constant density, H_2 charge pressure at room T is ~40 atm

-International safety certification (Directive 97/23/CE PED)

-Minimize walls and windows thickness

-Target shape and dimensions to :

- **maximize muon stop in gas**
- **to minimize distance gas – detectors**
- **to be compliant to allowable volume at Riken Port**

-H_2 compatible

... and, of course, all the above within time and cost constraints!

2016 Best solution

Target= Inner vessel with high P gas (44 bar)

- -Al alloy 6082 T6 cylinder D = 60 mm and L = 400 mm, inner volume of 1.08 l
- -Internally Ni/Au plated (L = 280 mm)
- -Cylinder side wall thickness = 3.5 mm
- -Wrapped in 20 layers of MLI
- -Front window D= 30 mm 2.85 mm thick
- -Three discs of 0.075 mm Al foil for window radiative shield
- -304L SS gas charging tube
- -304L SS cooler cold-end support
- -G10 mechanical strut
- -Two Cu straps for cooling

Vacuum vessel = outer cylinder (P atm)

- -Al6060 D=130 mm, 2 mm thick walls
- -≈30mm between inner/outer walls
- -Flanged Al window 0.8 mm thick
- -Pumping valve & harness feed-tru's

CRIOTEC IMPIANTI
spa Chivasso

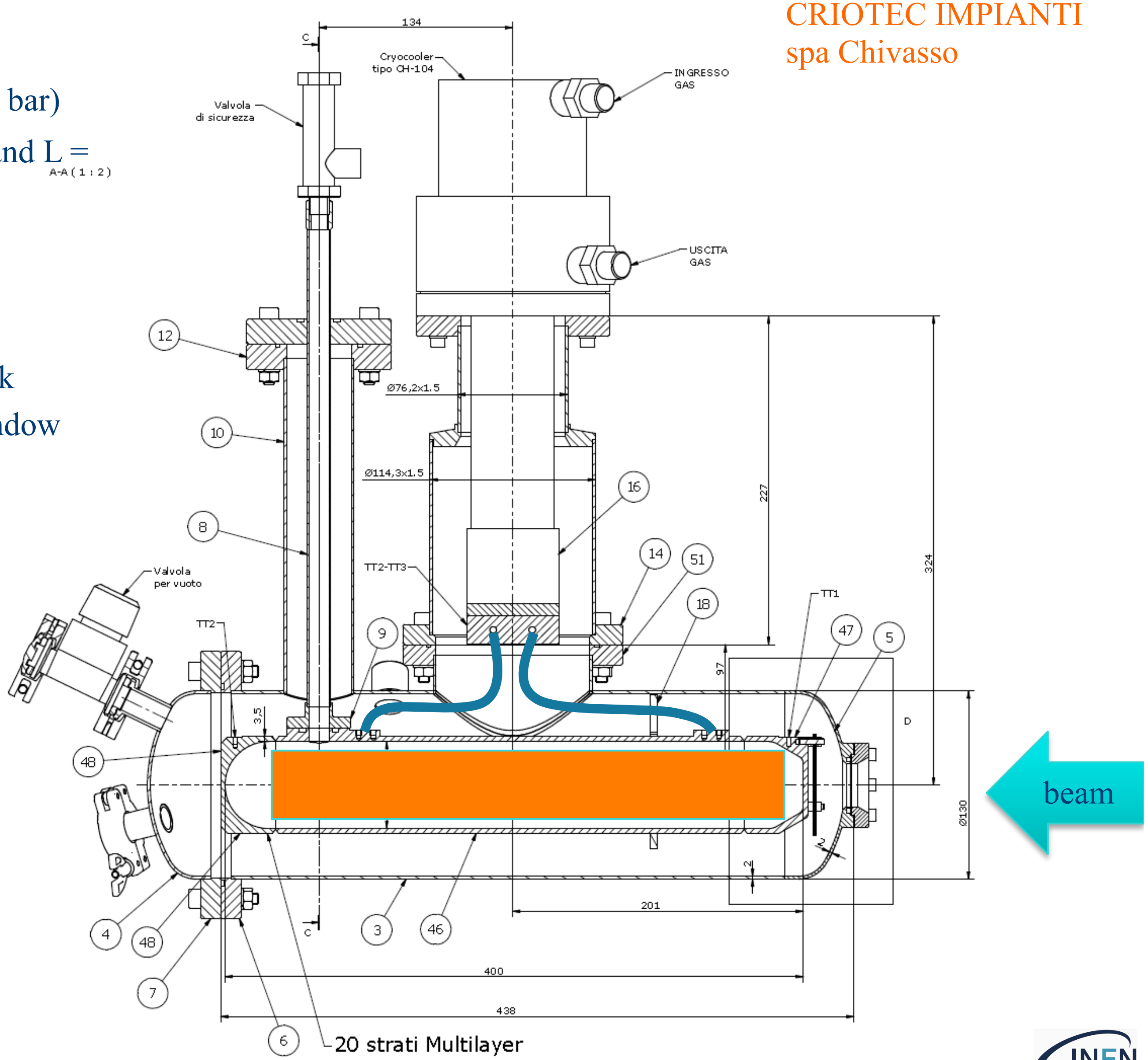

FAMU

INFN
Istituto Nazionale di Fisica Nucleare

Target in lab

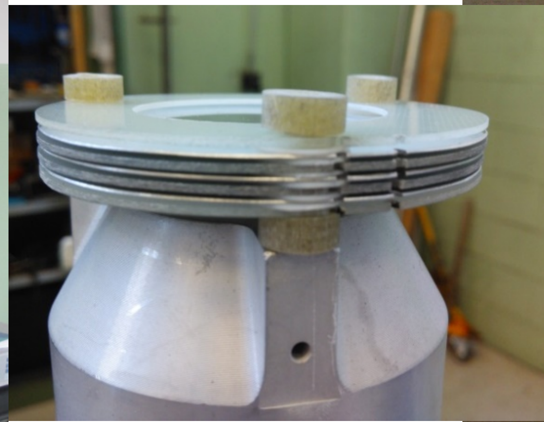

Target on beam line

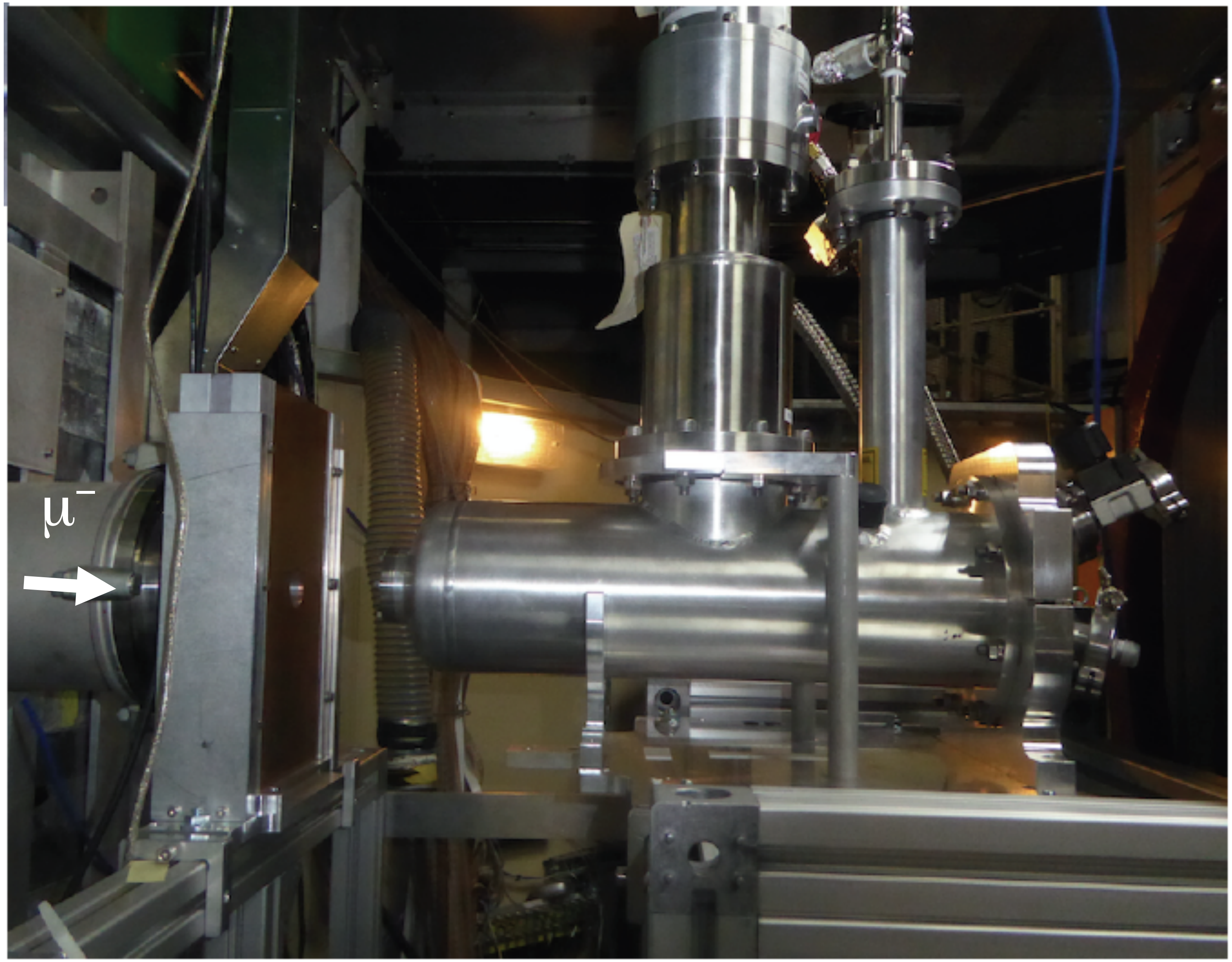

Thermal cycles 2016

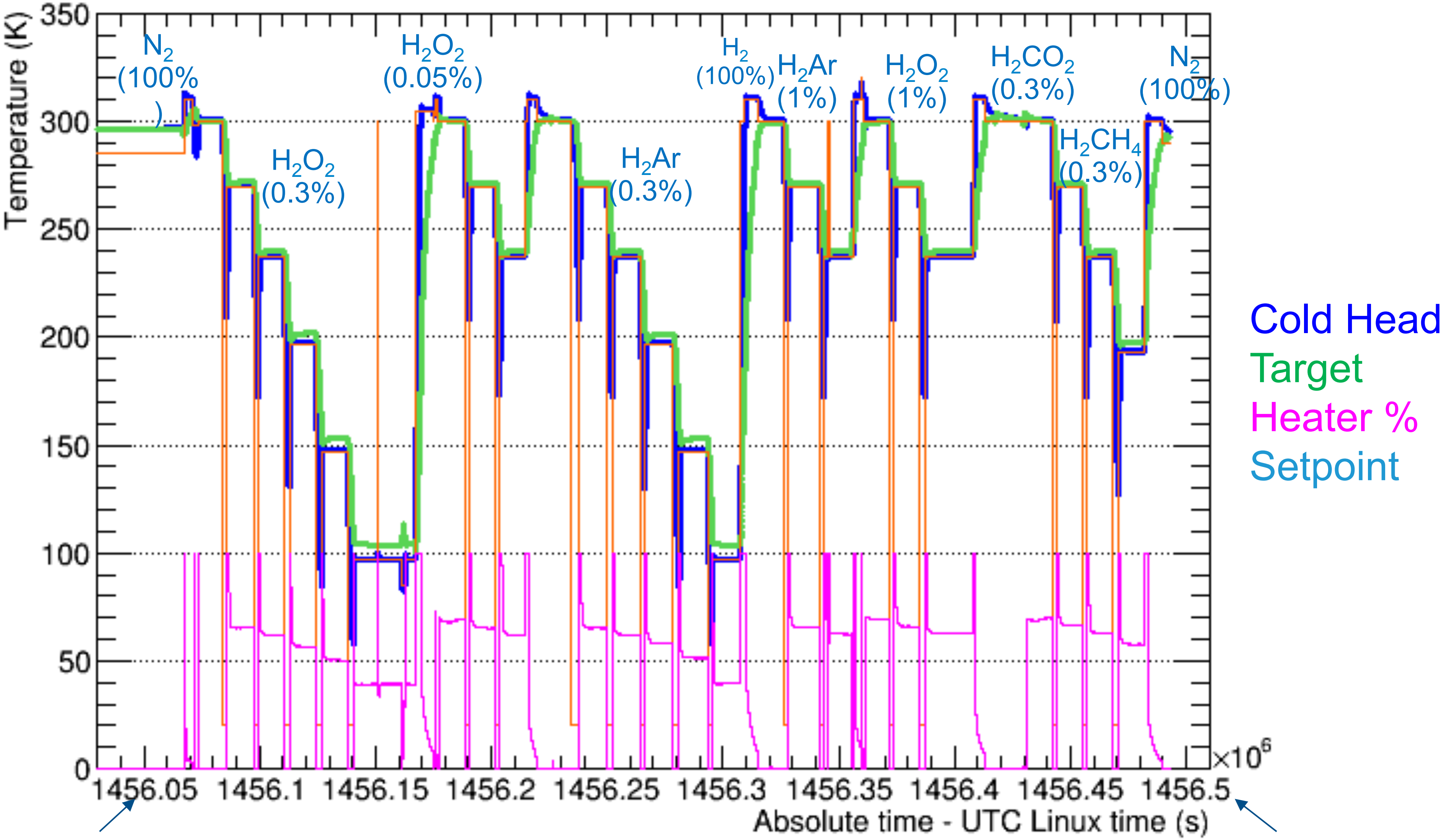

21/02/2016

26/02/2016

5 days: Feb 2016 measurements run

Detectors: suited for time-resolved X-ray spectroscopy

Germanium HPGe: low energy X-rays spectroscopy

ORTEC GLP:
Energy Range: 0 – 300 keV
Crystal Diameter: 11 mm
Crystal Length: 7 mm
Beryllium Window: 0.127 mm
Resolution Warrented (FWHM):
- at 5.9 keV is 195 eV (T_{sh} 6 μs)
- at 122 keV is 495 eV (T_{sh} 6 μs)

ORTEC GMX:
Energy Range: 10 – 1000 keV
Crystal Diameter: 55 mm
Crystal Length: 50 mm
Beryllium Window: 0.5 mm
Resolution Warrented (FWHM):
- at 5.9 keV is 600 eV (T_{sh} 6 μs)
- at 122 keV is 800 eV (T_{sh} 6 μs)

Detectors: suited for time-resolved X-ray spectroscopy

Lanthanum bromide scintillating crystals [$LaBr_3(Ce)$]:
fast timing X-rays detectors

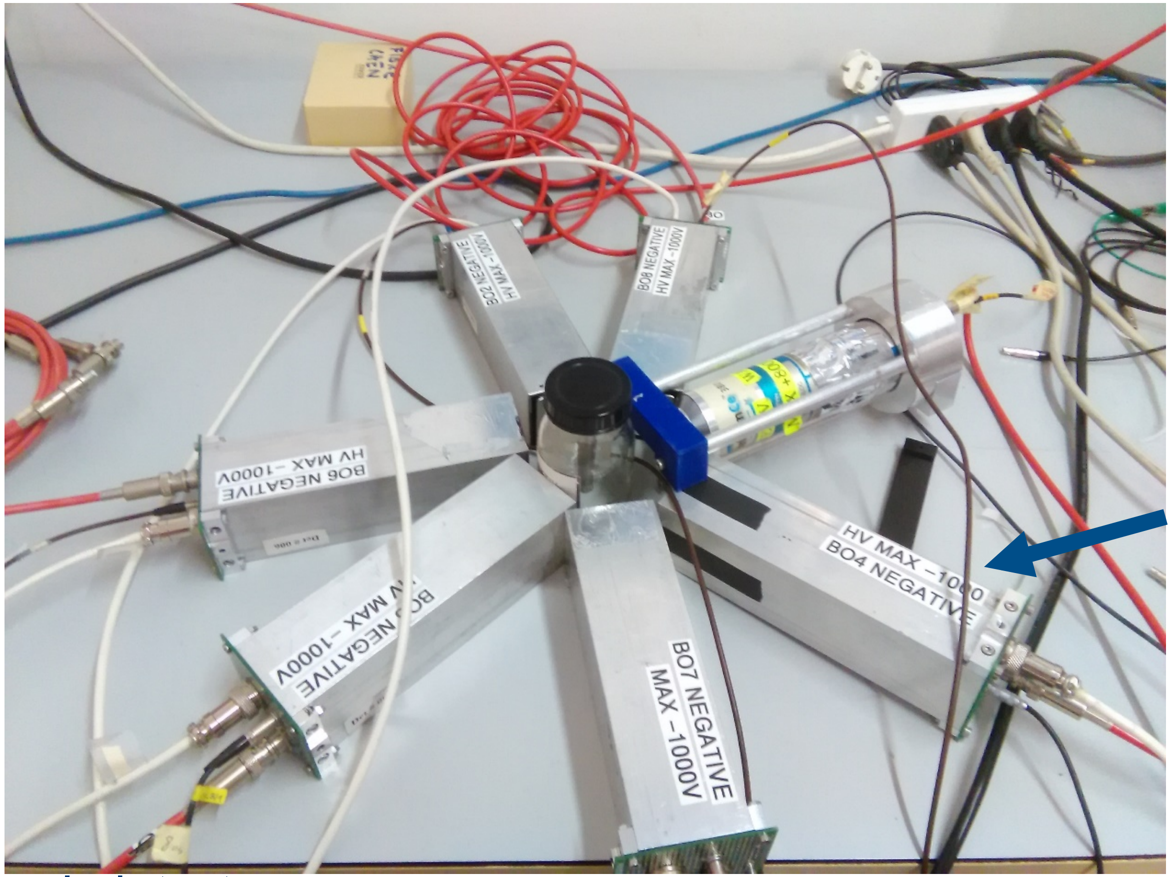

Lab test

8 cylindrical 1 inch diameter 1 inch long $LaBr_3$(5%Ce) crystals read by PMTs.

On purpose developed fast electronics and fast digital processing signal.

Star-shaped support for detectors

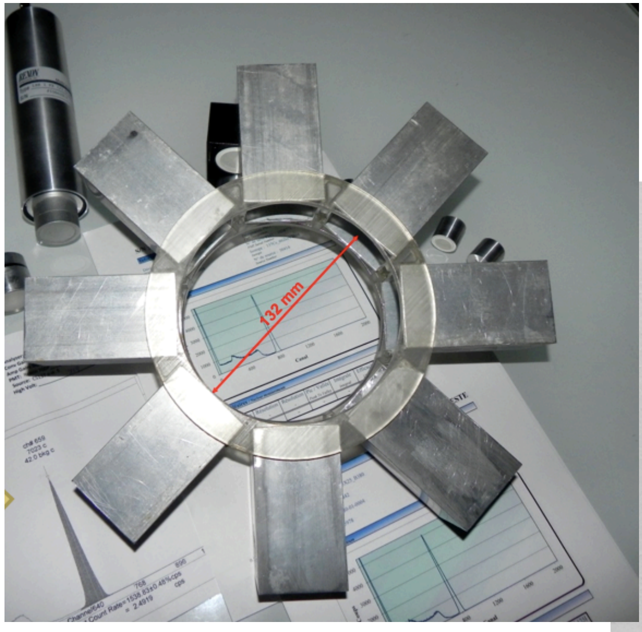

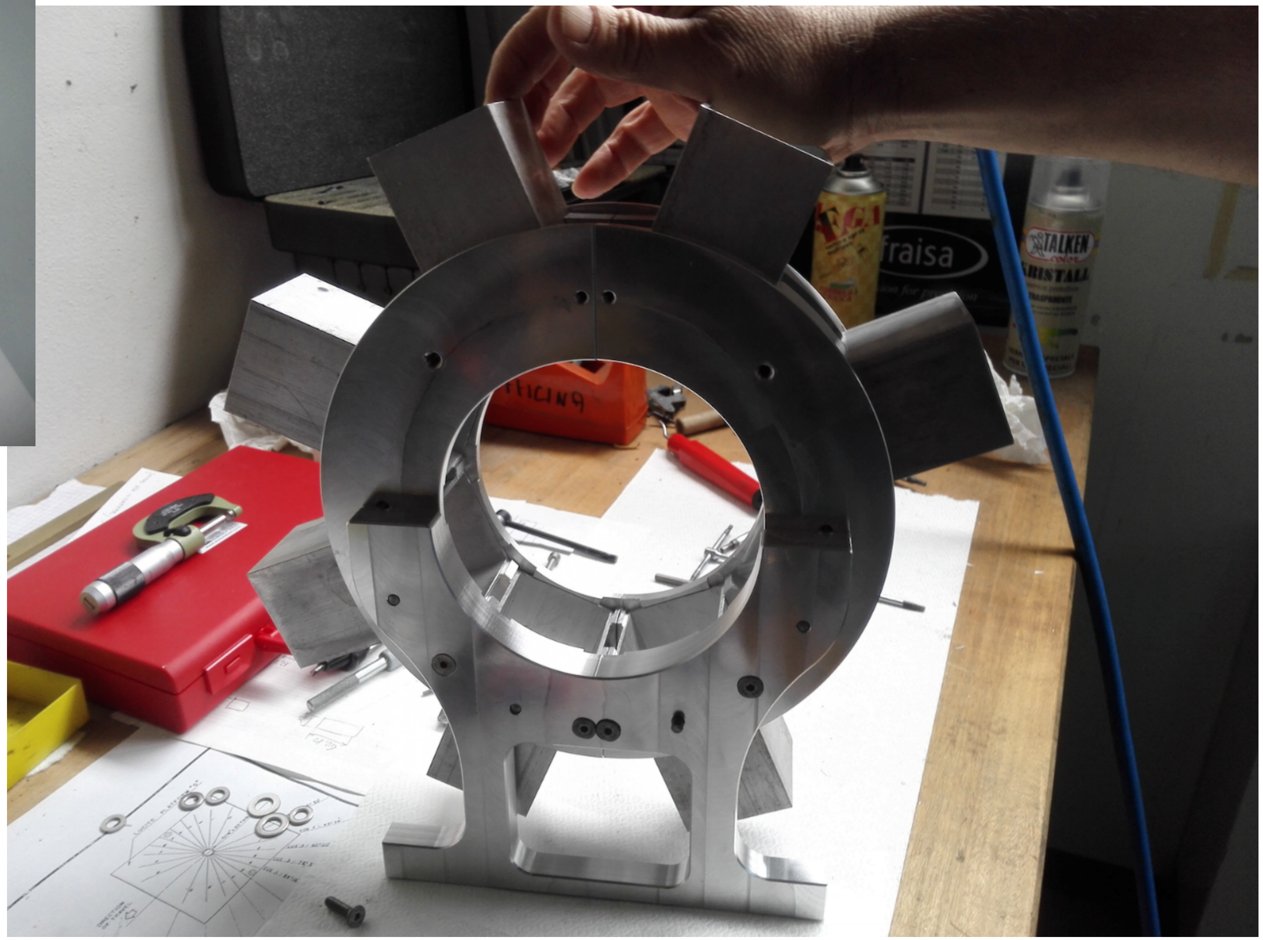

2016: experimental setup

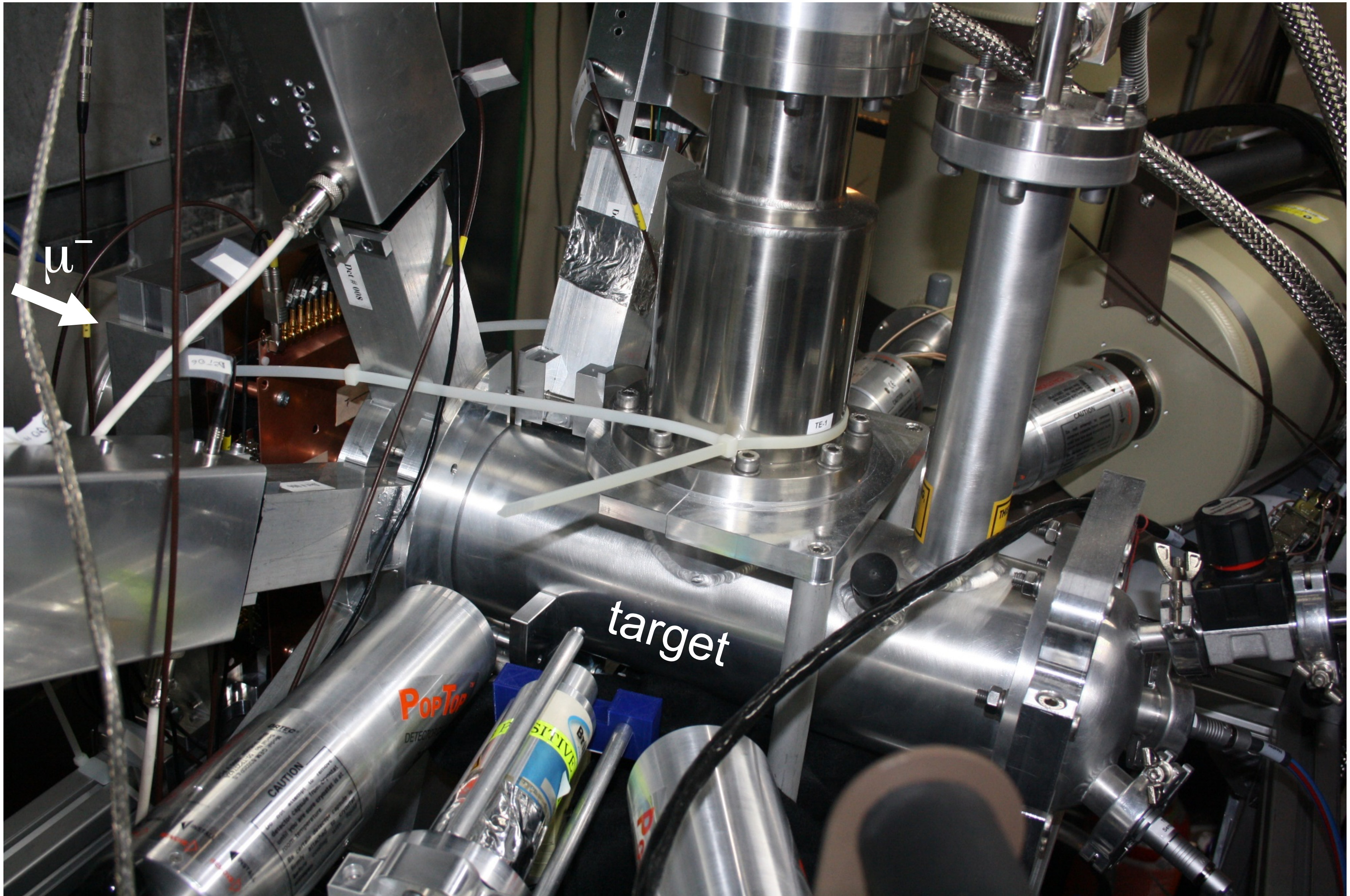

2016: experimental setup

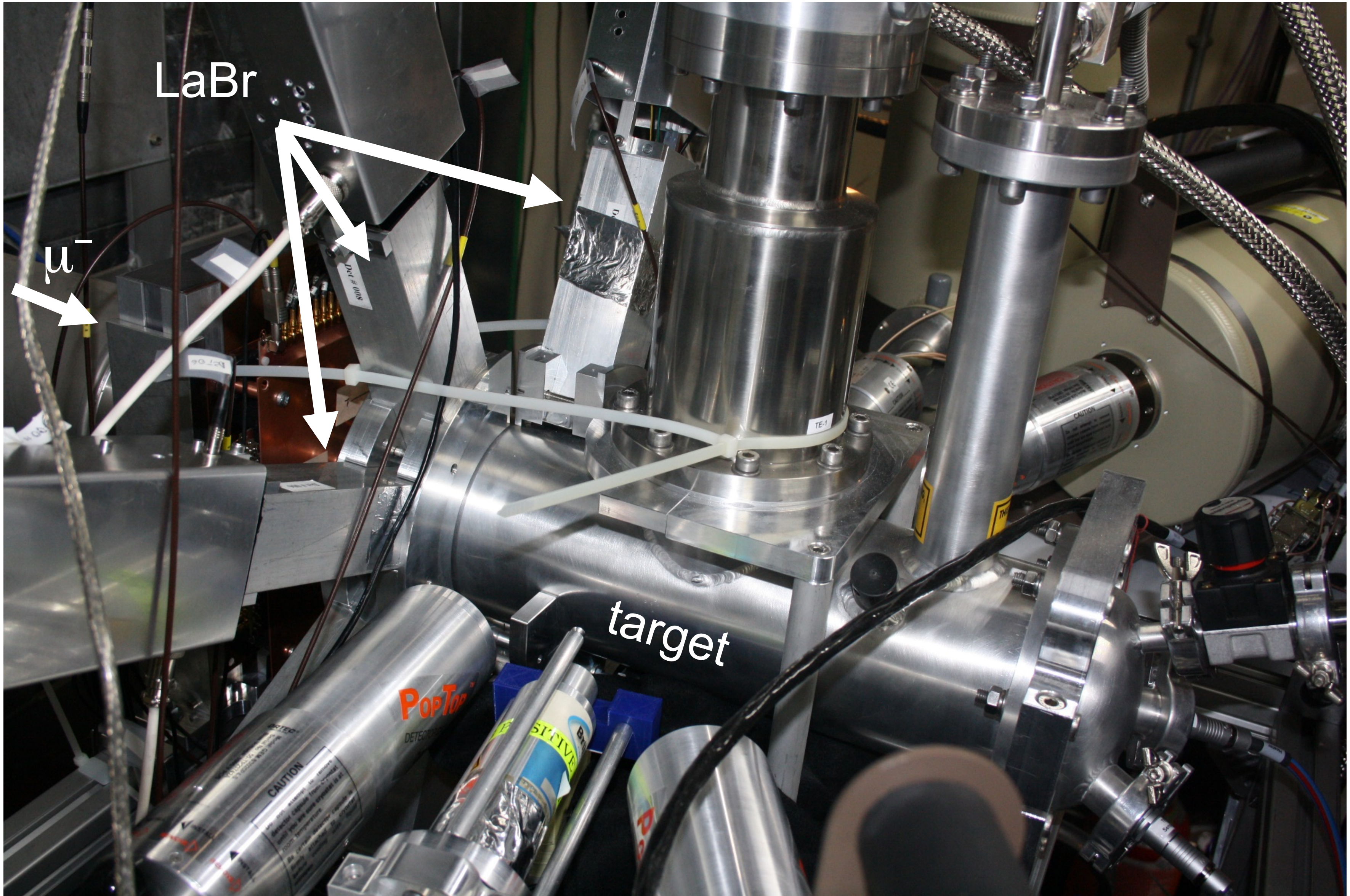

2016: experimental setup

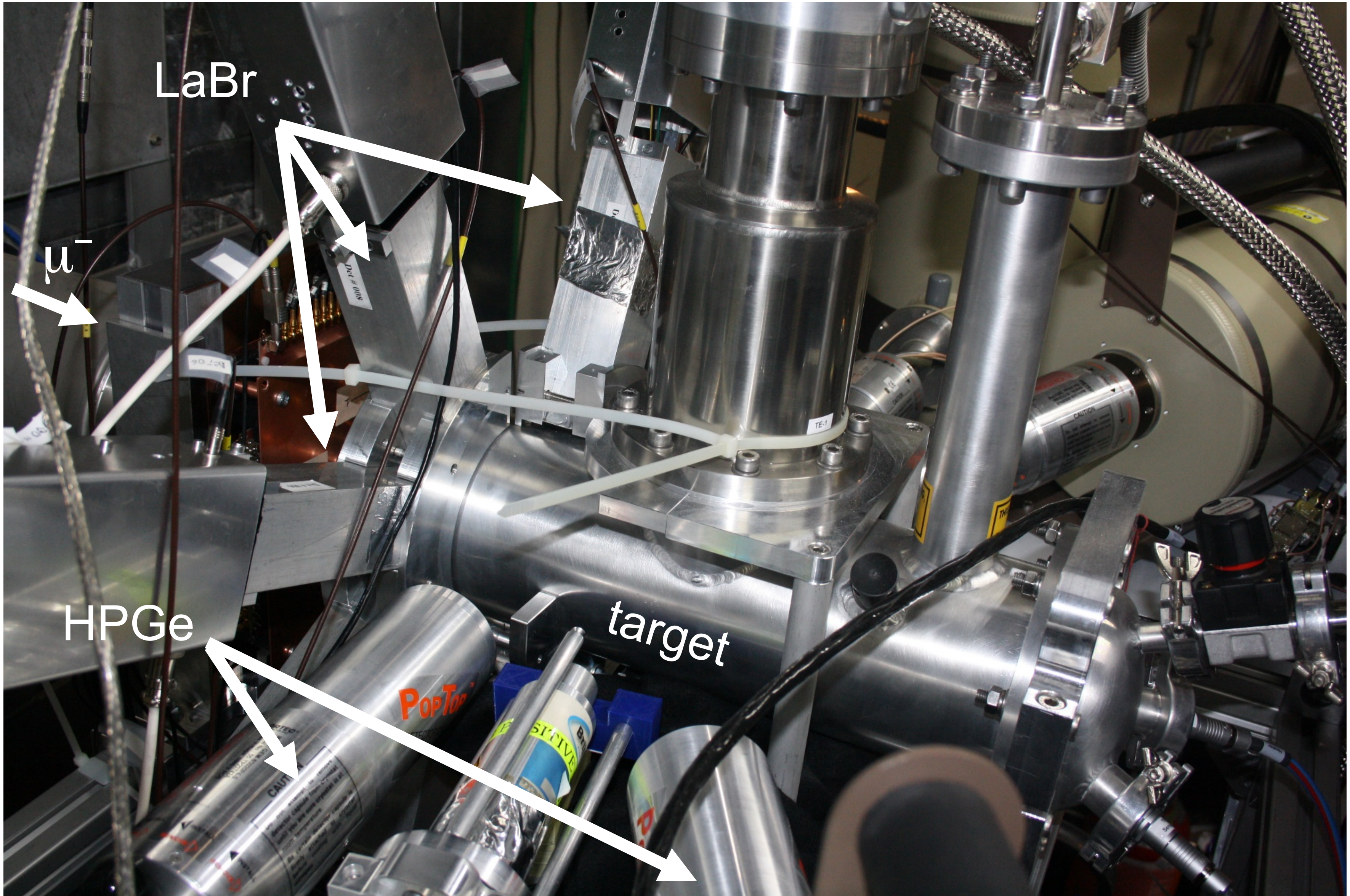

2016: transfer rate measurement

Steps:

1) fix a target temperature (i.e. mean kinetic energy

2) produce μp and wait for thermalization

3) study time evolution of Oxygen X-rays

4) repeat with different temperature

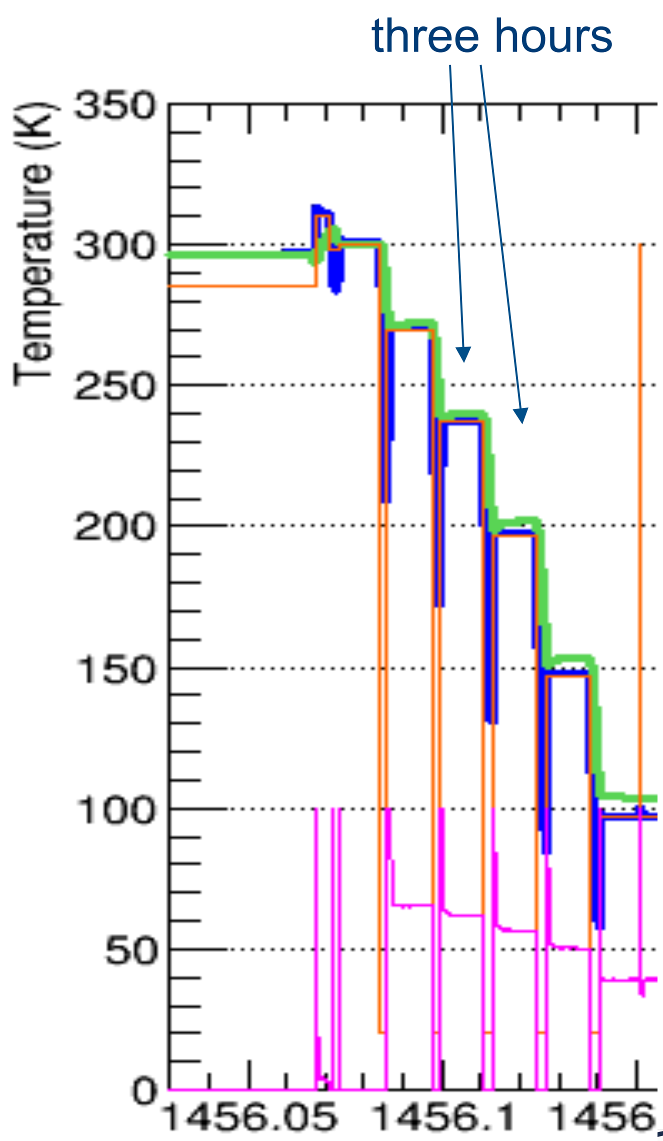

Target cryo performances: T control steps

2017 on beam: lowest temperature

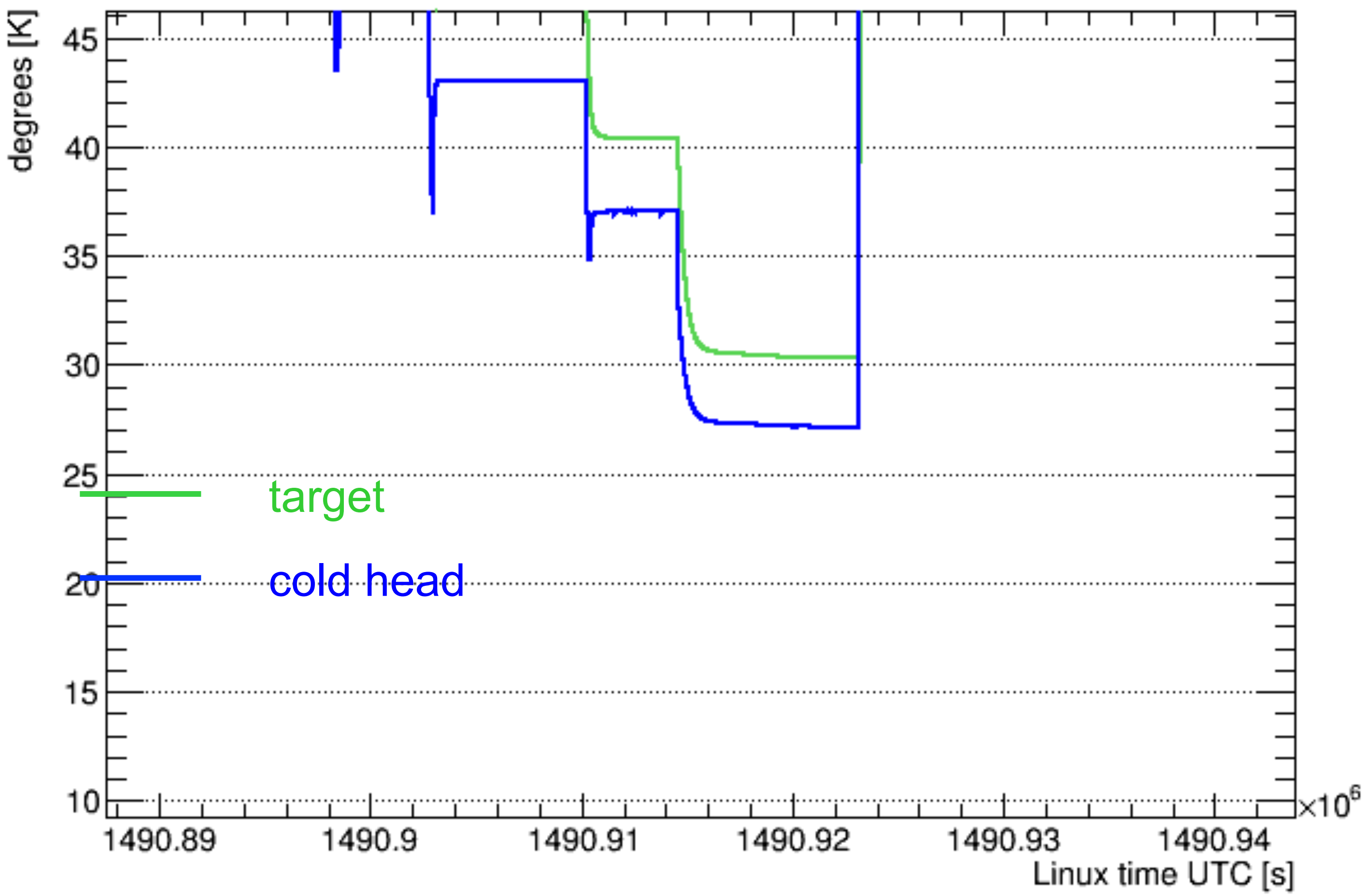

FAMU

INFN Istituto Nazionale di Fisica Nucleare

OUTLINE

- FAMU background & motivations
- The method to measure the hfs
  - laser
  - beam
  - target
  - detectors
- muon transfer rate measurements
- conclusions

Spectral lines measurements

Germanium detectors: excellent energy resolution

Pure H_2 target in aluminium container

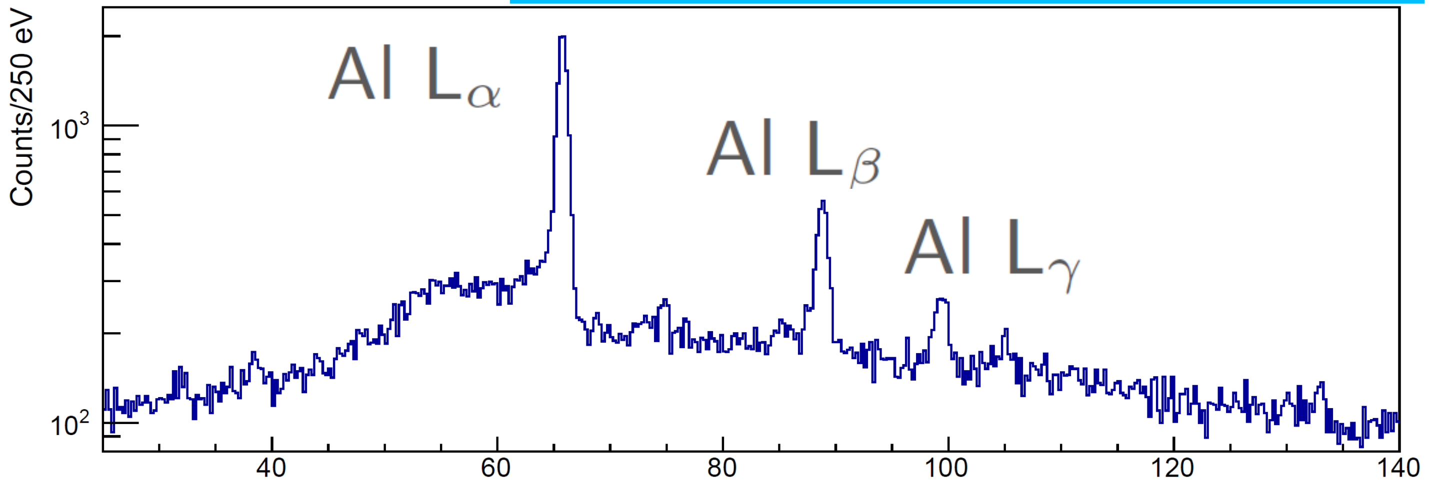

$H_2 + (4\%\ w/v)CO_2$ gas mixture in aluminium container

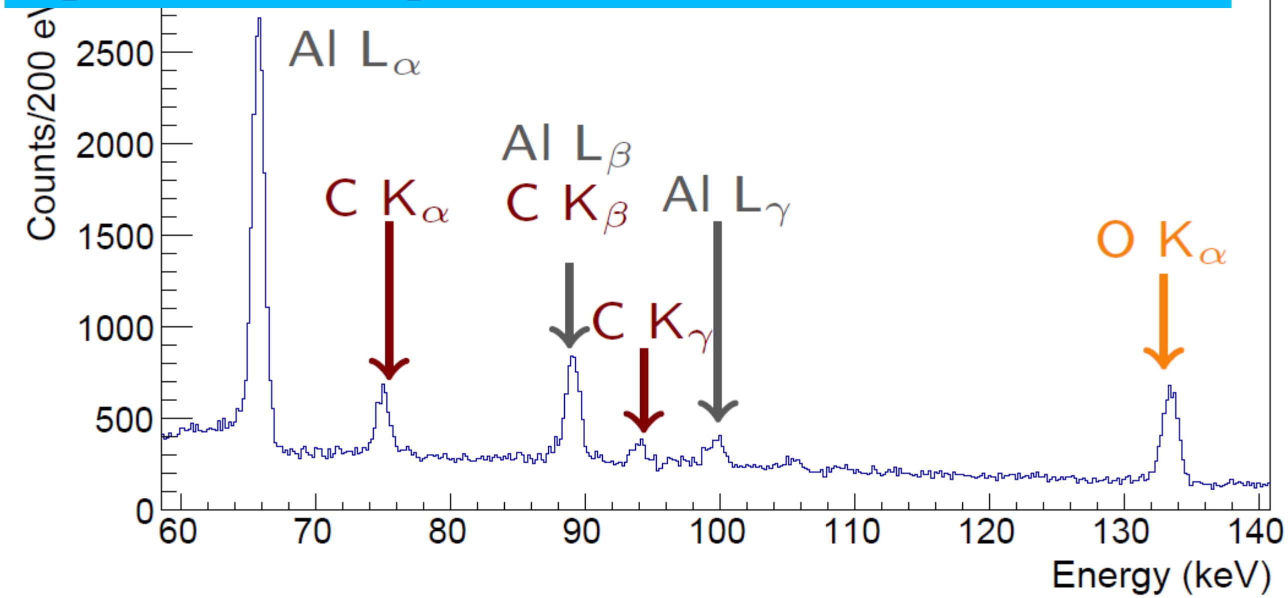

$LaBr_3$(5%Ce) scintillating crystals

$H_2 + (4\%\ w/v)CO_2$ gas mixture in aluminium container

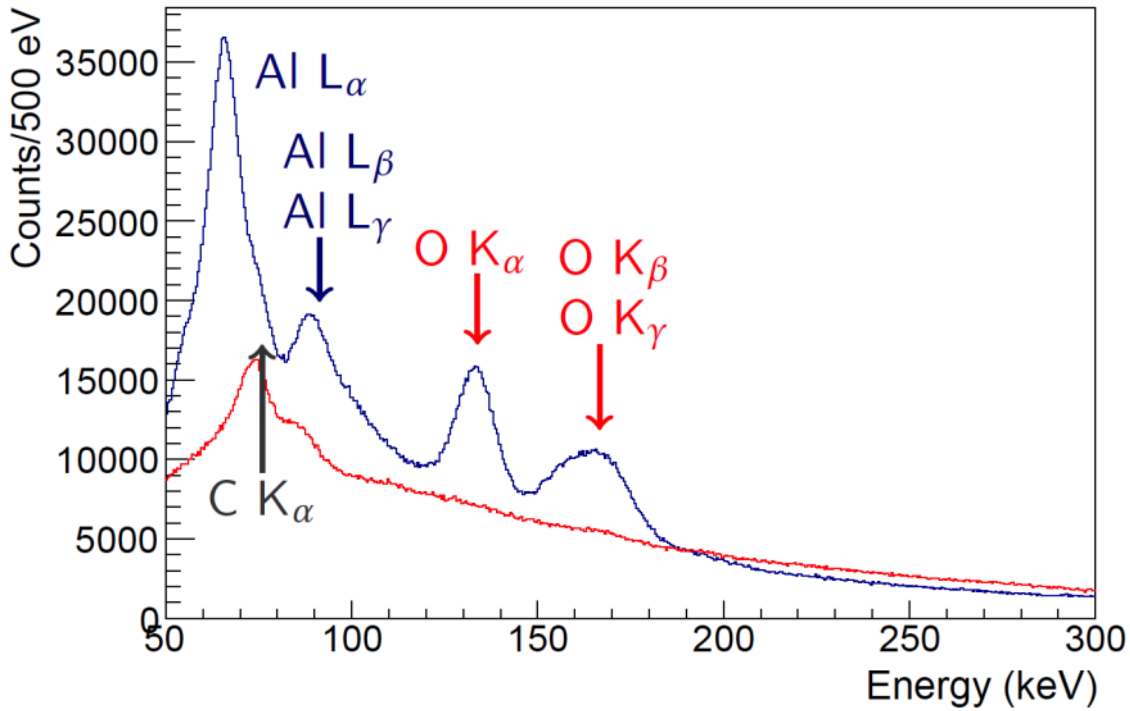

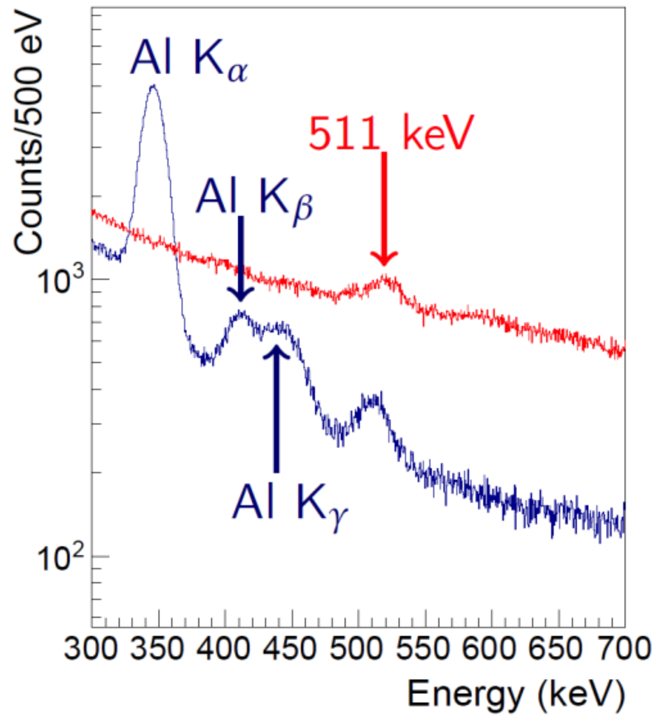

$LaBr_3$(5%Ce) scintillating crystals

$H_2 + (4\% \text{ w/v})CO_2$ gas mixture in aluminium container

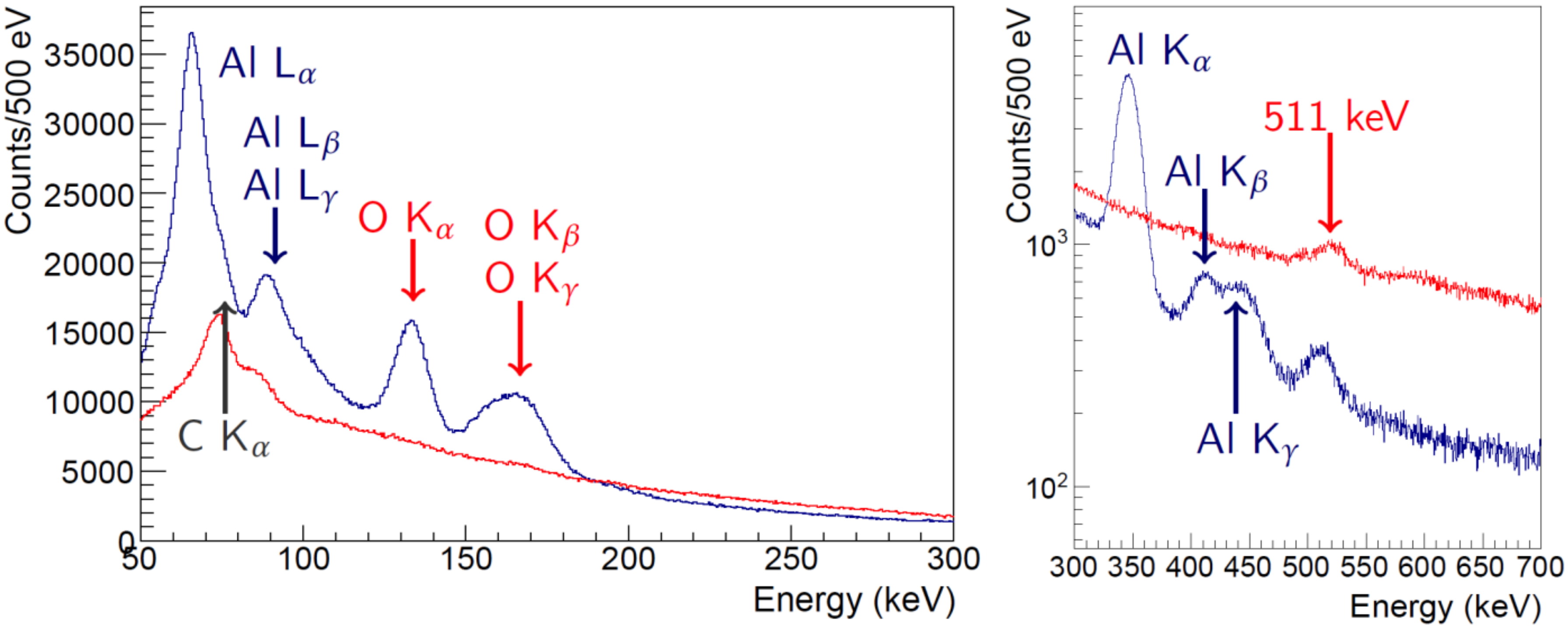

LaBr$_3$(5%Ce) scintillating crystals

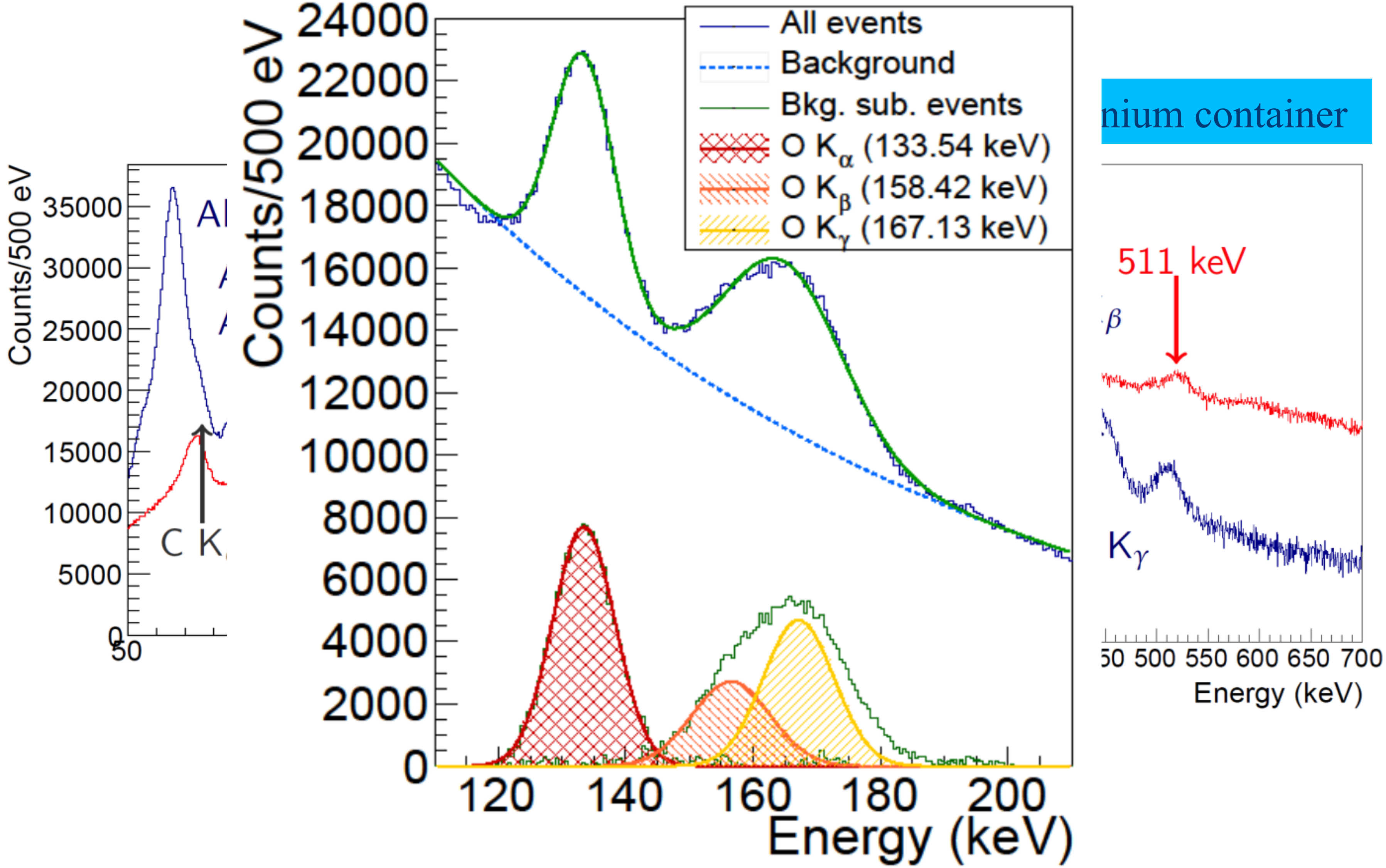

Muonic transfer rate measurement

$\mu p + Z \Rightarrow \mu Z + p$

Time spectrum: peaks and tails

Beam time structure

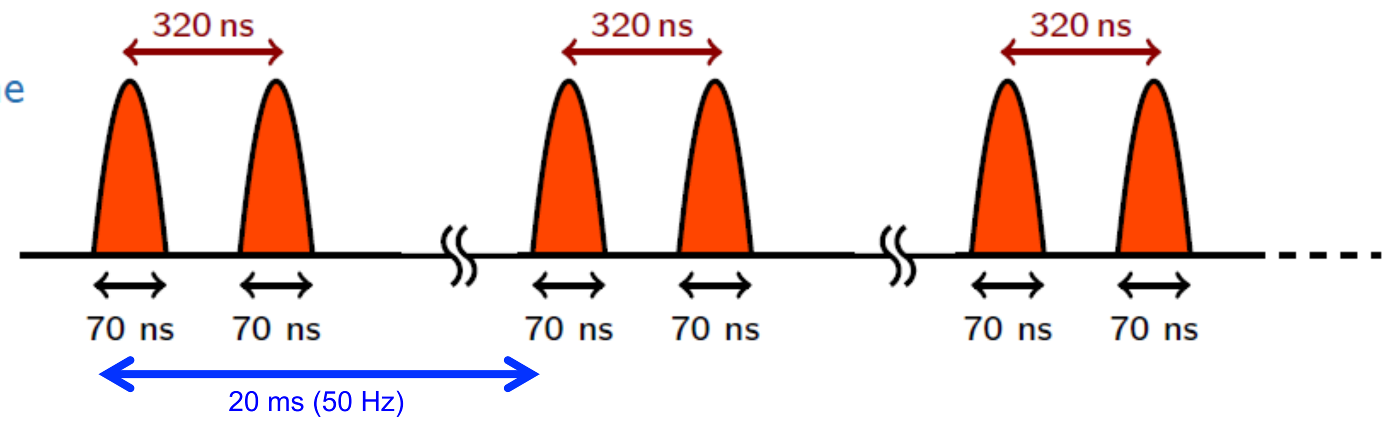

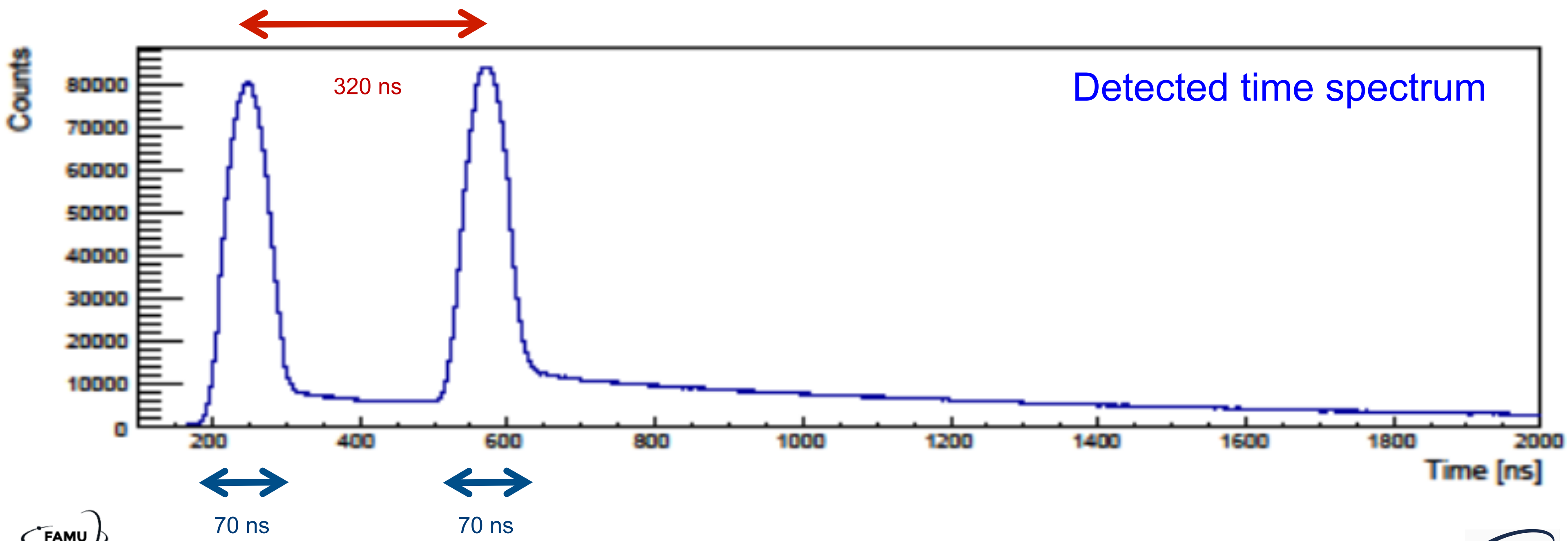

Peaks: prompt emission of X-rays

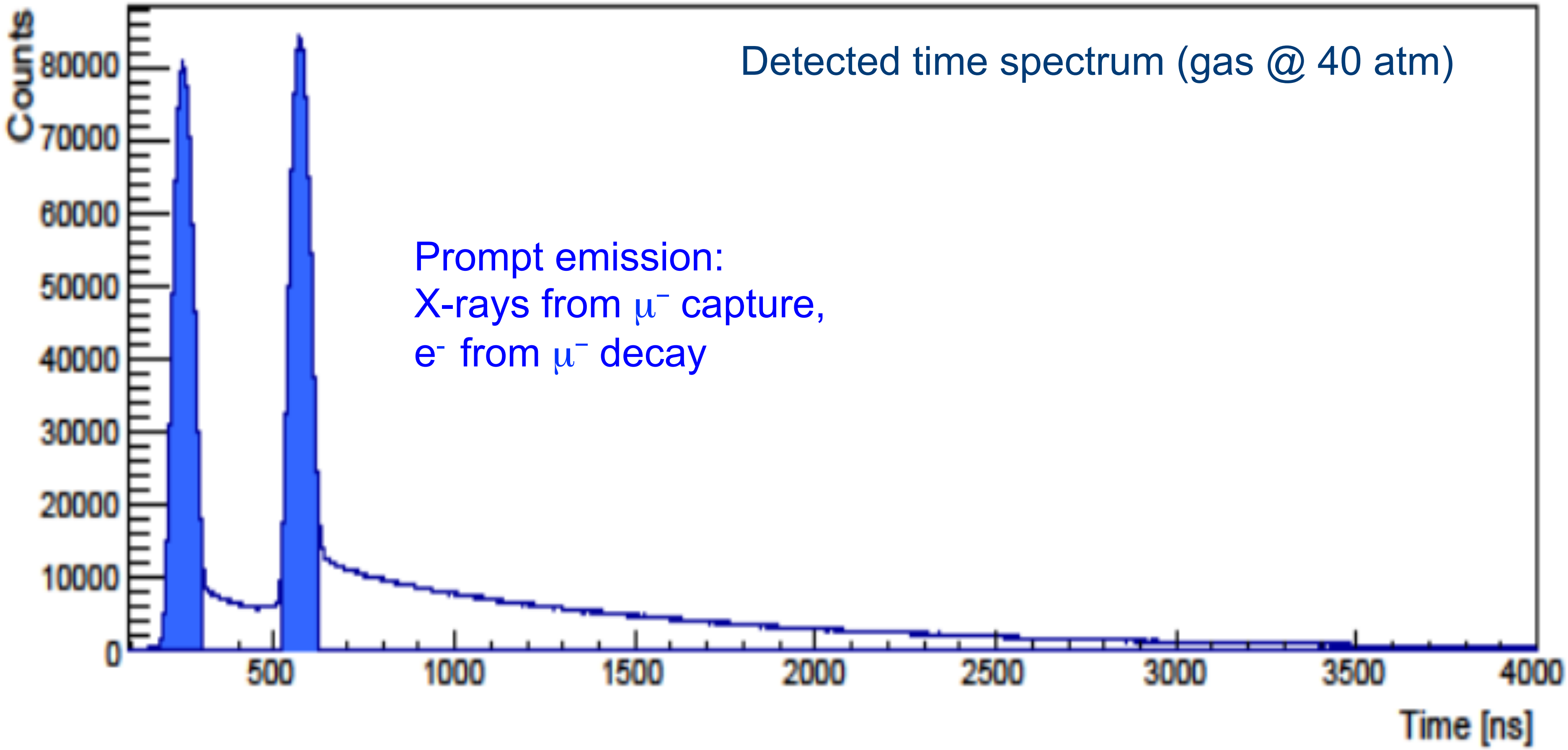

Tails: (bounded) muon live time

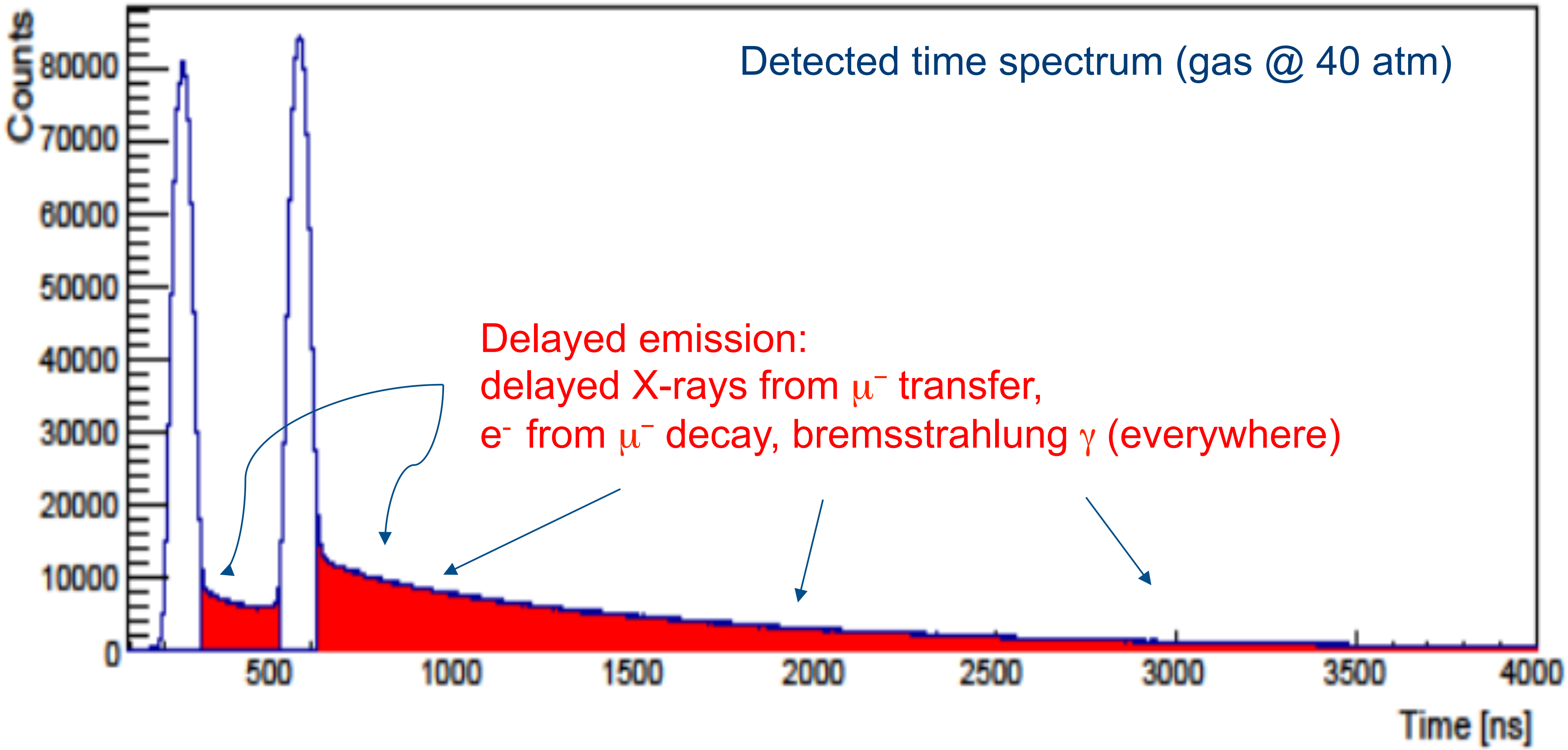

2016: transfer rate measurement

Steps:

1) fix a target temperature (i.e. mean kinetic energy of gas constant)
2) produce μp and wait for thermalization
3) study time evolution of Oxygen X-rays
4) repeat with different temperature

2016: transfer rate measurement

Steps:

1) fix a target temperature (i.e. mean kinetic energy of gas constant)
2) produce μp and wait for thermalization
3) study time evolution of Oxygen X-rays
4) repeat with different temperature

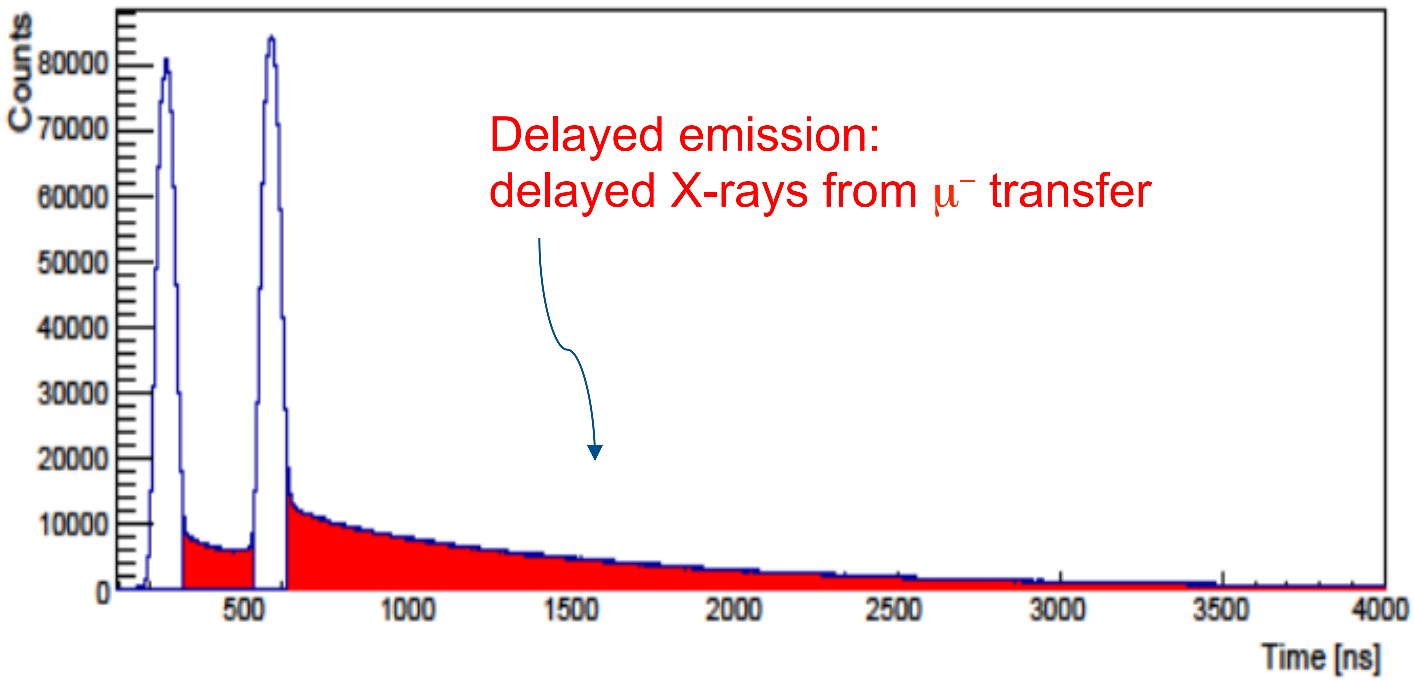

2016: transfer rate measurement

3) study time evolution of Oxygen X-rays

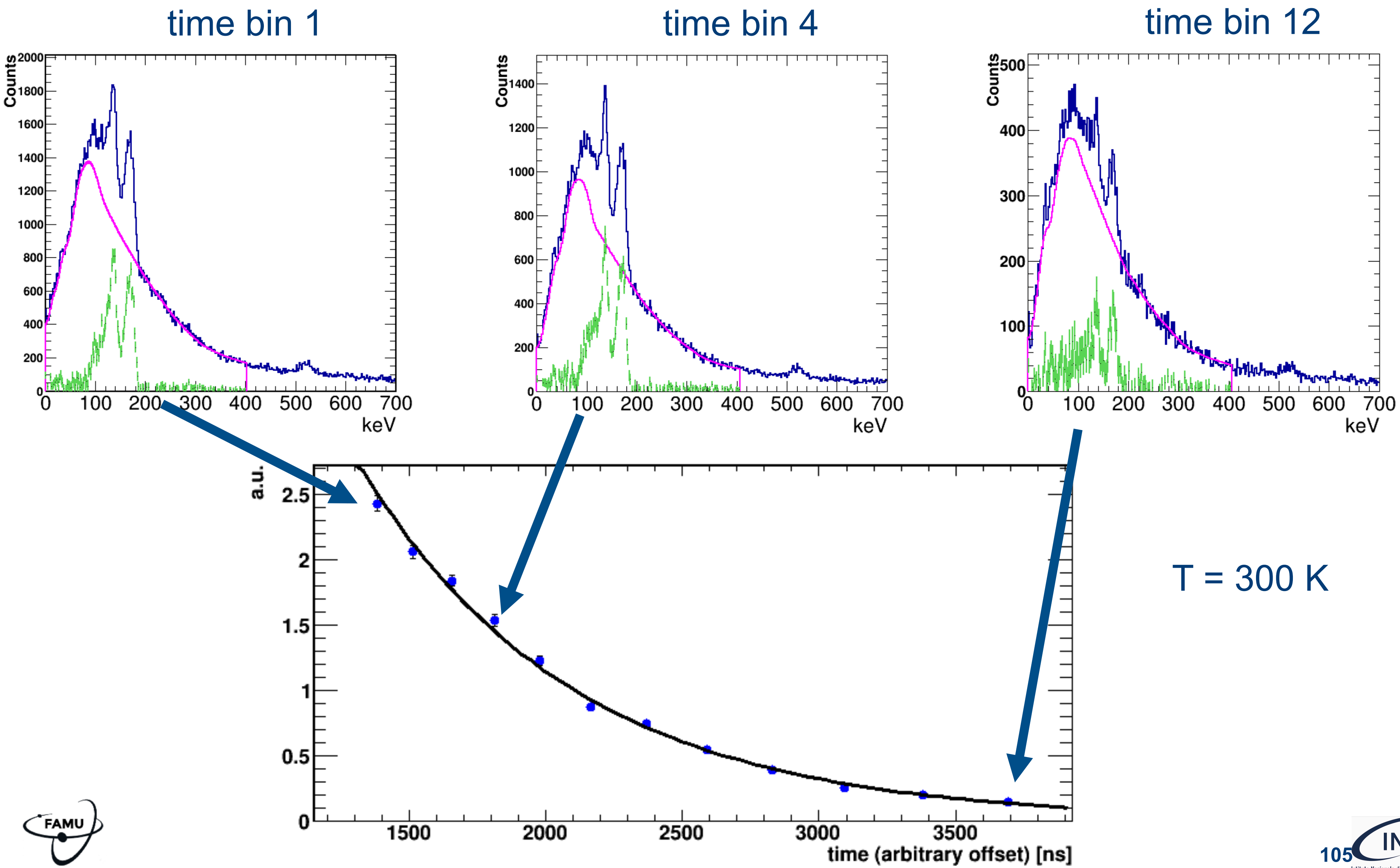

T = 300 K

2016: transfer rate measurement

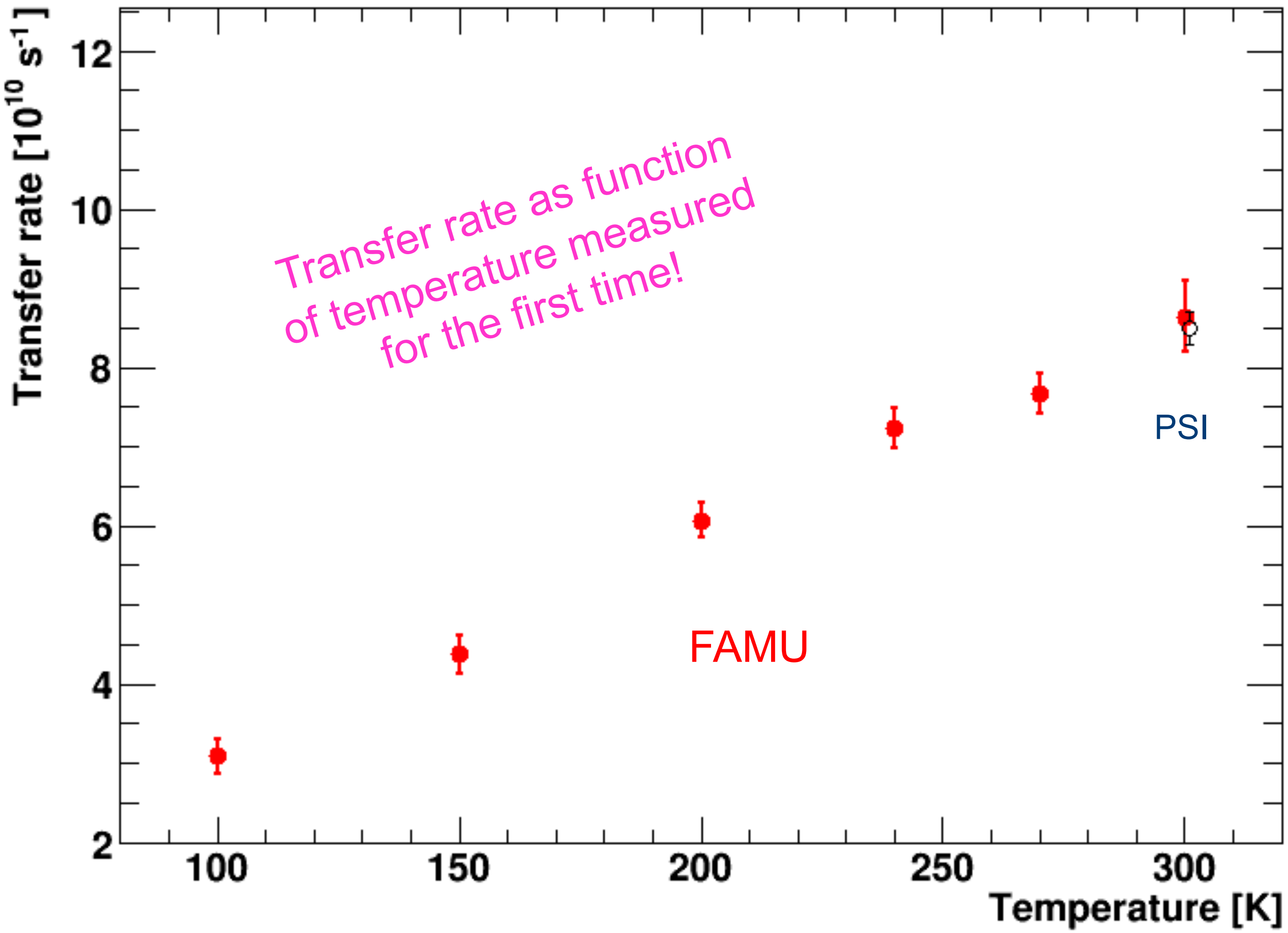

LaBr & HpGe

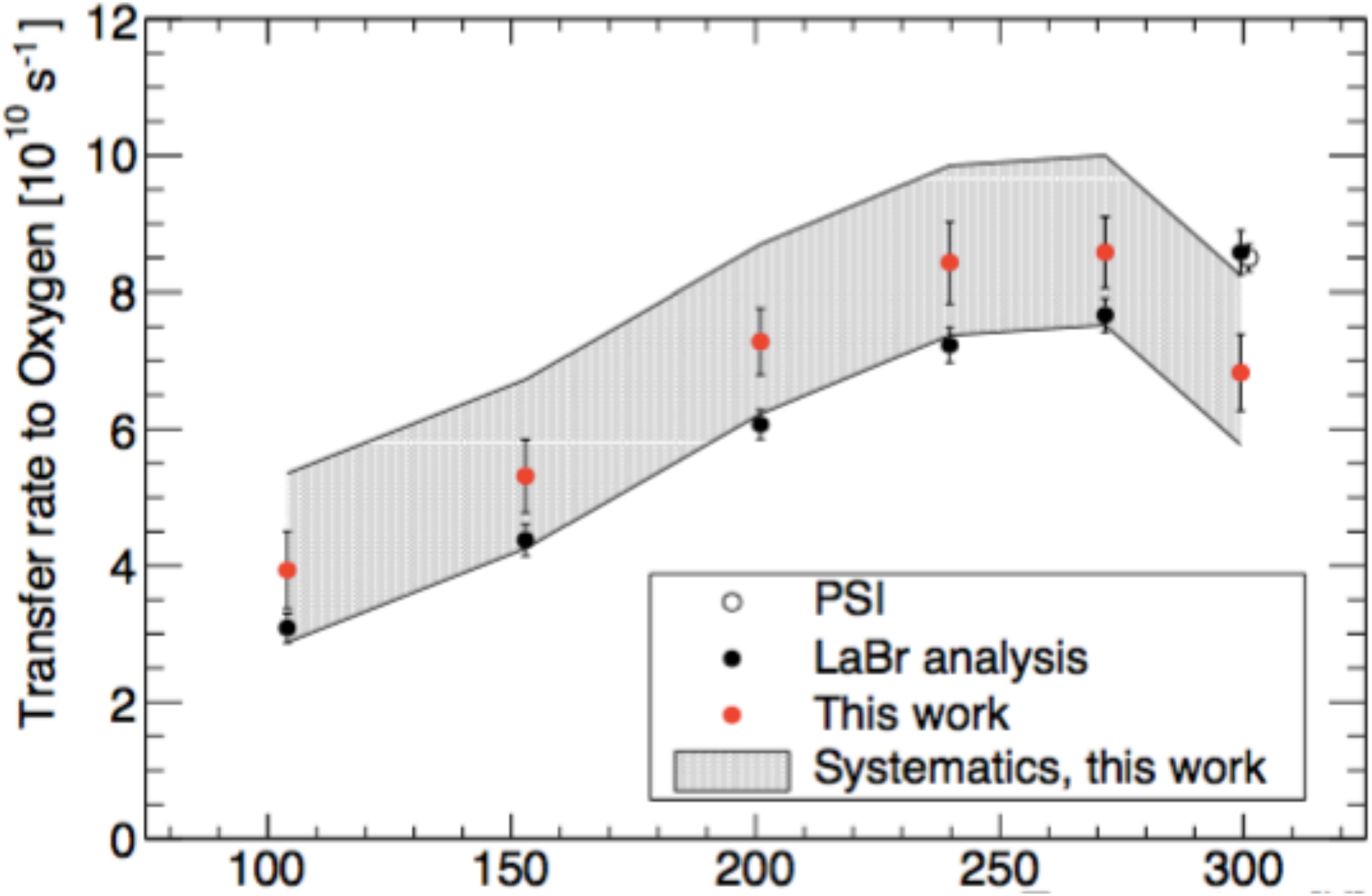

Transfer rate to Oxygen [10^{10} s^{-1}]
12
10
8
6
4
2
0
100
150
200
250
300
PSI
LaBr analysis
This work
Systematics, this work

Transfer rate up to 120 meV

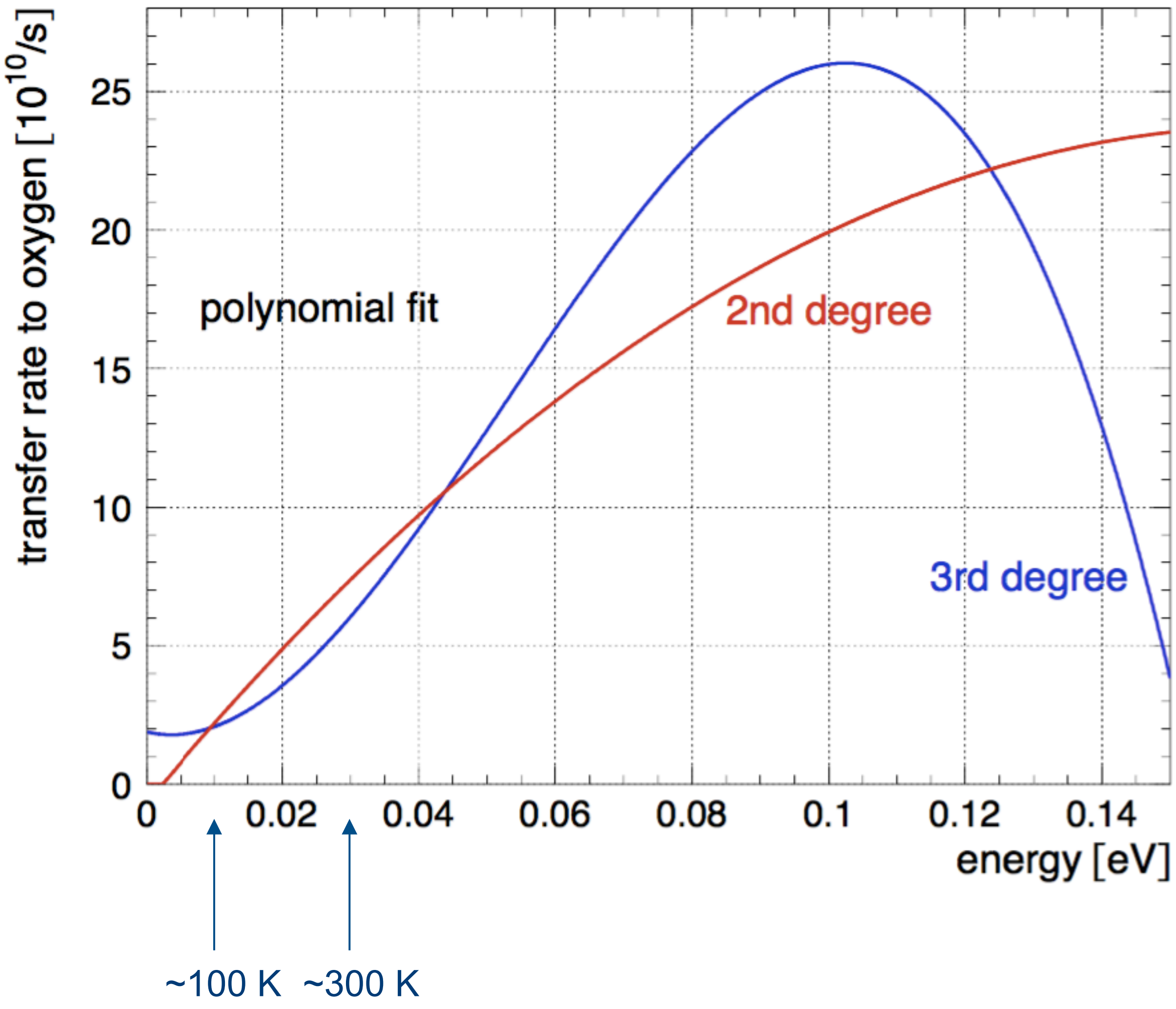

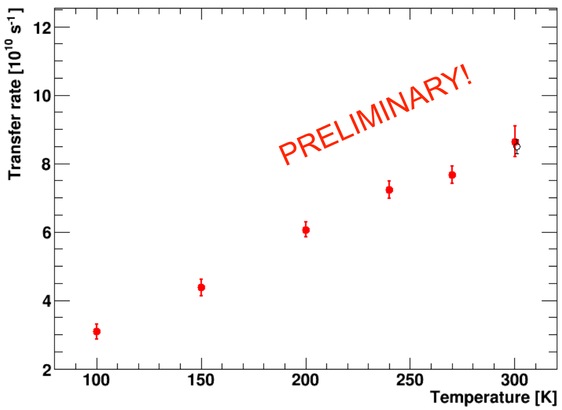

Transfer rate up to 120 meV

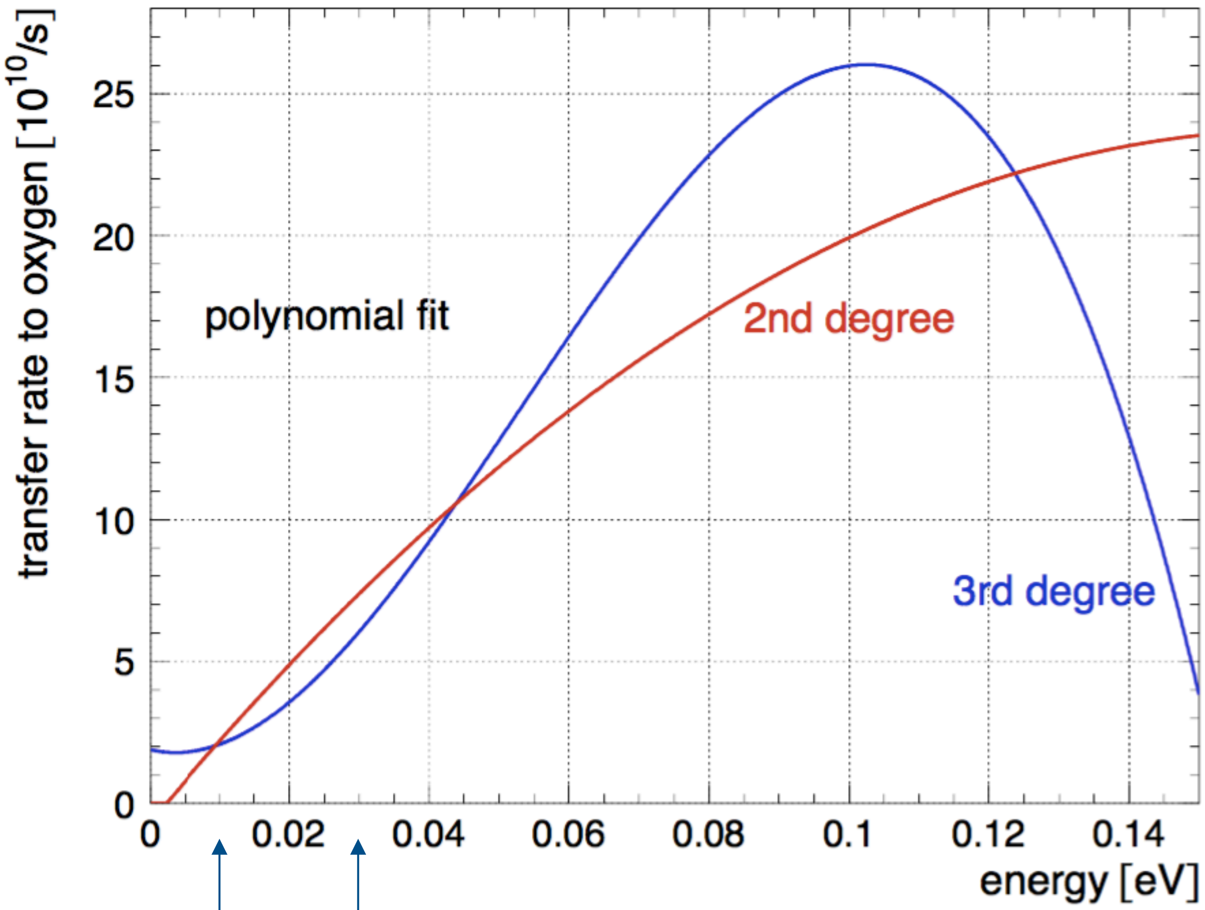

~100 K ~300 K

μp energy
after laser pulse

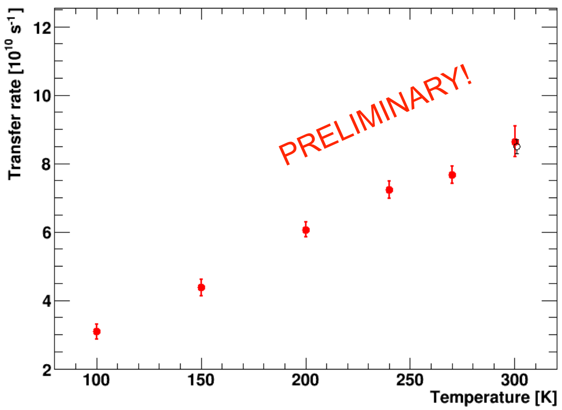

INFN
Istituto Nazionale di Fisica Nucleare

Study of best setup to maximize signal

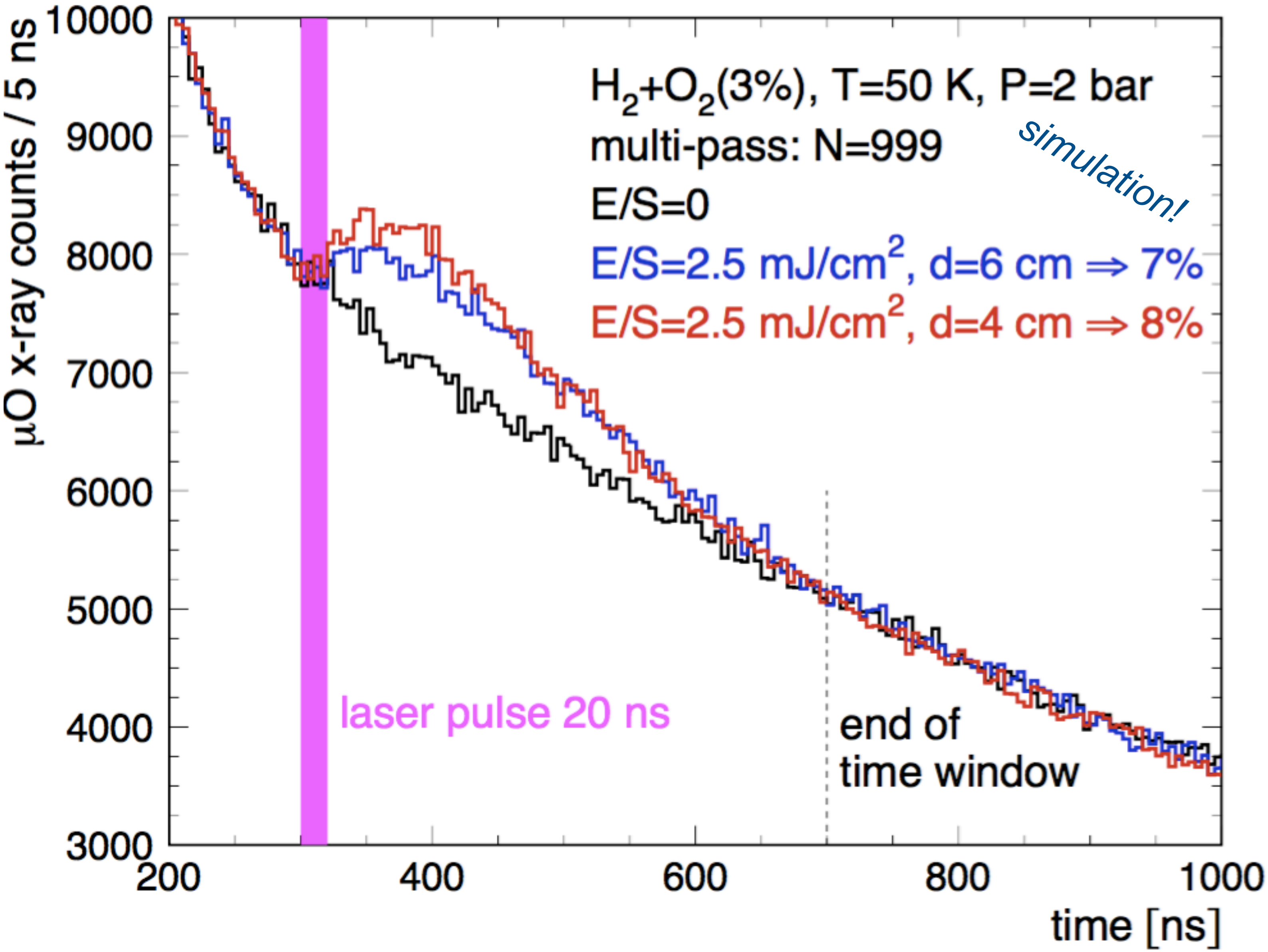

2018 target solution under study

Affinamento studio

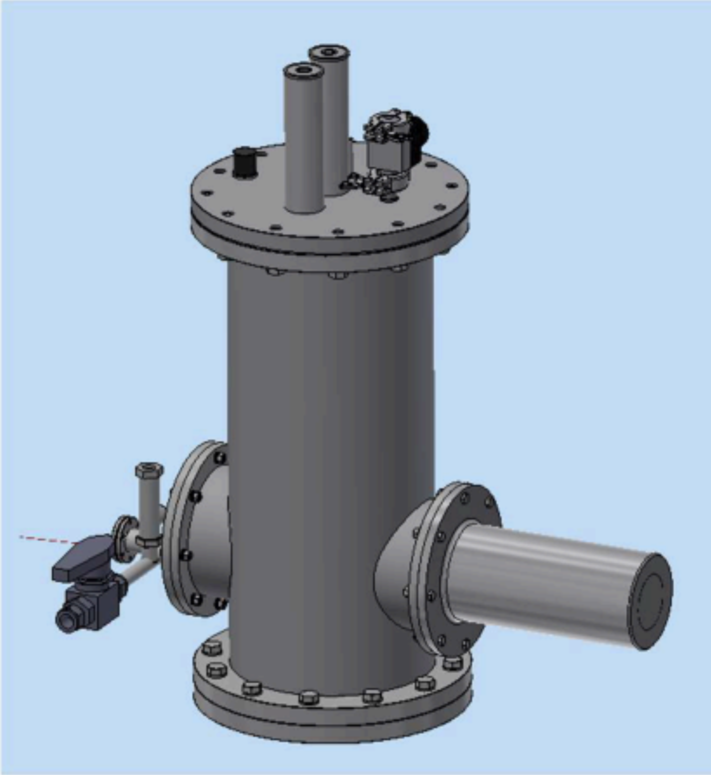

Analizzata la possibilità di evitare la flangia di estremità del Target

Studio copertura Target

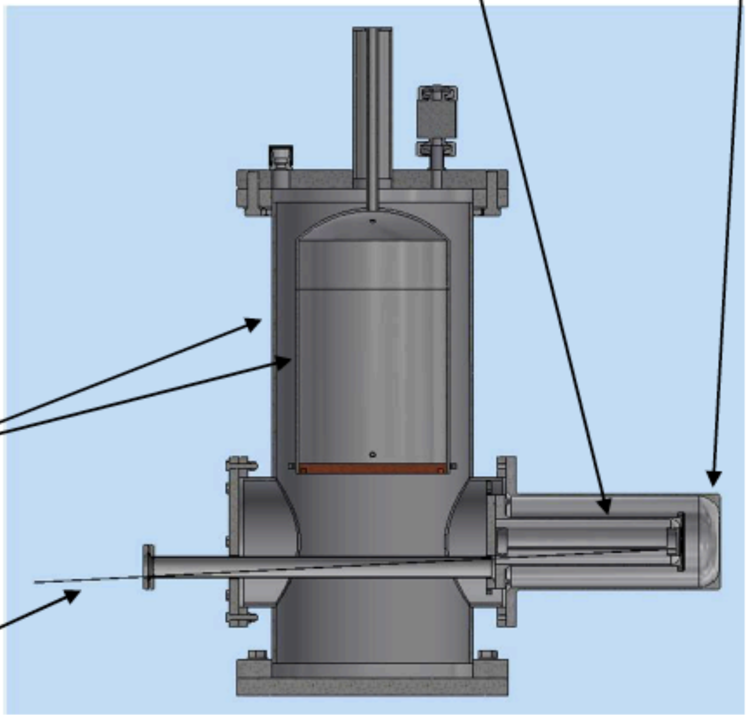

Nell'ottica di ridurre la lunghezza di percorso del laser, i diametri del criostato e del serbatoio sono stati ridotti a scapito della loro altezza

Analizzato percorso laser con inclinazione 0.050 rad

Target

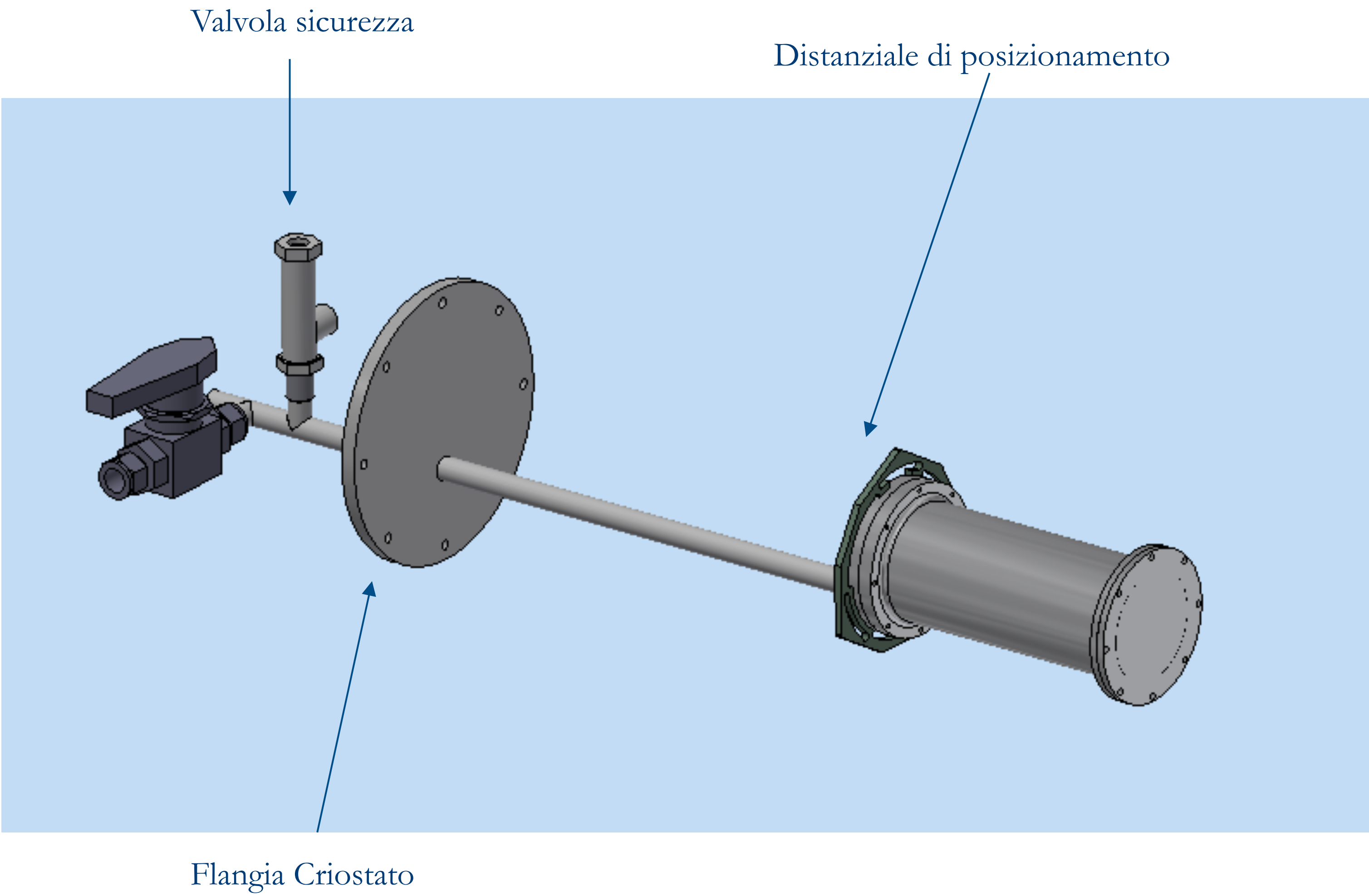
Valvola sicurezza
Distanziale di posizionamento
Flangia Criostato

Criotec IMPIANTI S.p.A.

Target - Layout

Valvola sicurezza

Distanziale di posizionamento

IPOTESI con specchi autoportanti fissati alla flangia

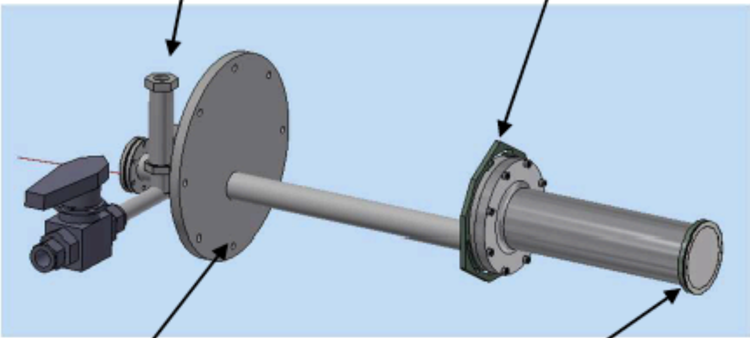

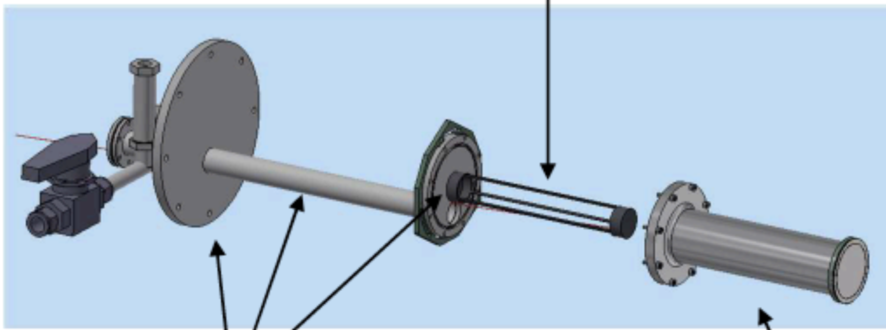

Flangia Criostato

Schermi termici Alluminio / PTFE

Parti in acciaio

Parti in alluminio senza flangia di estremità

Laser con inclinazione di 0.050 rad

RICHIESTE:

- possibilità di ridurre angolo massimo del laser (magari a 0.030 rad) in modo ridure i diametri del tubo e della flangia del Target

Target - Dettaglio

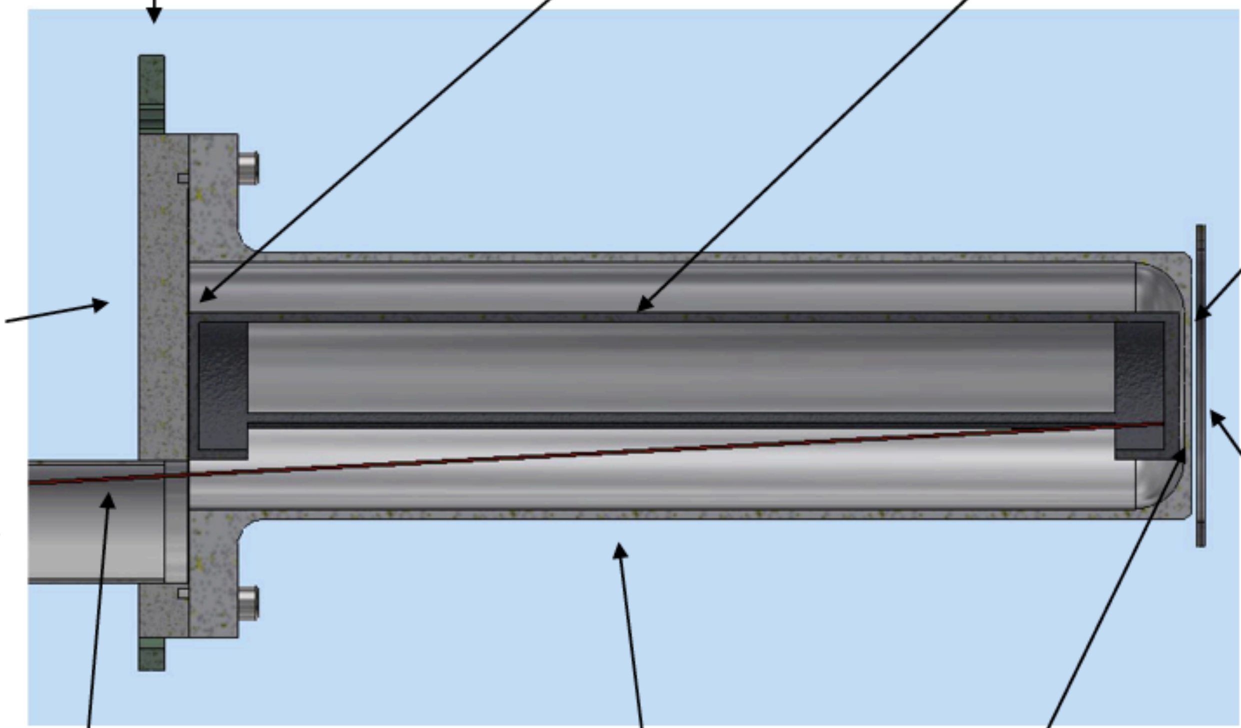

Muons beam density

GEOV07R0180K2BH2O2
like 2016 target (GEOV06R05300K40AH2O2) but with:

- gas : H2 O2(3%) (density: 0.877 kg/m3) temperature : 80 K
  pressure : 2 BAR
  berillium flange (vacuum vessel) : 0.3 mm aluminium entrance window : 0.5 mm
- no hodoscope
- no coating on entrance window (NB: in this version coating volumes just changed the material not the name nor the shape, hence there is a sub- mm shape distortion at the edges)

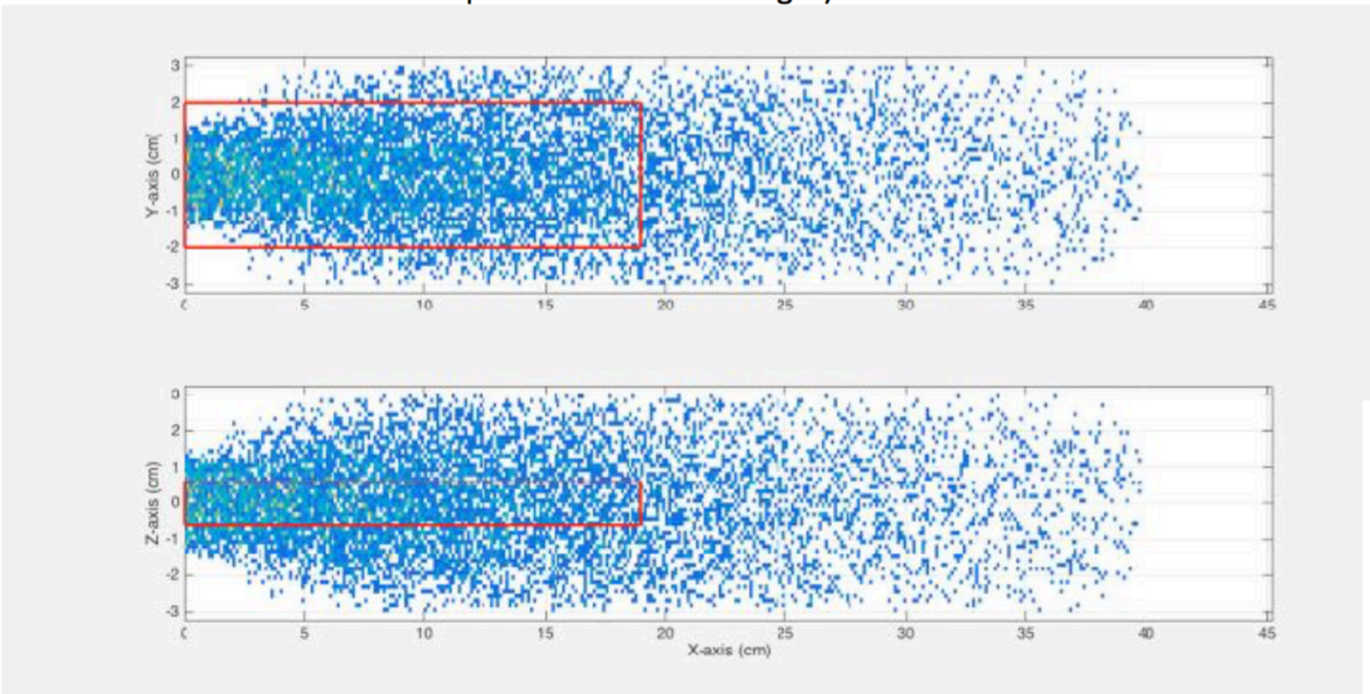

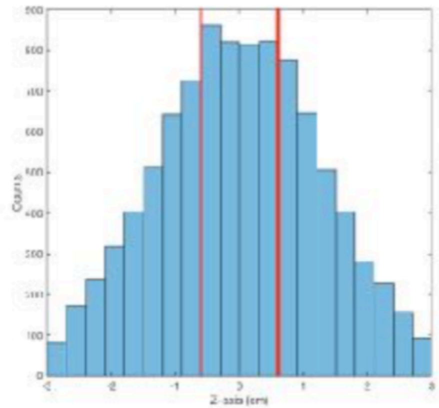

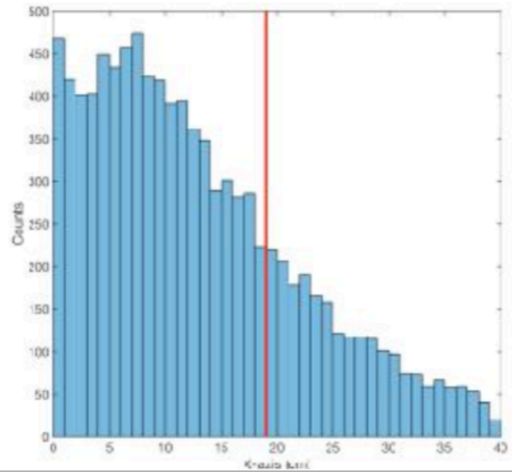

From Emiliano, july 2017.

Measurement plan

- From data analysis:
  - about 10 muon transferred events were observed per second per detector: with 16 detectors ~2 10^6 events/(3 hours) are expected.
- From simulations:
  - laser shot: ~6% event excess, i.e. about 10^5 events/(3 hours), enough statistics at a given fixed laser frequency.

➡ 6 hours = one step (0.1 nm) – half signal (laser), half background (no laser)

Rough scan: 420 hours to acquire 70 different laser frequencies.

Fine scan around resonance peak: 180 hours, 30 different laser frequencies.

Total time (with setup and preparation): ~40 days

Summary

- FAMU: investigation of the proton radius puzzle with HFS of $(\mu^{-}p)_{1S}$

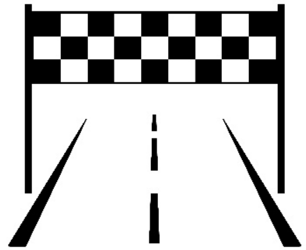

- An exciting journey:
  - started *25 years ago*
  - *most intense pulsed beam* in the world
  - *best detectors* for energy and time observation
  - *first time measurement* of the muon transfer rate to Oxygen
  - *innovative* and powerful laser system

Looking forward to perform the final measurement!

the FAMU collaboration

JINST

PUBLISHED BY IOP PUBLISHING FOR SISSA MEDIALAB

RECEIVED: *April 5, 2016*
ACCEPTED: *April 11, 2016*
PUBLISHED: *May 12, 2016*

Steps towards the hyperfine splitting measurement of the muonic hydrogen ground state: pulsed muon beam and detection system characterization

The FAMU collaboration

A. Adamczak,[a] G. Baccolo,[b] D. Bakalov,[c] G. Baldazzi,[d] R. Bertoni,[b] M. Bonesini,[b] V. Bonvicini,[e] G. Campana,[d] R. Carbone,[e] T. Cervi,[g,h] F. Chignoli,[b] M. Clemenza,[b] L. Colace,[i,j] A. Curioni,[b] M. Danailov,[e,f] P. Danev,[c] I. D'Antone,[d] A. De Bari,[g,h] C. De Vecchi,[h] M. De Vincenzi,[i,k] M. Furini,[d] F. Fuschino,[d] K.S. Gadedjisso-Tossou,[e,l] D. Guffanti,[e] A. Iaciofano,[i] K. Ishida,[m] D. Iugovaz,[e] C. Labanti,[d] V. Maggi,[b] A. Margotti,[d] M. Marisaldi,[d] R. Mazza,[b] S. Meneghini,[d] A. Menegolli,[g,h] E. Mocchiutti,[e] M. Moretti,[b] G. Morgante,[d] R. Nardò,[h] M. Nastasi,[b] J. Niemela,[l] E. Previtali,[b] R. Ramponi,[n] A. Rachevski,[e] L.P. Rignanese,[d] M. Rossella,[h] P.L. Rossi,[d] F. Somma,[i,o] M. Stoilov,[c] L. Stoychev,[e,l] A. Tomaselli,[h,p] L. Tortora,[i] A. Vacchi,[e,q,1] E. Vallazza,[e] G. Zampa[e] and M. Zuffa[d]

[a] *Institute of Nuclear Physics, Polish Academy of Sciences, Radzikowskiego 152, Kraków, PL31342 Poland*
[b] *National Institute for Nuclear Physics (INFN), Sezione di Milano Bicocca, Piazza della Scienza 3, Milano, Italy*
[c] *Institute for Nuclear Research and Nuclear Energy, Bulgarian Academy of Sciences,*

2016 JINST 11 P05007

Istituto Nazionale di Fisica Nucleare

Summary

The FAMU project represents the quantum leap towards the realization of the first, long awaited, measurement of

$\Delta E^{hfs}(\mu^{-}p)_{1S}$ the hyperfine splitting (hfs) in the 1S state of muonic hydrogen.

- An exciting journey:
  - started *25 years ago*
  - *most intense pulsed beam* in the world
  - *best detectors* for energy and time observation
  - *first time measurement* of the muon transfer rate to Oxygen
  - *innovative* and powerful laser system

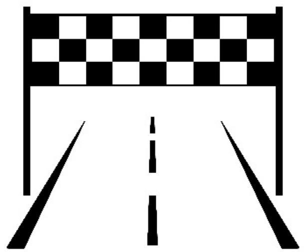

Looking forward to perform the final measurement!

Thanks!

INFN Istituto Nazionale di Fisica Nucleare

	Hydrogen		Muonic Hydrogen	
	magnitude	uncertainty	magnitude	uncertainty
E^{F}	1420 MHz	0.01 ppm	182.443 meV	0.1 ppm
δ^{QED}	$1.16\,10^{-3}$	$< 0.001\,10^{-6}$	$1.16\,10^{-3}$	10^{-6}
δ^{rigid}	$39\,10^{-6}$	$2\,10^{-6}$	$7.5\,10^{-3}$	$0.1\,10^{-3}$
δ^{recoil}	$6\,10^{-6}$	10^{-8}	$1,7\,10^{-3}$	10^{-6}
δ^{pol}	$1.4\,10^{-6}$	$0.6\,10^{-6}$	$0.46\,10^{-3}$	$0.08\,10^{-3}$
δ^{hvp}	10^{-8}	10^{-9}	$0.02\,10^{-3}$	$0.002\,10^{-3}$

The term δ^Z is related to the Zemach radius r_Z by means of

$$\delta^Z = 2\alpha\,(1+k) \times M_\mu M_p/(M_\mu + M_p)\ r_Z$$

$k=0.0152$ is a QED correction

δ^Z is approximately $\delta^Z = -7.3 \times 10^{-3}$.

Using phenomenological data the proton polarizability term δ^{pol} has been evaluated to $\delta^{pol} = (0.46 \div 0.08) \times 10^{-3}$

E. Cherednikova et al., Nucl. Phys. A703, 365 (2002).

The uncertainty in the value of the Zemach radius obtained with respect to r_Z is limited by the uncertainty of δ^{pol} to about 1%.
Knowing r_Z with the accuracy of $\delta r_Z = 0.01$ fm
will allow to confirm or reject the existence of any peculiarities in the μ-p interaction and assess a vision on the proton size puzzle.

note

- nuclear physics and metrology
- theory summary uncertainty evaluation
  - nuclear structure
  - two photon exchange
  - inelastic nuclear-nucleon polarizabilit
  - CJ @ TIFPA ECT*

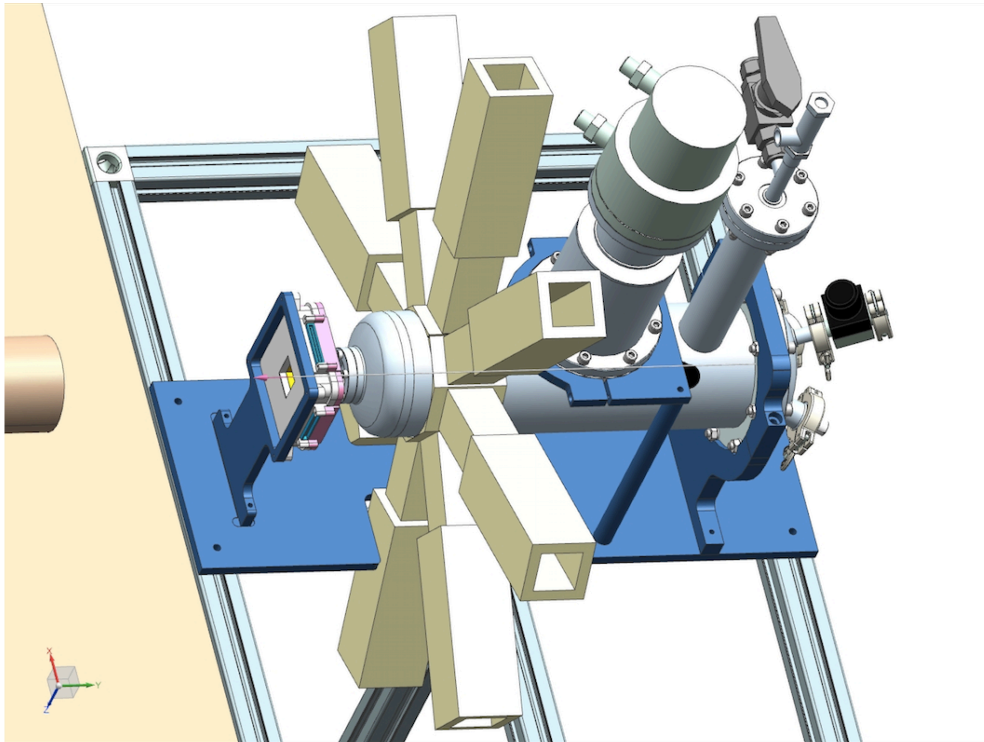

Andrea Vacchi

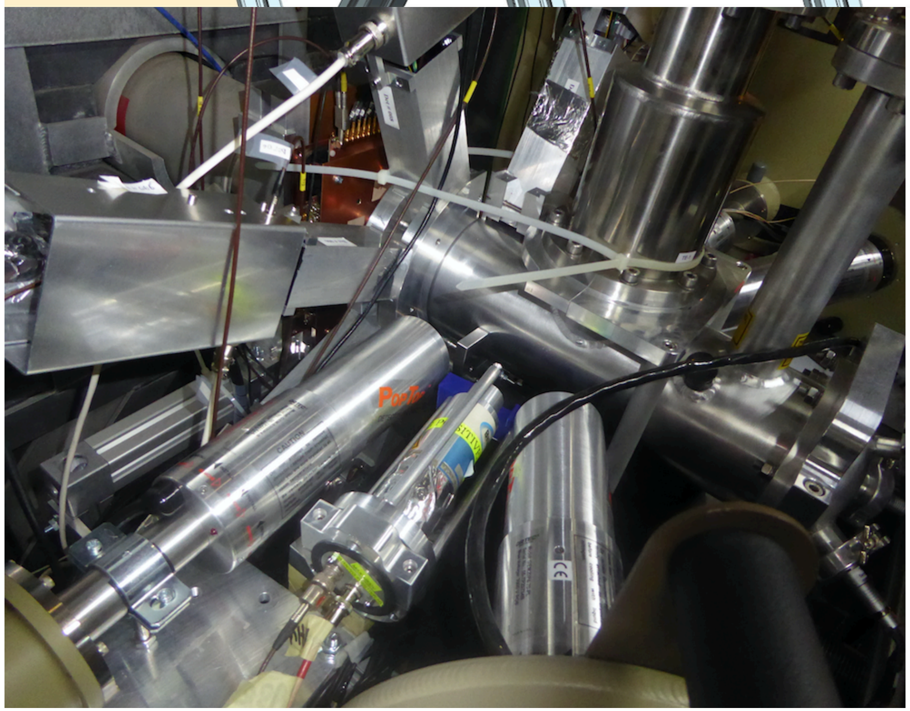

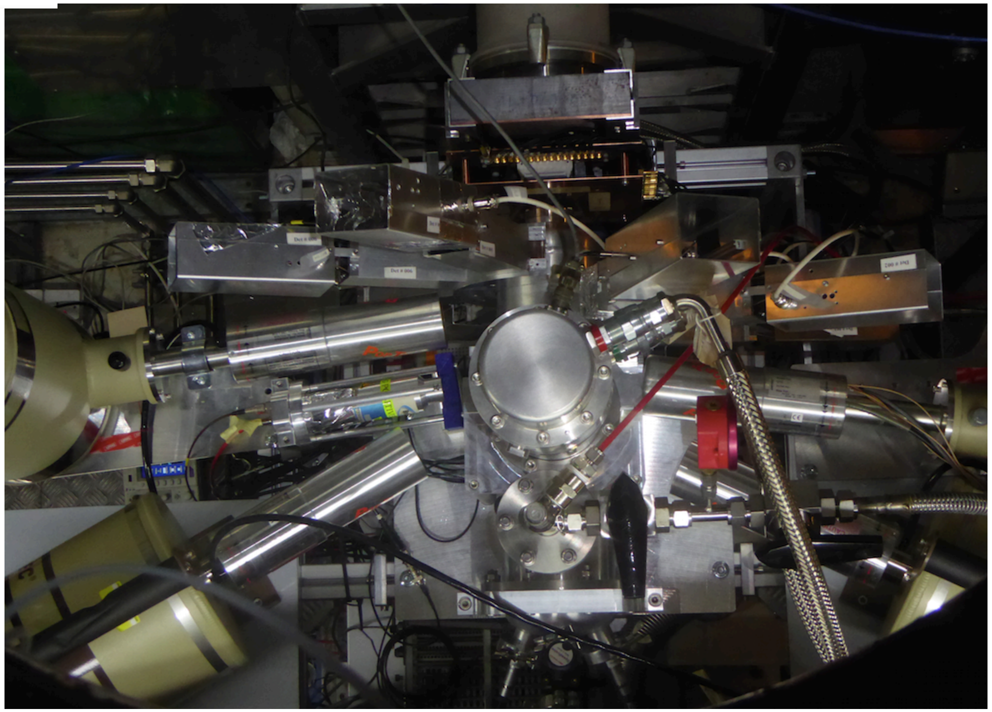

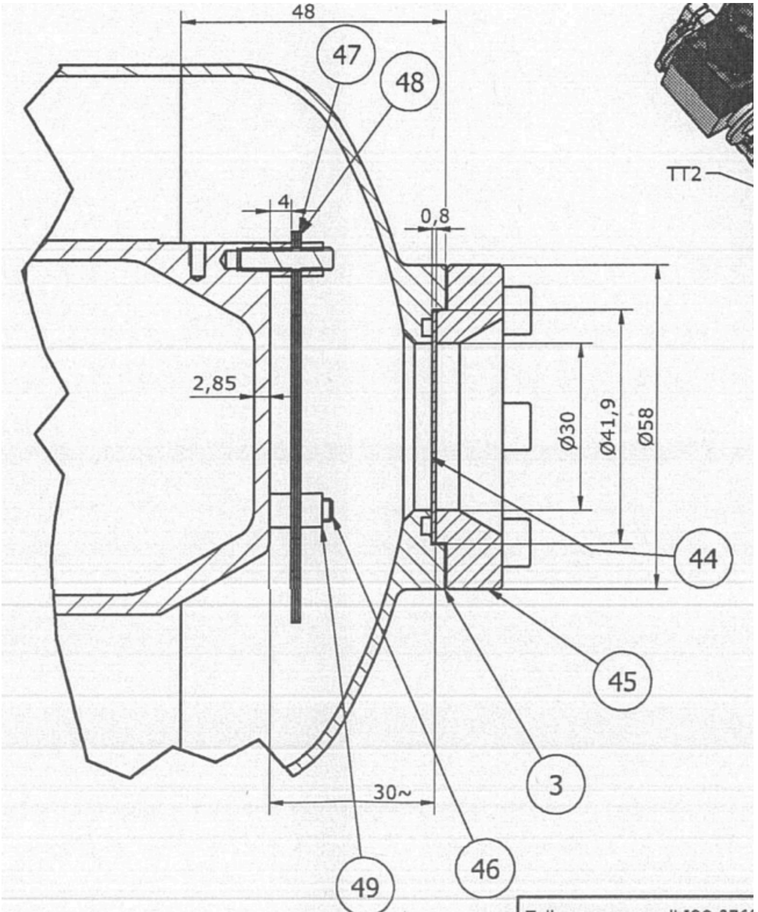

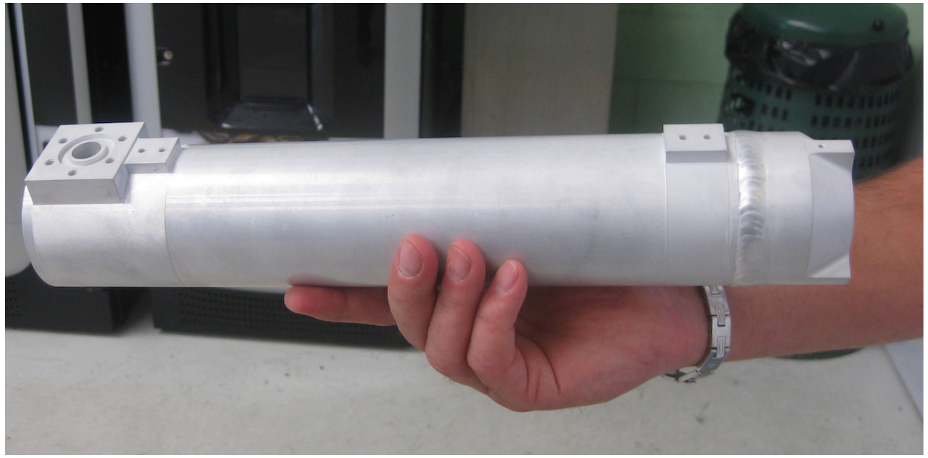

internal coating Ni+Au

nuclear capture of the muons in heavy nuclei is fast (less than 100 ns this eliminates the noise from muon decay electrons.

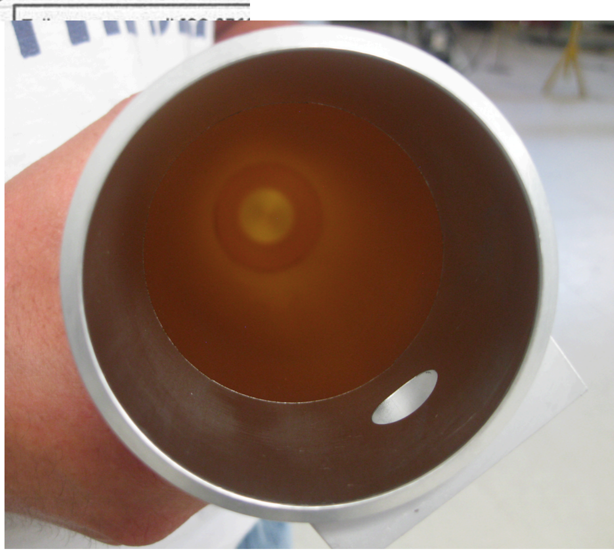

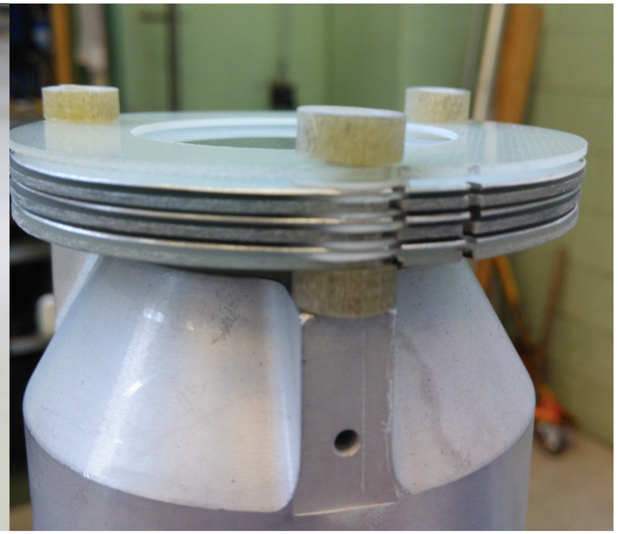

FAMU

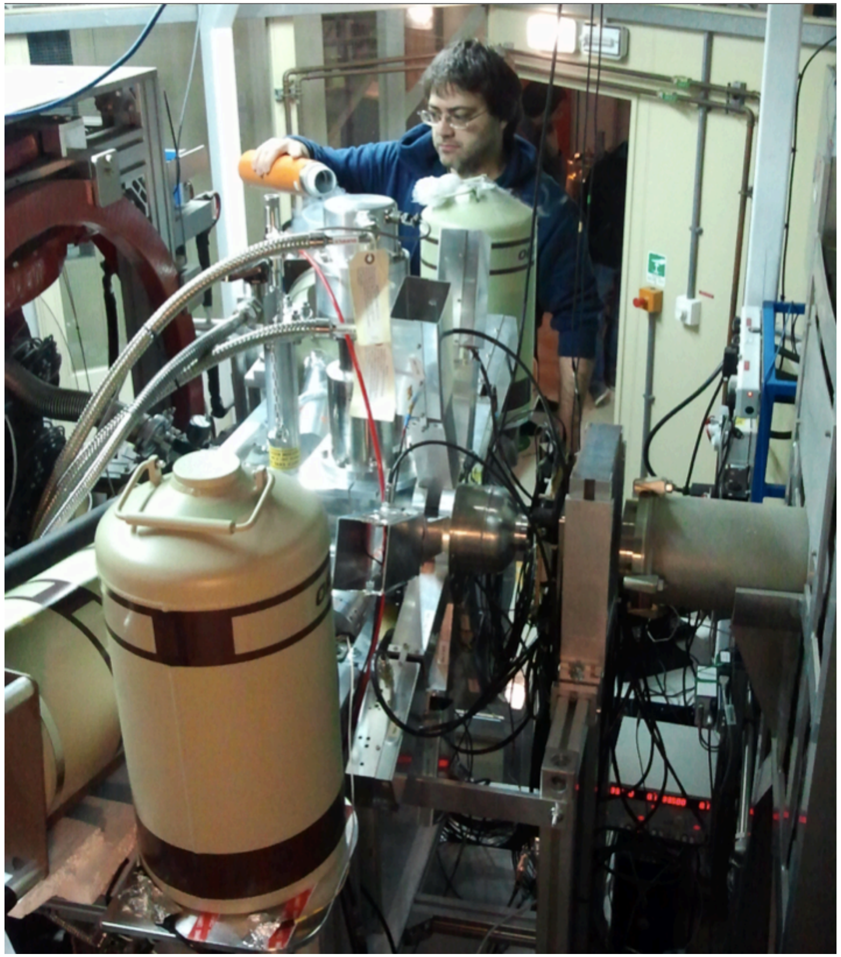

Gas system

critical aspects:

- pressure measurement precision
- gas mixture composition precision

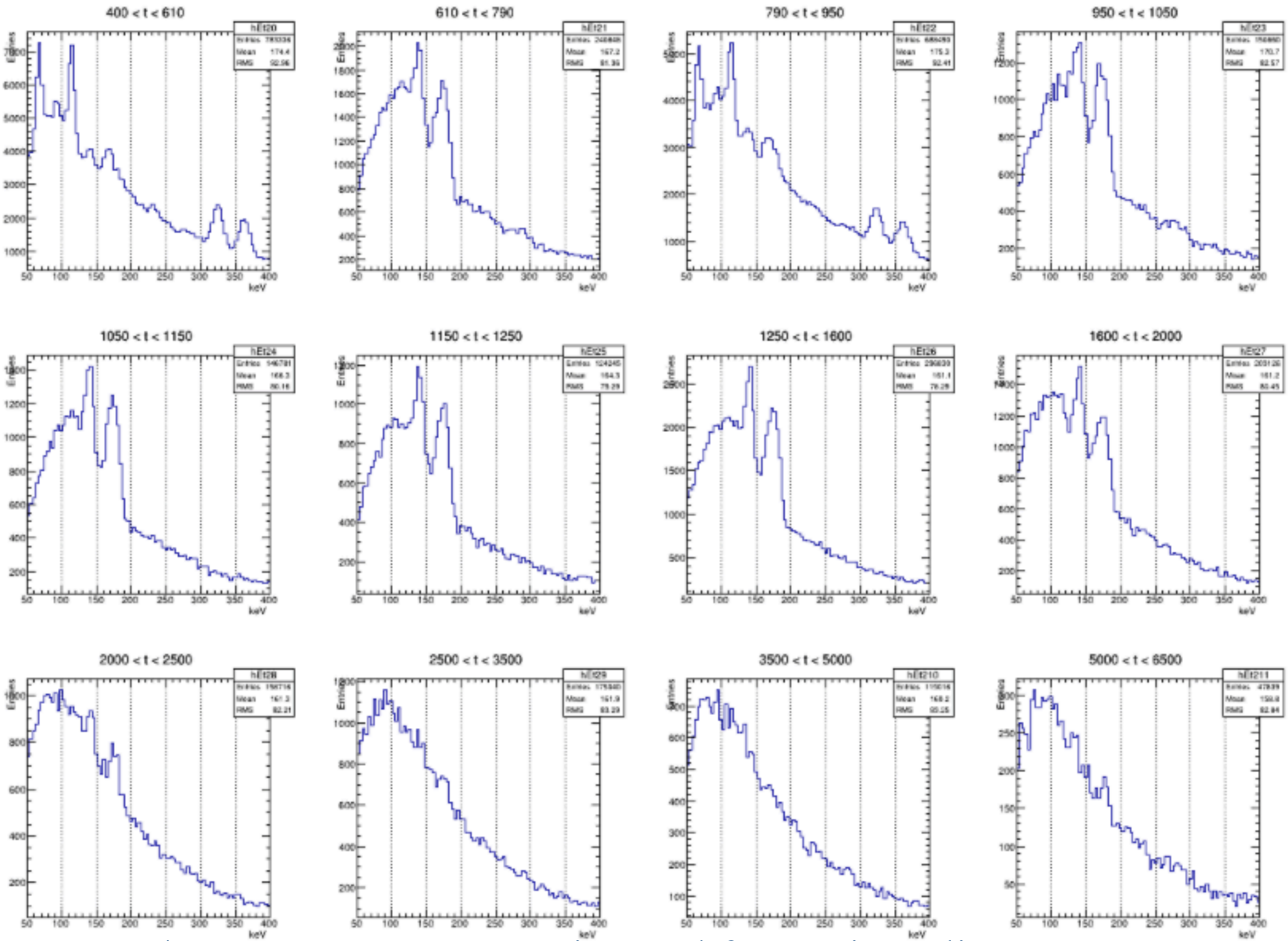

H/O2 1% energy spectra integral for 12 time slices

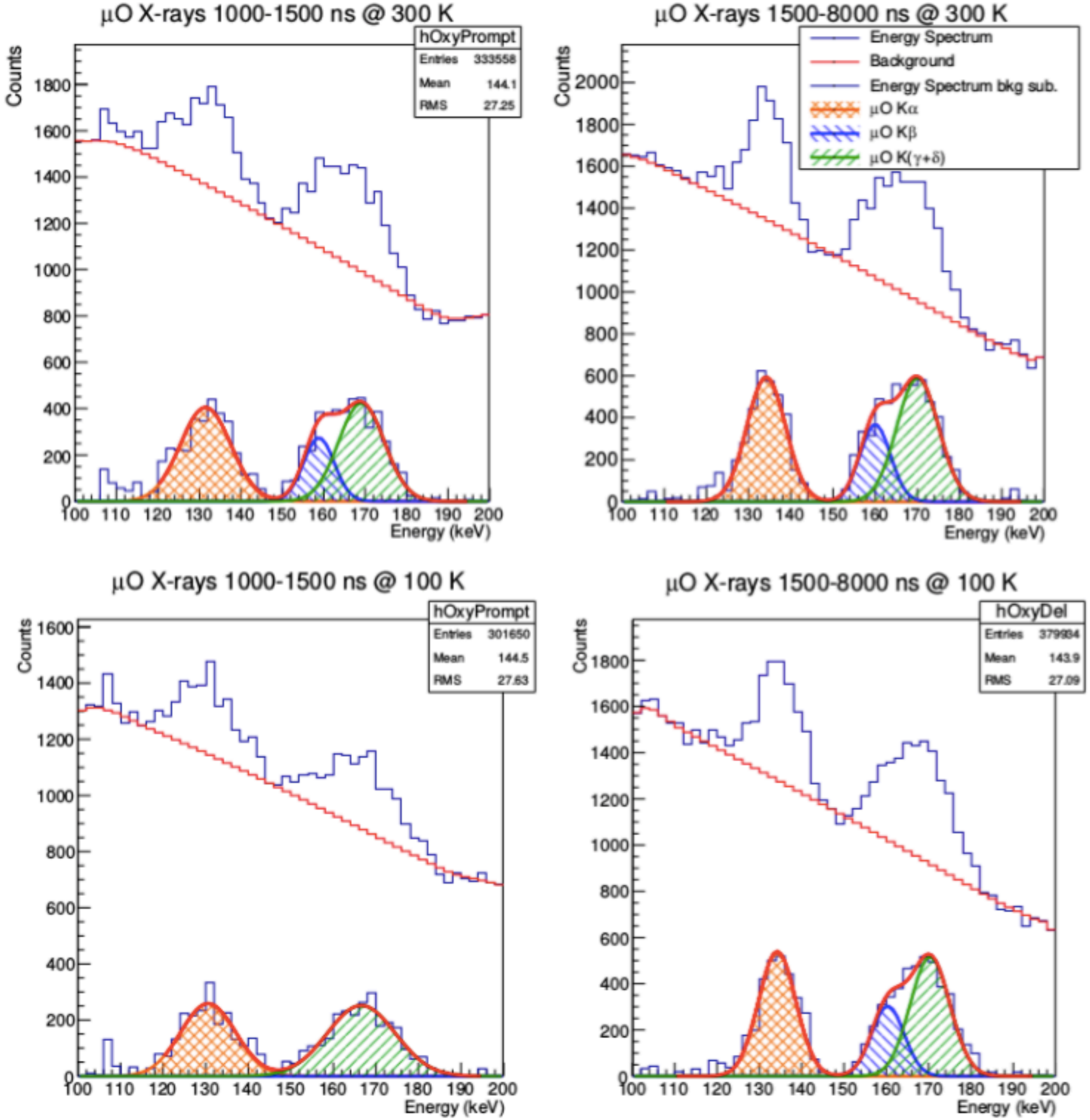
μO X-rays 1000-1500 ns @ 300 K
hOxyPrompt
Entries 333558
Mean 144.1
RMS 27.25
μO X-rays 1500-8000 ns @ 300 K
Energy Spectrum
Background
Energy Spectrum bkg sub.
μO Kα
μO Kβ
μO K(γ+δ)
μO X-rays 1000-1500 ns @ 100 K
hOxyPrompt
Entries 301650
Mean 144.5
RMS 27.63
μO X-rays 1500-8000 ns @ 100 K
hOxyDel
Entries 379934
Mean 143.9
RMS 27.09
Counts
Energy (keV)

Energy spectrum – H2O2(0.3%) – HPGe GLP

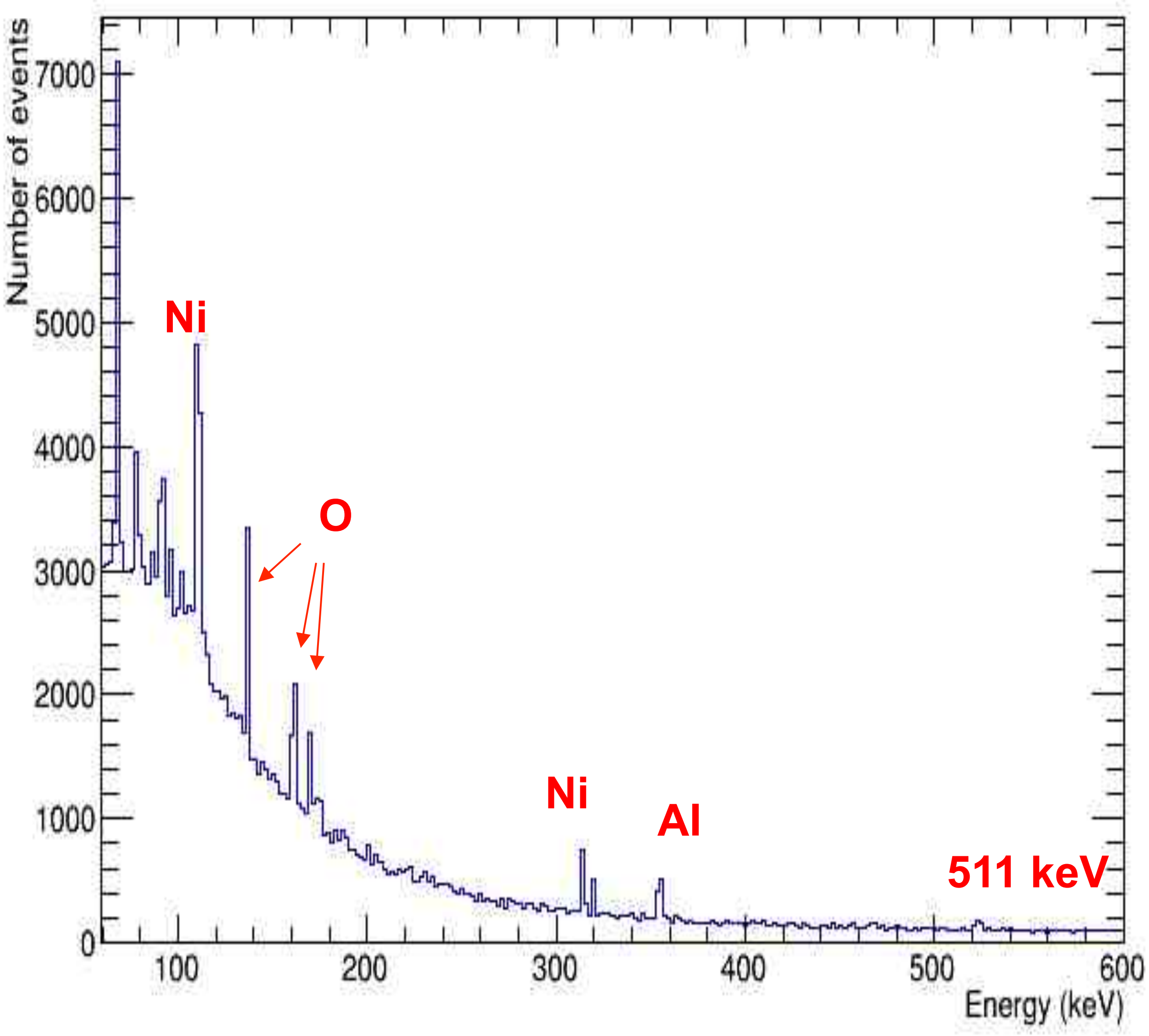

concluding

- Beam and detectors characterization concluded
- Study of the transfer in gas mixture at different temperatures and concentrations done – analysis on going
- Laser in procurement phase
- experiment on a solid ground

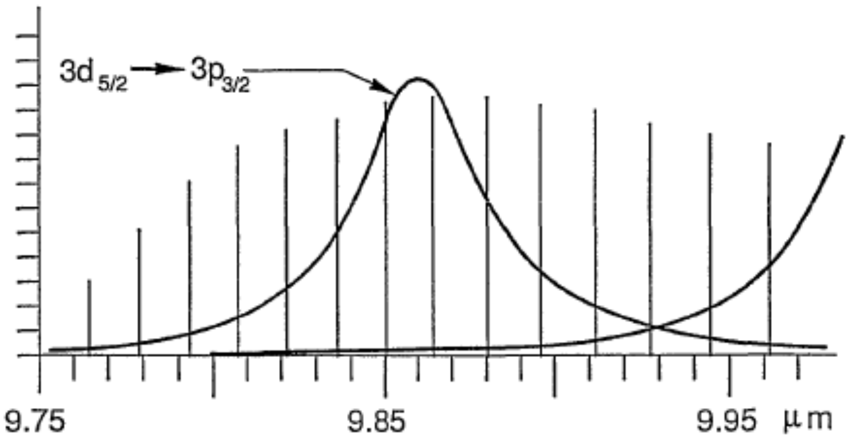

Fig. 4 : $^{13}C\,^{18}O_2$ laser transitions: 001-020 [II] P branch.

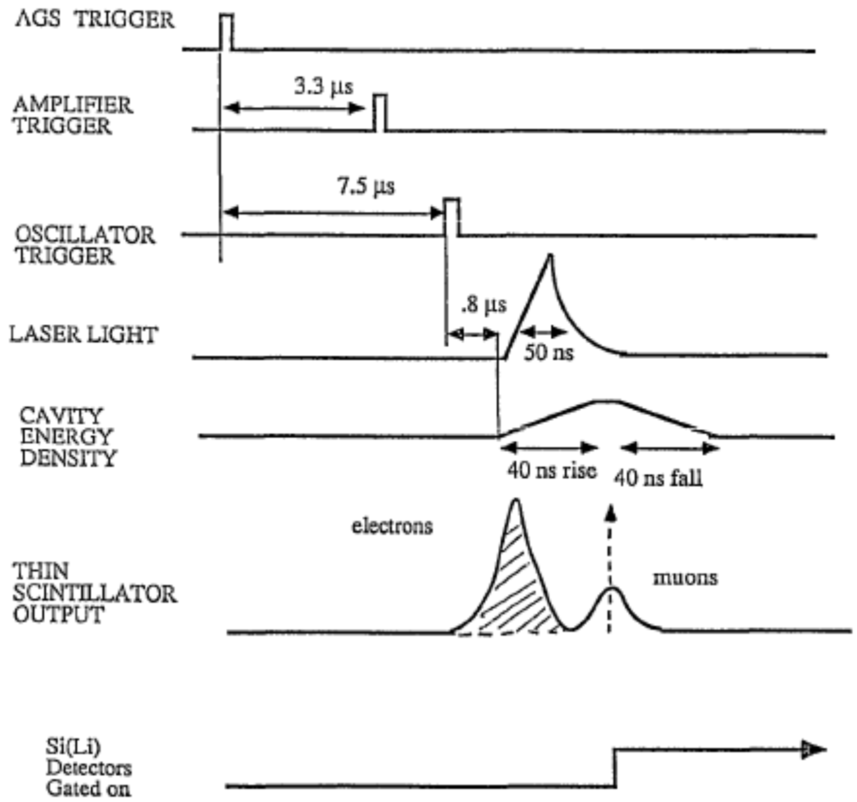

Fig. 5 : Timing of laser system.

Table 2. MUST's Gantt chart.

Year	$1_{(1/2)}$	$1_{(2/2)}$	$2_{(1/2)}$	$2_{(2/2)}$	$3_{(1/2)}$	$3_{(2/2)}$	$4_{(1/2)}$	$4_{(2/2)}$
WP 1 - implementation complete simulation software								
1.1 implementation of the complete simulation software								
WP 2 - Development of final spectroscopic gas target								
2.1 optical cavity characterization & integration								
2.2 laser + opt. path safety study and assessment.								
2.3 final gas target assembly of the lay-out including, optical path and multi-pass cavity								
2.4 RIKEN-RAL preliminary data collection new target-cavity								
WP 3 - Development of the MUST laser source								
3.1 procurement of MUST upgrade laser system for > 5 mJ								
3.2 integration and calibration of the final laser system								
WP 4 - Muon beam and X-ray detecting system								
4.1 LaBr & HPGe detector's elements procurement								
4.2 LaBr & HPGe detectors progressive assembly and test								
4.3 Silicon Drift Detectors SDD beam monitor assembly								
4.4 integration, diagnostics and calibration detectors system								
WP 5 - Measurement of μH HFS of and r_Z								
5.1 first spectroscopy run resonance search								
5.2 high statistics data collecting sessions								
5.3 preliminary data analysis and study of systematics								
5.4 second tour of data collection								
5.5 data analysis, and theory simulations preliminary results								
6.6 determination of the Zemach radius of the proton								

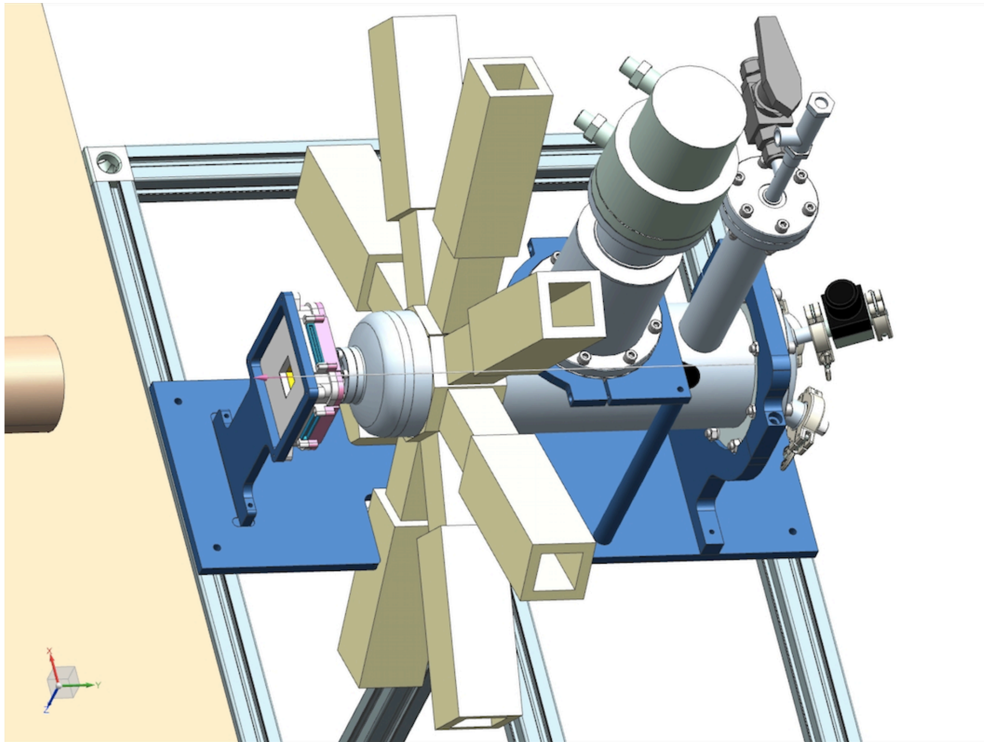
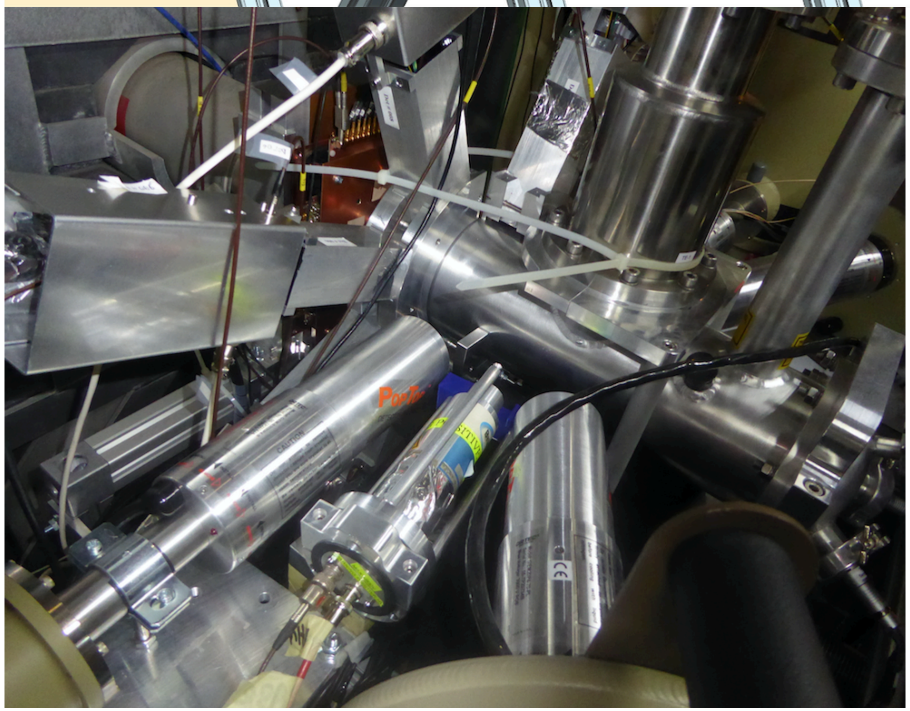
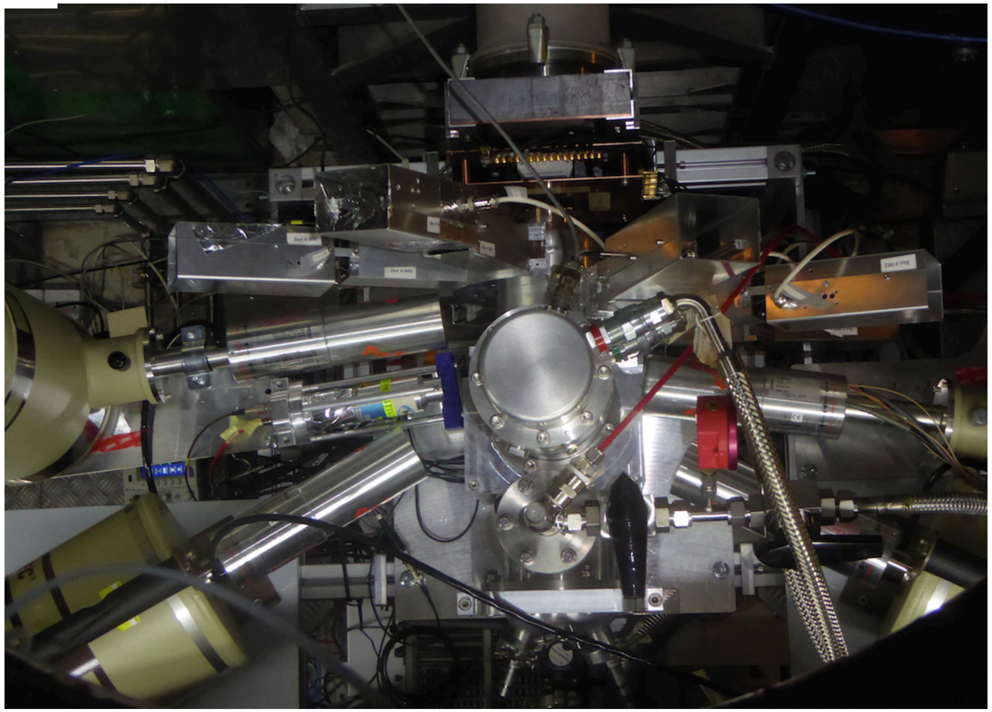

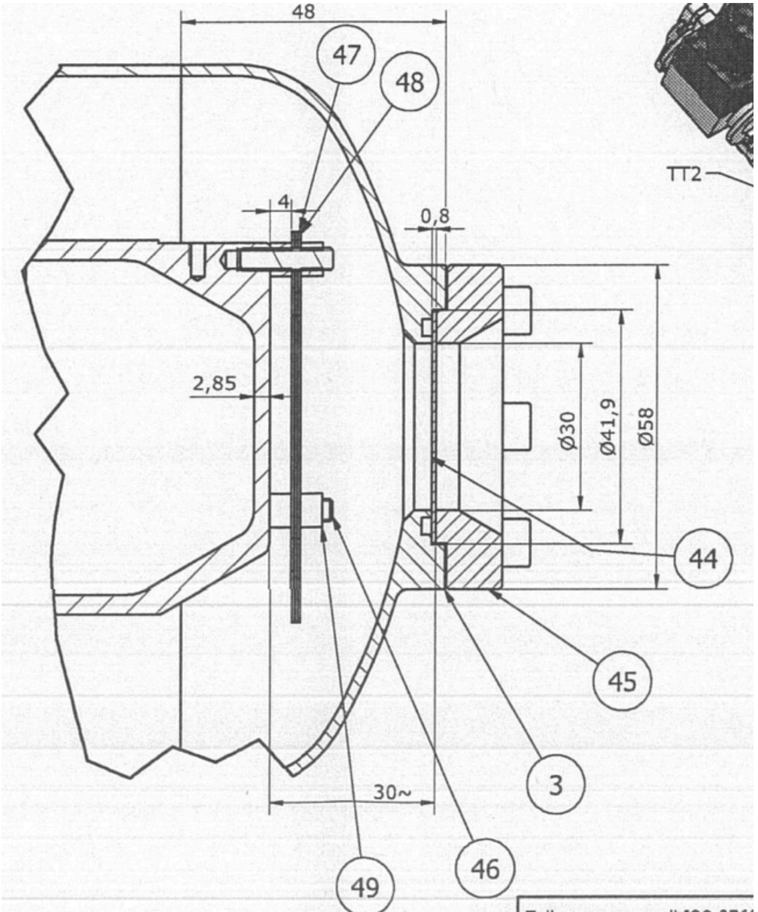

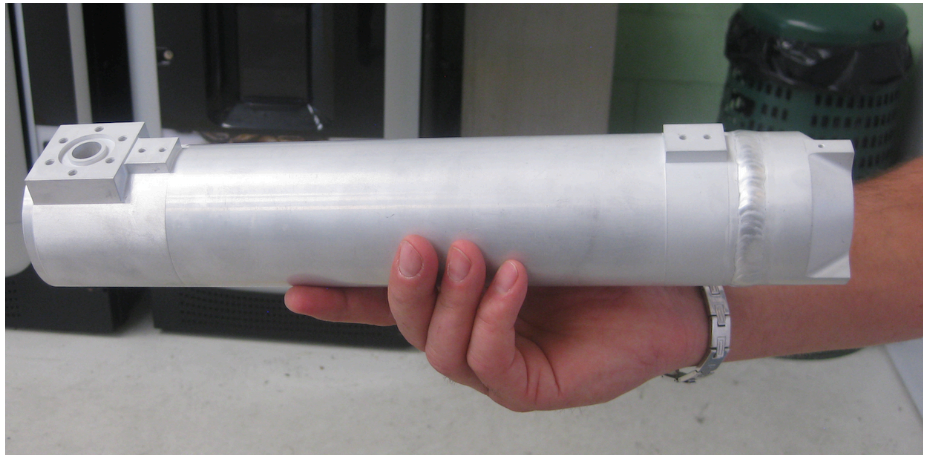

internal coating Ni+Au

nuclear capture of the muons in heavy nuclei is fast (less than 100 ns this eliminates the noise from muon decay electrons.

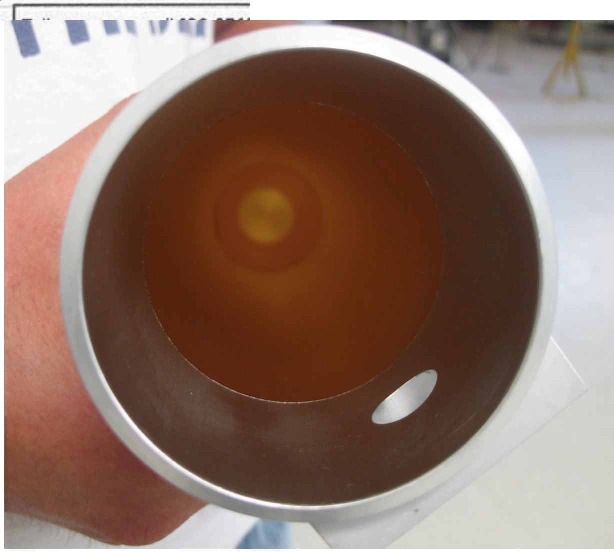

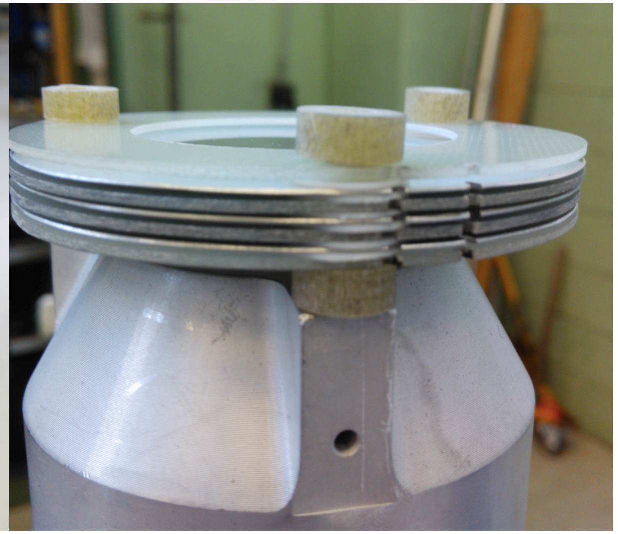

FAMU

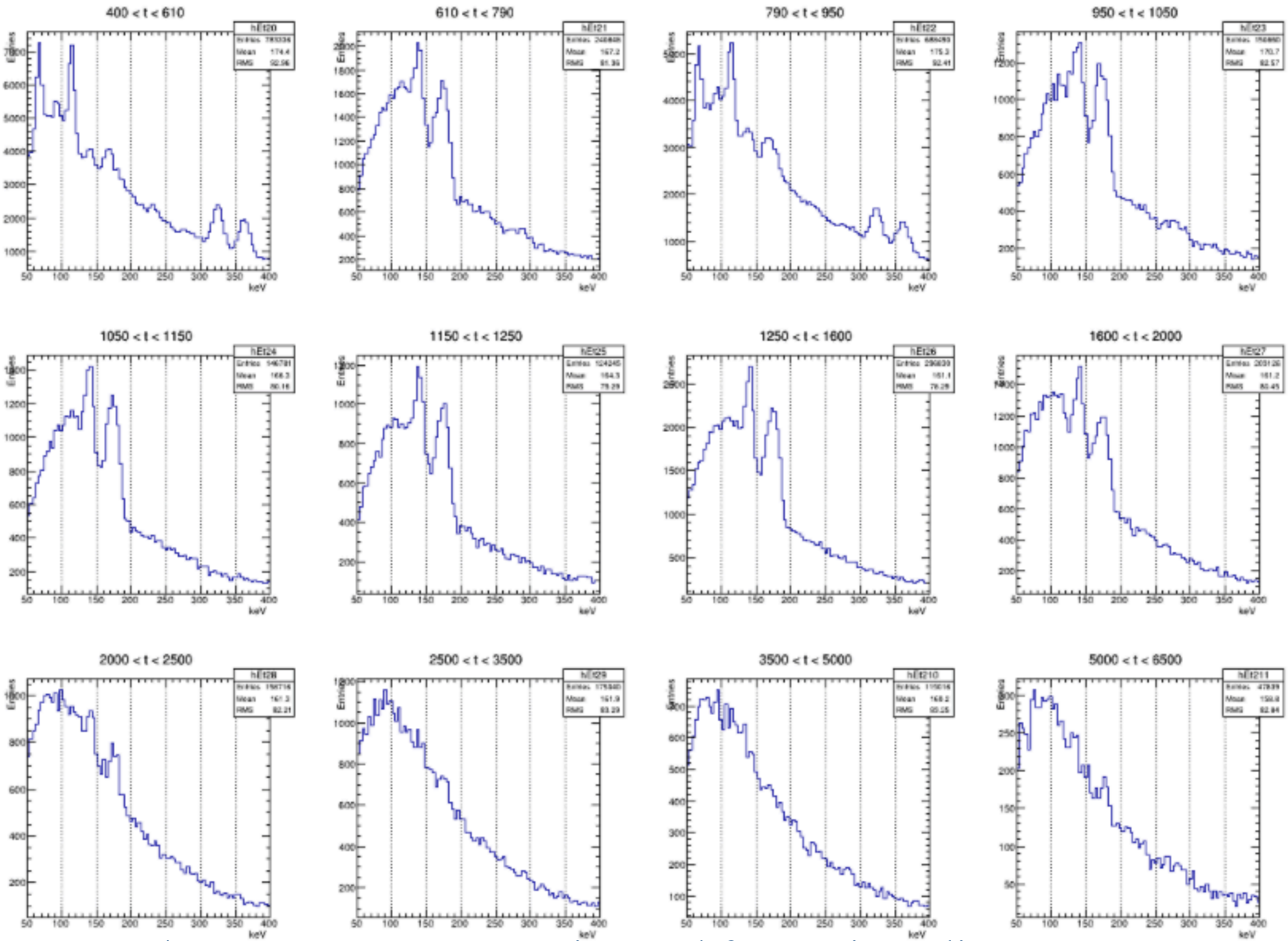

H/O2 1% energy spectra integral for 12 time slices

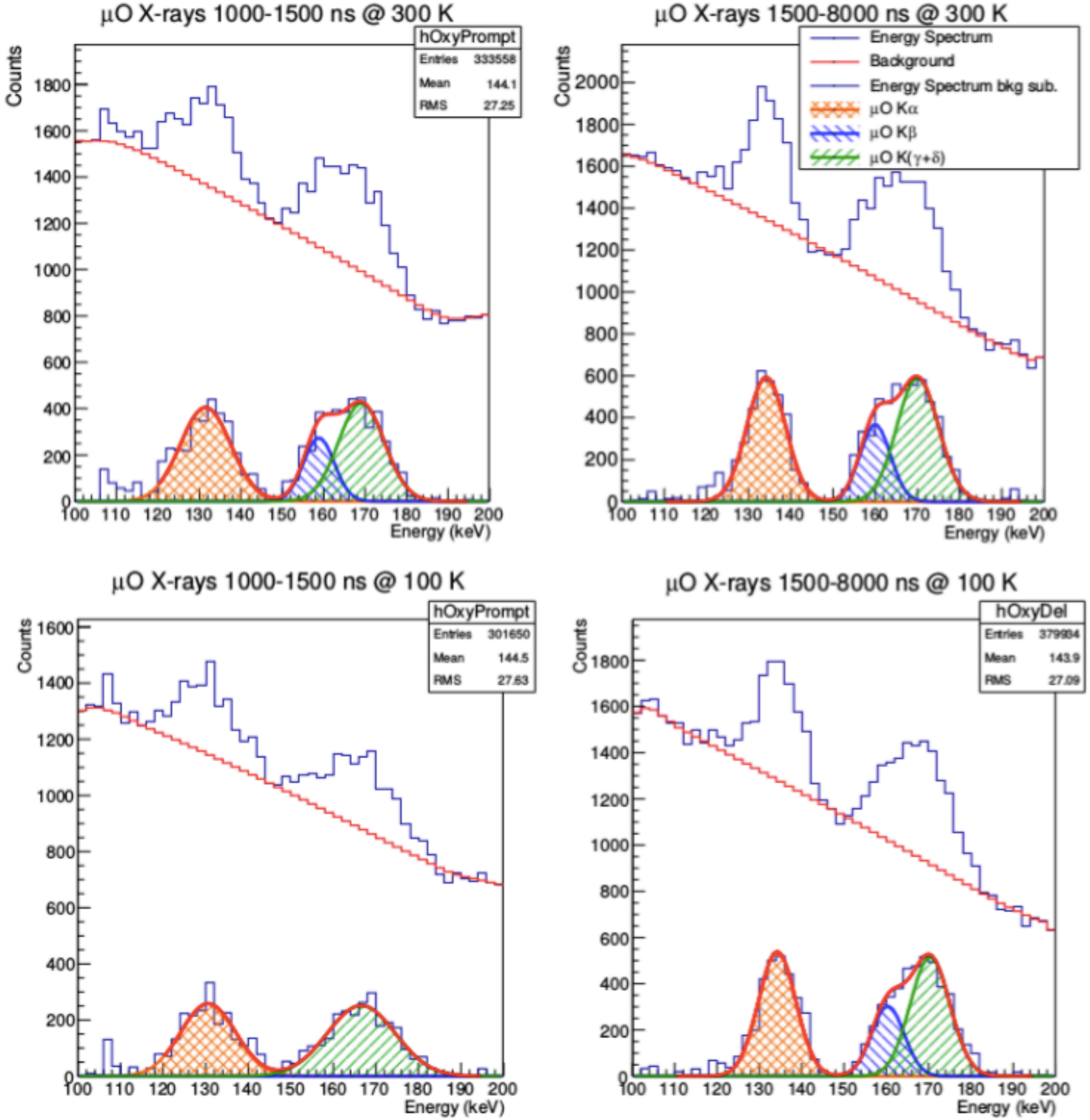
μO X-rays 1000-1500 ns @ 300 K
hOxyPrompt
Entries 333558
Mean 144.1
RMS 27.25
μO X-rays 1500-8000 ns @ 300 K
Energy Spectrum
Background
Energy Spectrum bkg sub.
μO Kα
μO Kβ
μO K(γ+δ)
μO X-rays 1000-1500 ns @ 100 K
hOxyPrompt
Entries 301650
Mean 144.5
RMS 27.63
μO X-rays 1500-8000 ns @ 100 K
hOxyDel
Entries 379934
Mean 143.9
RMS 27.09
Counts
Energy (keV)

FAMU

FAMU Preparatory Phase

First Temperature dependence measurement of the muon transfer to oxygen Λ(T) in the epithermal range

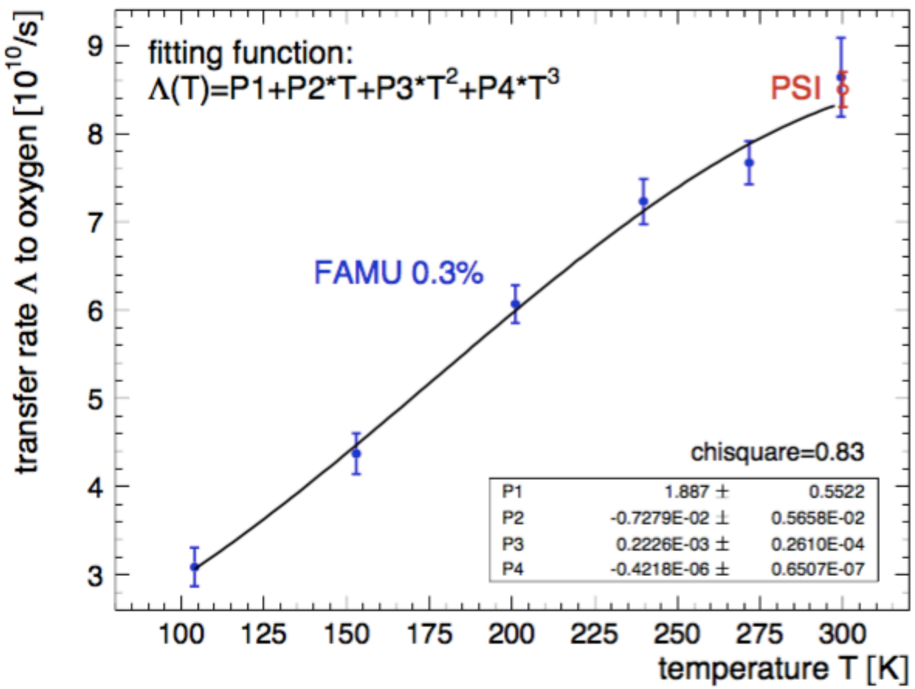

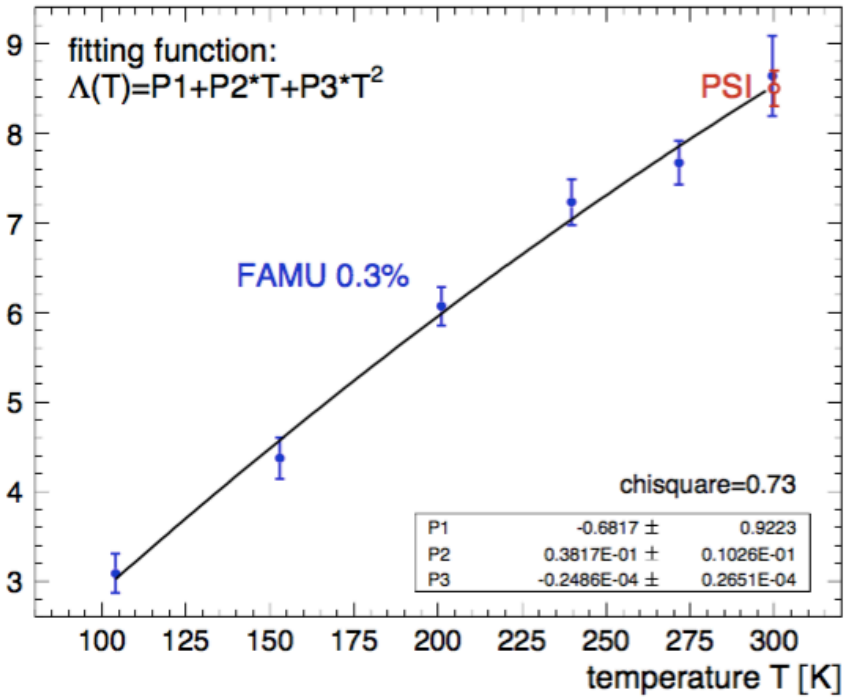

Transfer rate up to 120 meV

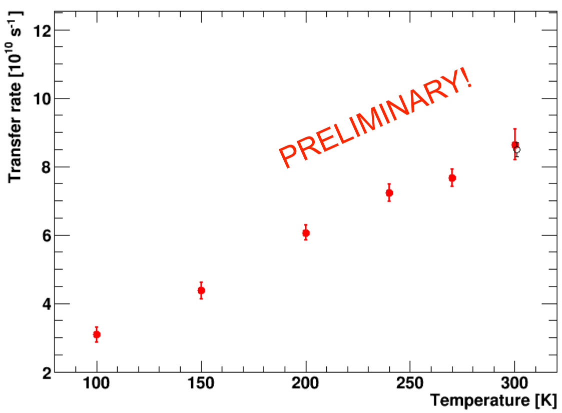

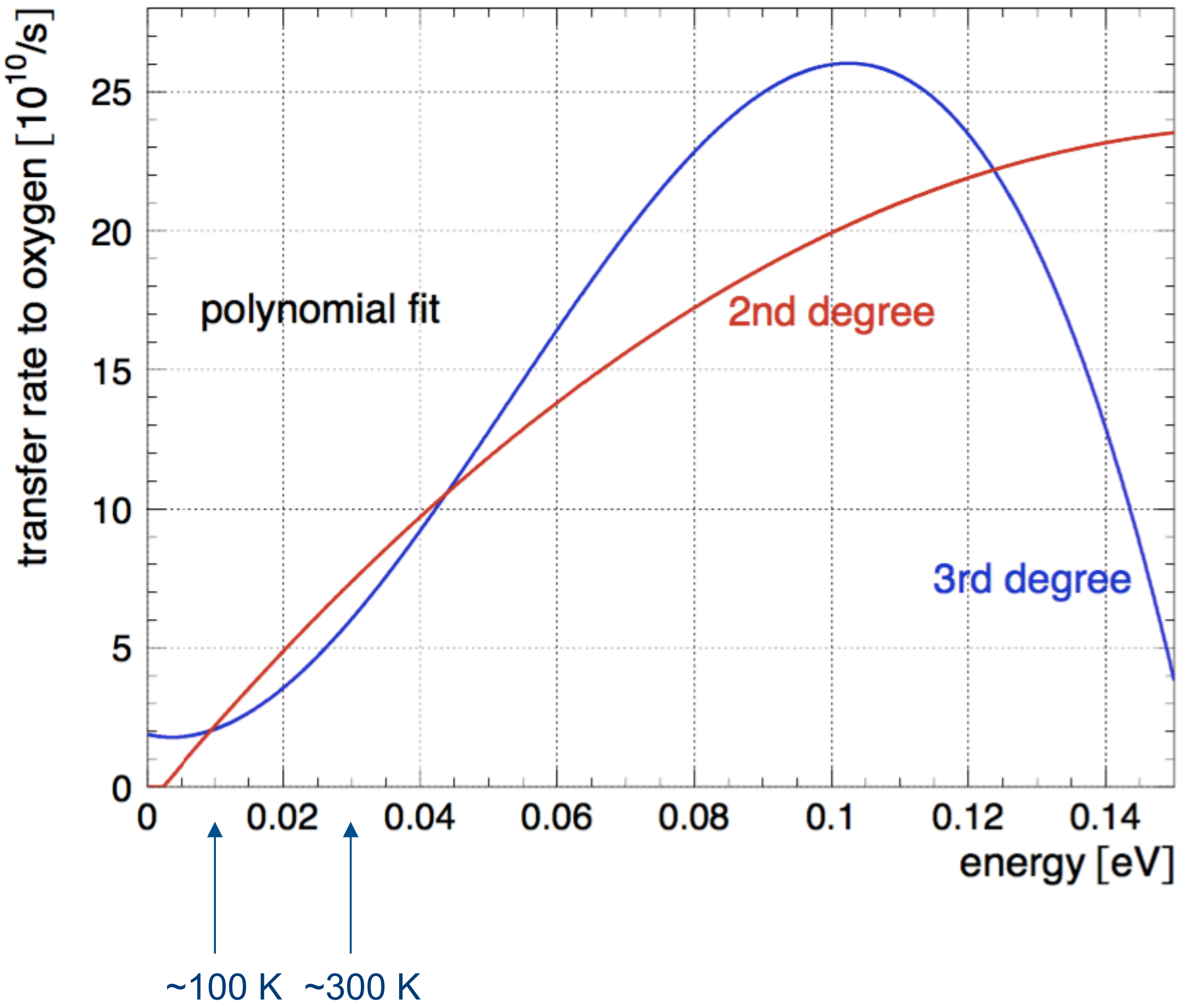

Transfer rate up to 120 meV

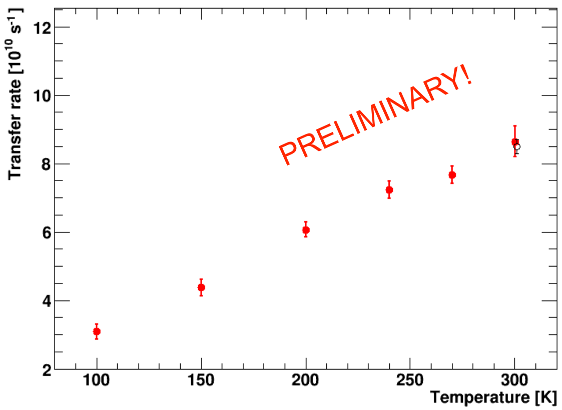

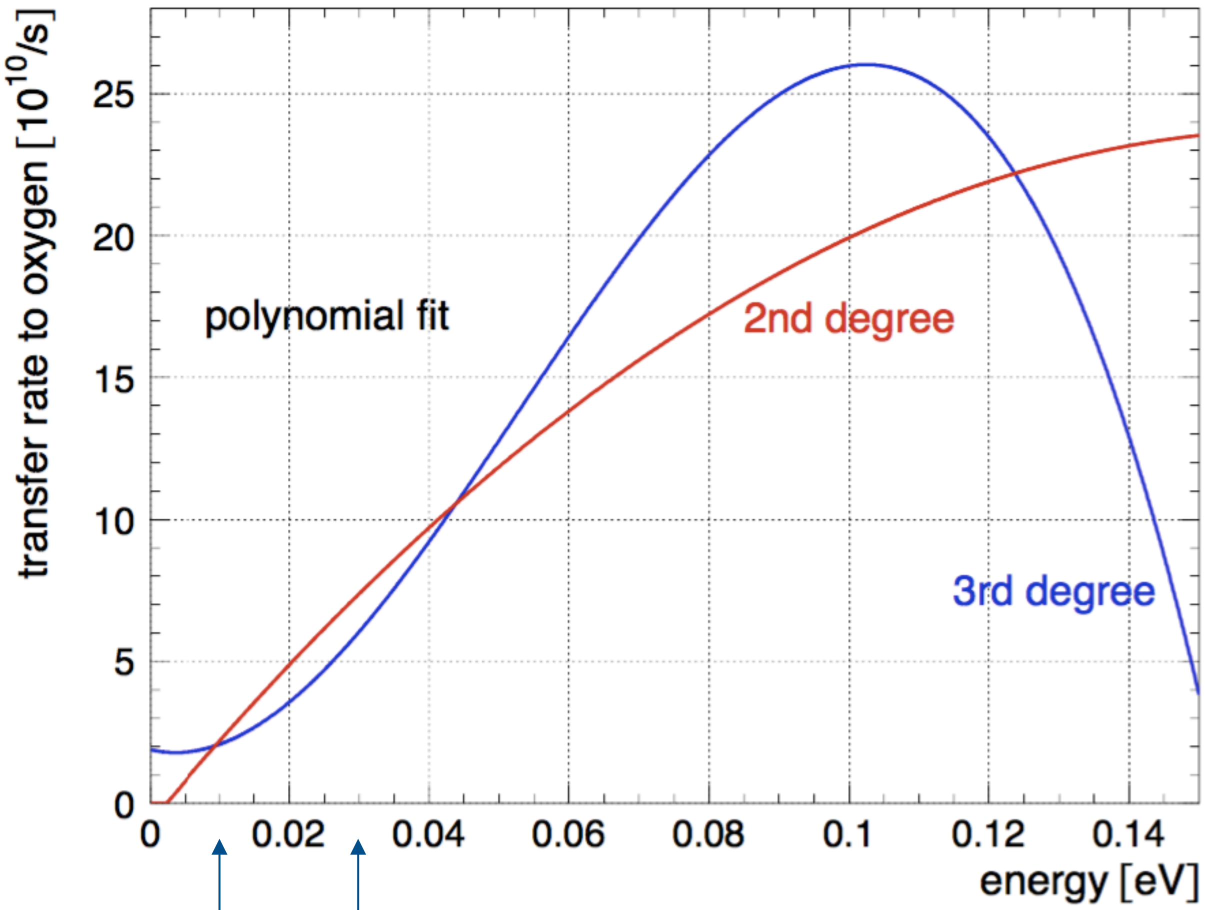

~100 K ~300 K

μp energy
after laser pulse

Study of best setup to maximize signal

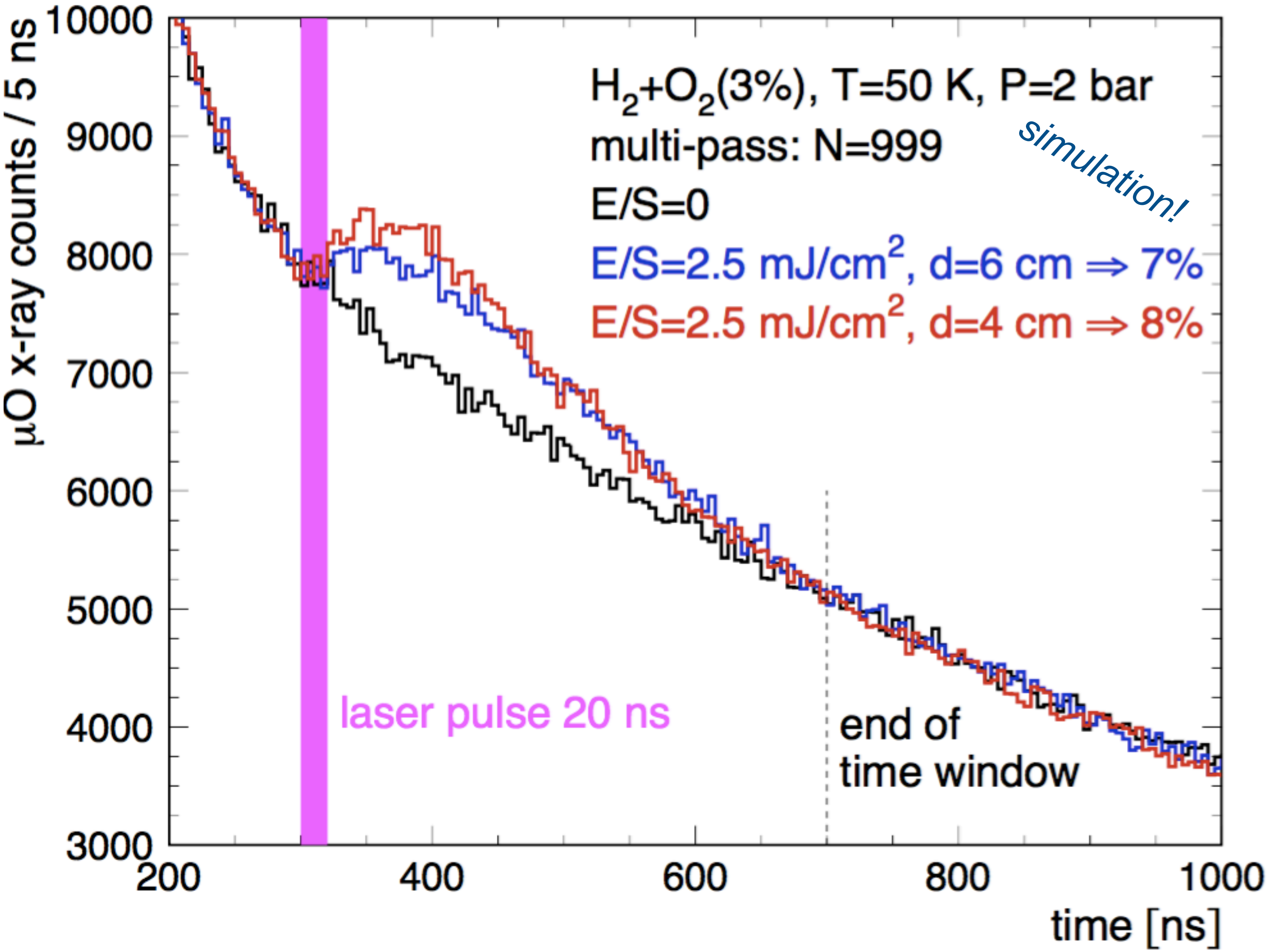

Full MC simulation using realistic laser-field profile and new pressure and concentration conditions A.A. D.B.

Optimized efficiency

5 millions muons 50K, 2 bar and oxygen 3%

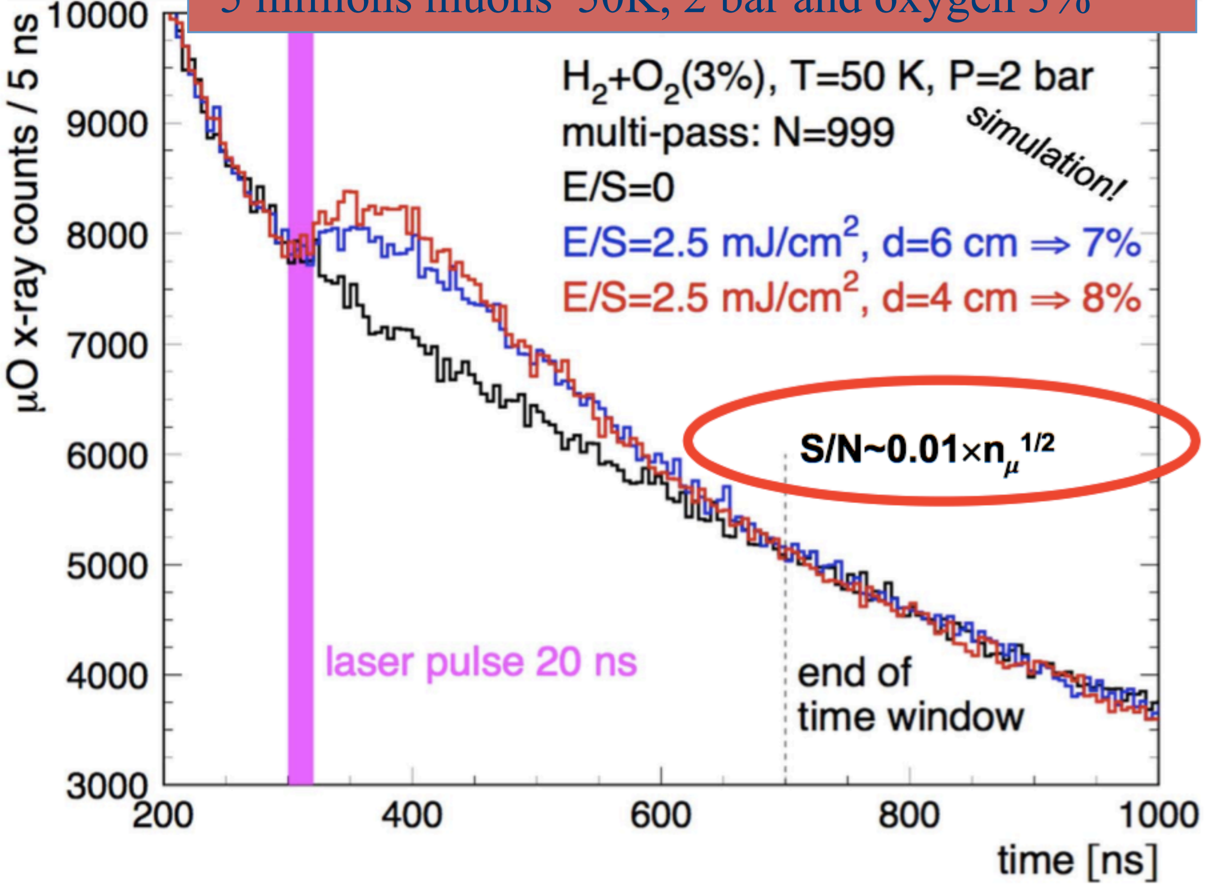

To accelerate the muon transfer to oxygen => concentration O2 3% (weigth).
Target pressure, 2 bars to enhance delayed transfer events.
The *simulation has been performed at 2 bars without the time structure of the RIKEN-RAL beam*, in order to clearly see the main processes and effects.

The laser is turned on at 300 ns.
The laser pulse of 20 ns is marked by the magenta line. Then the laser field stays in the multipass cavity until extinction at about 1300 ns. The spectra are parametrized by E/S - laser power per unit of the laser-beam section. For E/S-2.5 mJ/cm^2, the effect reaches 7%.
The variable "d" denotes a distance between the mirrors of a laser cavity. The number of muon stops (5 millions) was equal for every case.

FAMU

INFN
Istituto Nazionale di Fisica Nucleare

- The Proton Radius Puzzle: Why We All Should Care
- SERIES
- Physics Colloquium
- PRESENTER
- Gerald A. Miller, University of Washington
- November 17, 2017 11:00AM to 12:00Pm
- Colloquium
- **Abstract:** A new scalar boson that couples to the muon and proton can simultaneously solve the proton radius puzzle and the muon anomalous magnetic moment discrepancy. Using a variety of measurements, we constrain the mass of this scalar and its couplings to the electron, muon, neutron, and proton. Making no assumptions about the underlying model, these constraints and the requirement that it solve both problems limit the mass of the scalar to between about 100 keV and 100 MeV. We identify two unexplored regions in the coupling constant-mass plane. The implications of recent experiments are discussed.
-

Measurement of the proton Zemach radius from the hyperfine splitting energy in ground-state muonic hydrogen

M. Sato,[*1] S. Aikawa,[*2] K. Ishida,[*1] M. Iwasaki,[*1,*2] S. Kanda,[*3] Y. Ma,[*1] Y. Matsuda,[*4] T. Matsuzaki,[*1] K. Midorikawa,[*5] Y. Oishi,[*1] S. Okada,[*1] N. Saito,[*5] A. Takamine,[*6] K. Tanaka,[*1,*4] H. Ueno,[*1] and S. Wada[*5]